Integrated Master in Chemical Engineering

Interfacing Metal-Organic Frameworks with Structured Supports

Master Thesis

Developed for the course

Development Project in a Foreign Institution

Mariana Garcia Domingos

TU Delft - Delft University of Technology
Faculty of Applied Sciences
DelftChemTech, Section Catalysis Engineering

Chemical Engineering Department

Graduating Professor: **Freek Kapteijn**

Daily Supervisors: **Enrique Ramos**
Jorge Gascon
Evaluator in the home institution**: Professor José Luís Figueiredo**

July 2009

Acknowledgments

This project can be seen as a quest to find ways to use MOFs as catalysts. And it was with uttermost joy and surprise that along this journey I met so many people that were like catalysts to me and my project.

I spent five months looking for answers that could give some contribution in this complex new subject, and found many of them among the ones that helped me and whose help I now acknowledge.

First of all, I would like to express my gratitude to Professor Freek Kapteijn for the opportunity to work in his group and the challenges posed that were a good source of motivation.

Secondly, I will be always grateful to Jorge Gascon for all the support and feedback, the knowledge transmitted and, of course, for answering, with lots of patience my long emails with questions and doubts.

I would also like to acknowledge Professor José Luís Figueiredo, my evaluator in FEUP, for reading my monthly reports and giving his opinion about the work developed.

Then, it is impossible to forget the help given by Enrique Ramos in supervising me, always available even when he was busy with other issues. I must also thank him, for hearing me all the times that I was despairing with no good results (I know it was not an easy task).

Thanks also to Jana Juan Alcaniz, my laboratory mate, I spent only five months with her but I am sure that I will miss her. I have learned a lot with her sense of work and organization and I found a friend always there to give me a hug.

I am also forever grateful to my Erasmus mate Sofia, who had to hear all my complaints about everything and nothing, sometimes almost 24 hours a day, thanks to my office mates, for the great environment and for having always nice words to say when the things were not going as we expected.

Thanks to the technical support Harrie, Kevin, Bart and Willy and also thanks to Joana and Chao who made me feel at home.

I also acknowledge my catalysts working by distance, JU, IO, Mário, Márcia and Recta. Really special thanks to Simão for all the wonderful moments we spent together, that made him a good source of inspiration. Thanks a lot! And let’s continue dreaming!

Last but definitely not the least, thanks to the state of the art catalysts of my life, whose performance continues unbeatable: my parents, Guilherme e Lourdes, my lovely sister, Gui, my grandparents, Agostinho, Emília e Luíza, and my grandaunt, Té, who always help me in conquering life and are responsible for the person that I am.

Abstract

Some attrition can occur when performing a reaction with Metal-Organic Frameworks, MOFs, in a slurry operation system. In order to maintain the catalytic properties of the material and also to avoid its loss during the, after reaction, separation and purification processes, a new approach for using Metal-Organic Frameworks in catalysis was studied, which consisted of coating a structured support, as Cordierite, with MOF.

The MOF studied within this project was MIL-101 (Cr). Firstly, a direct impregnation of Chromium Oxide followed by both microwave and hydrothermal synthesis was tested and compared using two different supports: cordierite monoliths and α-alumina disks.

Due to some uncertainty about the origin of the crystals being synthesized a different route was tested, consisting of a secondary growth after different seeding techniques. First the most appropriate particles to be used as seeds were studied. In α-alumina disks, seeds were applied on the support by dip and spin coating, followed by a secondary growth. The effectiveness of the methods was then compared. In order to apply some seeding techniques in a monolithic support, a previous wash coating with α-alumina was done using also two different procedures that differ essentially in the total time of the monolith preparation, before the secondary growth, and in the temperature of calcination.

After obtaining a layer of MIL-101 (Cr) on a monolithic support, several catalytic tests were performed. The reaction chosen was Knoevenagel condensation which can be catalyzed by bases. Two different bases, Guanidine Nitrate and 1,5,7-Triazabicyclo[4.4.0]dec-5-ene, were grafted into the MOF by a post-synthetic modification and, before starting performing reactions in a monolithic stirrer reactor, some studies were done in a slurry system to find out if the grafting was effective and a activity for the reaction was introduced with the grafting.

Then, some catalytic tests involving a MOF grafted and covered on the monolith were tried but several obstacles were encountered that are also discussed, as part of the scope of this project.

MIL-101 (Cr) was interfaced successfully with both α-alumina disks and cordierite monoliths wash-coated with α-alumina. The most promising way for seeding the disks was spin coating but a clear layer of MOF was obtained in cordierite monoliths using a dip coating and followed by vacuum treatment. The two bases grafted in MOFs proved to make it an active catalyst even after three runs, using it as particles. Regarding the reaction using monoliths, the basicity was introduced in the MOF coated although relevant catalytic activity is still to be encountered.

Key words: MIL-101 (Cr), coating, seeding, support and monoliths

Table of Contents

Table of Contents i
List of Figures iii
List of Tables vi
Notation and Glossary vii
1 Introduction and Motivation 1
2 State of the Art 8
3 Interfacing MIL-101 (Cr) with monoliths – Precursor Impregnation 14
3.1 Introduction 14
3.2 Experimental Work 14
3.3 Impregnation of Chromium Oxide as Precursor on Cordierite 15
3.4 Impregnation of Chromium Oxide as Precursor on α-alumina disks 19
4 Interfacing MIL-101 (Cr) with monoliths - Seeding Techniques 21
4.1 Introduction 21
4.2 Experimental work 21
4.3 Preparation of the most appropriate nanoparticles 25
4.4 1st Step Interfacing MIL-101 (Cr) with α-alumina disks by dip coating and spin coating 28
4.5 2nd Step Interfacing MIL-101 (Cr) with Cordierite wash-coated with α-alumina 31
5 Catalytic Performance in Slurry Operation 36
5.1 Post-synthetic modification of MIL-101 (Cr) 36
5.2 Knoevenagel Condensation Reaction 37
5.3 Experimental work 38
5.4 Grafting with Guanidine Nitrate 39
5.5 Grafting with 1,5,7-Triazabicyclo[4.4.0]dec-5-ene 40
6 Monolithic Grafting and First Studies using a Monolithic Stirrer Reactor 43
7 Conclusions and Recommendations for Future Work 48
7.1 Conclusions 48
7.2 Recommendations for Future Work 49
8 References 50
Appendix 1 MOFs with catalytic applications known so far 55
Appendix 2 Characterization Methods 57
Appendix 3 XRD pattern of Cordierite impregnated with Chromium Oxide before and after synthesis 61
Appendix 4 Synthesis using Chromium Oxide Particles 63

Appendix 5 Thermo Gravimetric Analysis of the Samples with Chromium Oxide Impregnated in Air using an air flow 65

Appendix 6 N_2 Adsorption Isotherms obtained for MIL-101 (Cr) particles with different synthesis reactants concentration 67

Appendix 7 BET Method 69

Appendix 8 *t* method 71

Appendix 9 XRD Pattern and TGA of MIL-101 (Cr) particles synthesized using different reactants concentration 73

Appendix 10 SEM micrographs of α-alumina disk after a secondary growth in a sample seeded with dip coating 75

Appendix 11 Thermo Gravimetric Analysis of a Monolith after Secondary Growth and without a wash-coated with α-alumina 77

Appendix 12 SEM micrographs of Cordierite Wash-Coated with α-alumina and after Secondary Growth in Static Oven 79

Appendix 13 Thermo Gravimetric Analysis of the MIL-101 (Cr) covered in monoliths and with HPA encapsulation 81

Appendix 14 First Experimental Setup tested for the Monolithic Stirrer Reactor 85

Appendix 15 Poster Presented in MOFCAT Workshop 2009 - Metal Organic Frameworks on the Road to Applications in Oslo 87

List of Figures

Figure 1- Evolution history of crystalline microporous materials.The 15th International Zeolite Conference (IZC) held in 2007 was entitled "From zeolites to Porous Materials: The 40th Anniversary of International Zeolite Conference". At the last IZC MOFs were also classified into a new class of zeolitic materials [3]. 1

Figure 2 -Number of Metal-Organic Framework structures reported in the Cambridge Stuctural Database (CSD) from 1978 through 2006.The bar graph illustrates the recent dramatic increase in the number of reports, while the inset shows the natural log of the number of structures as a function of time, indicating the extraordinarily short doubling time for MOF structures, compared to the total number of structures archived in the database [5]. 2

Figure 3 -Pore diameter as a function of pore volume. Blue circles, sorption and crystal MOF structures; red squares, crystal MOF structures; yellow diamonds, some typical zeolites [7]. 3

Figure 4 – SEM micrograph of IRMOF-3 samples before and after reaction [14]. 4

Figure 5 – Basic Building units and crystal structure of MIL-101 (Cr)[17], [15].. 5

Figure 6 – Diagram illustrating the activities performed in order to interface MIL-101 (Cr) with monoliths. 6

Figure 7- A hexagonal large-pore structure of POST-1 with trinuclear secondary building units.Three pyridyl groups pointing to the pore, Zn atoms in green, oxygen in red, nitrogen blue, C atoms in white and C atoms in pyridil groups In yellow [27]. 10

Figure 8 – The pore structure of rho-ZMOF (left) and the encapsulated $[H_2TMPyP]^{4+}$ *porphyrin in rho-ZMOF* α*-cage (right). Solvent molecules and hydrogen atoms are omitted for clarity [10]* 11

Figure 9 – SEM micrographs of a) monolith (Cordierite), b) monolith with chromium oxide, and c) Monolith with MIL-101 (Cr)). 16

Figure 10- SEM micrographs of the layer obtained. 16

Figure 11 – Isotherms obtained for the monolith, monolith with Chromium Oxide impregnated, monolith with MIL-101 (Cr). 17

Figure 12 – TGA results for monolith with MIL-101 (Cr) both with microwave and hydrothermal synthesis and its derivative. 18

Figure 13 -SEM micrographs of the monolith impregnated with Chromium Oxide – a), monolith after hydrothermal synthesis of MIL-101(Cr)-b). 18

Figure 14 – SEM micrographs of a) α*-alumina disk after2 hours of direct synthesis; b)* α*-alumina disk after a secondary growth during 10 hours.* 19

Figure 15 – XRD patterns of α*-alumina disks after direct synthesis with impregnation of Chromium Oxide;* α*-alumina disk after a secondary nucleation during 10 hours.* 20

Figure 16 – Schematic representation of spin coating technique [67]. 23

Figure 17 – Pictures of the set up used for Dip-coating in four different moments. 24

Figure 18 – SEM micrograph of MIL-101 (Cr) obtained with samples 2.5 more concentrated than the standard conditions. 26

Figure 19- Nitrogen Adsorption Isotherm of the sample synthesized with the standard conditions 2.5 times diluted (blue line-desorption curve; black line-adsorption curve). 26

Figure 20 –SEM micrograph for powder samples synthesized 2.5 times diluted and a magnification of 60 000. 27

Figure 21 – SEM micrograph and atomic distribution in a cross section of a α-alumina disk after hydrothermal synthesis using dip coating seeding. 28

Figure 22 – XRD pattern of α-alumina disk surface after hydrothermal synthesis and with a previous seeding using dip coating technique. XRD pattern of MIL-101 (Cr) samples for comparison effects. ... 29

Figure 23-SEM micrographs of MIL-101 (Cr) hydrothermal synthesis in α-alumina disks (A and B) and microwave synthesis (C and D). 29

Figure 24 –XRD pattern of a-alumina samples with microwave and hydrothermal synthesis. 30

Figure 25 – SEM micrograph of α-alumina disk cross sectional view with the respective atomic distribution of Chromim (yellow dots) and Alumina (red dots) 31

Figure 26 –Picture of the monolith synthesized using A procedure and static oven and a scheme illustrating the problem encountered. 32

Figure 27 – Monolith after synthesis in rotatory oven and following procedure A and B for preparing the monoliths. 32

Figure 28 SEM micrographs of monoliths prepared with Procedure A) general overview of the α-alumina coating; B) surface of the monolith after being coated with α-alumina; c) cross sectional view of the monolith after secondary growth on a rotatory oven. 32

Figure 29 – SEM micrographs with a higher magnification with the octahedral geometry of the crystals perfectly clear- a) and b)- and the presence of MIL-101 (Cr) all over the channel. –c). 33

Figure 30 – SEM micrographs of monoliths prepared with procedure B a) monolith with just the coating; b) monolith after secondary growth in a rotatory oven. 33

Figure 31 –Raman Spectra of the monolith's surface after secondary growth and with the coating prepared by both Procedure A and B and also MIL-101 powder. 34

Figure 32 – TGA of MIL-101 (Cr) covered in the monoliths and respective derivative. 35

Figure 33 – Structure of MIL-101 (CR)A-trimeric building unit; B-Terephthalic acid; C-edges of the supertetrahedra; D Ball and stick representation E-3 D schematic representation .Chromium octahedral, oxygen and fluorine and carbon are in green, red and blue. 37

Figure 34 –Reaction Scheme of Knoevenagel Condensation. 38

Figure 35 – DRIFT spectra of guanidine nitrate, MIL-101 (Cr) and MIL-101 (Cr) grafted with guanidine. 39

Figure 36 –Yield versus time for homogeneous reaction with guanidine nitrate and the heterogeneous catalyst, in three consecutive runs. 39

Figure 37 – DRIFT spectra of1,5,7-Triazabicyclo[4.4.0]dec-5-ene, MIL-101 (Cr)and MIL-101(Cr) grafted with both bicycle in the standard amount (1 mol of base per mol of OH group) and half of that quantity and after performing 3 runs of reaction..... 40

Figure 38 – N_2 adsorption isotherms of MIL-101(Cr), MIL-101(Cr) grafted with 1,5,7-Triazabicyclo[4.4.0]dec-5-ene and MIL-101(Cr) grafted with half of the amount of 1,5,7-Triazabicyclo[4.4.0]dec-5-ene.. 41

Figure 39 - Yield versus time for homogeneous reaction with 1,5,7-Triazabicyclo[4.4.0]dec-5-ene and the heterogeneous catalyst, in three consecutive runs. 42

Figure 40 –TGA analysis of the monolith grafted with guanidine and the corresponding derivative. ... 44

Figure 41 – Monolithic support for a monolithic stirrer reactor bare cordierite and cordierite impregnated with MIL-101 (Cr). 45

Figure 42 – Conversion versus time for the reaction carried on the monolithic slurry reactor using, in powder, the same quantity of MIL-101 (Cr) that is on the monolith surface. 45

Figure 43 –Reaction Results of the last trial, performing the washing and the grafting in the monolithic stirrer reactor and using 4 monoliths. 46

Figure 44 – XRD pattern of the codierite, cordierite impregnated with Cr_2O_3 and after direct synthesis MIL-101 (Cr). 61

Figure 45- SEM Picture after the synthesis of MIL-101 (Cr) with Chromium Oxide. 63

Figure 46 – XRD patterns of the powder obtained when performing a synthesis with Chromium Oxide. 64

Figure 47 – TGA Results of the samples with direct synthesis both by Microwave and Hydrothermal Synthesis after Chromium Oxide Impregnation and with Helium an Air flow. 65

Figure 48 – N2 Adsorption Isotherms of MIL-101 (Cr) powder samples synthesized using a) standard conditions; b) 1.5 times more diluted synthesis conditions; c) 2 times more diluted synthesis conditions and d) 2.5 times more diluted synthesis conditions (blue is the dessorption curve and black the adsorption).. 68

Figure 49 – XRD patterns of MIL-101 (Cr) samples from the most diluted (50 mL) to the standard (20mL). 73

Figure 50 – TGA of MIL-101 (Cr) synthesized with different amount of water from the most diluted (50 mL) to the standard (20mL). 73

Figure 51 – SEM micrographs of: α-alumina disk top layer covered with MIL-101 (Cr) after dip coating technique –left image and cross sectional view of the same alumina disk. 75

Figure 52 – SEM micrograph of an α-alumina cross-sectional view..... 75

Figure 53 - TGA of MIL-101 (Cr) covered in the monoliths without doing a wash-coated with α-alumina and its derivative..... 77

Figure 54 – SEM micrographs of the sample with a wash coat with α-alumina and with the Secondary Growth performed in a Static Oven..... 79

Figure 55 – Different representations of Phosphotungstic Acid molecule. Oxygen, Tungsten and Phosphorous are represented by red, blue and yellow, respectively. 82

Figure 56 – TGA of MIL-101 (Cr) covered in the monoliths with HPA encapsulated and respective derivative 83

Figure 57 – First experimental setup tested. 85

List of Tables

Table 1 – BET surface area and Pore volumes calculated for each sample prepared. 26

Table 2 - TON and TOF values of the samples grafted with MIL-101 (Cr) guanidine after each run. 40

Table 3 – TON and TOF values of the samples with MIL-101 (Cr) grafted with 1,5,7-Triazabicyclo[4.4.0]dec-5-ene, after each run, and also of the homogeneous catalyst. 42

Table 4- Catalogue of known MOFs and summary of reactions catalyzed [10] 55

Table 5 – Characterization Methods Performed in each sample, ... 59

Notation and Glossary

Acronyms

AAO	Anodic Aluminium Oxide
APS	3-aminopropyltrialkoxysilane
ATC	Adamantane Tetracarboxylate
Bdc	1,4-benzenedicarboxylate
BINOL	1,1'-bi-2-naphthol
Bpdc	biphenyl-4,4'-dicarboxylate
Bpy	4,4′-bipyridine
Btb	benzene-1,3,5-tribenzoate
Btc	1,3,5-benzenetricarboxylate
BET	Brunauer, Emmett and Teller
CUS	Coordinatively Unsaturated Metal site
cpsi	Cells per square inch
Dabco	1,4-diazabicyclo[2.2.2]octane
DETA	diethylenetriamine
Dpyg	1,2-di(4-pyridyl)glycol
DRIFT	Diffuse Reflectance Infrared Fourier Transform
HKUST	Hong Kong University of Science and Technology
HPDC	4,5,9,10-tetrahydropyrene-2,7-dicarboxylate
HPA	Heteropoly Acid
ECA	Ethyl-cyanoacetate
ED	Ethylenediamine
MIL-101	Material of the Lavoisier Institute 101
MOF	Metal-Organic Framework
NDC	naphthalene-2,6-dicarboxylate
Pdc	pyridyl-2,6-dicarboxylate
POST-1	$\left[Zn_3(\mu_3-O)(1-H)_6\right]\cdot 2H_3O\cdot 12H_2O$
Pyz	Pyrazine
Pzdc	Pyrazine-2,3-dicarboxylate
SAM	Self Assembled Monolayer
SBU	Secondary Building Unit
SEM	Scanning Electron Microscopy
ST	Supertetrahedra
TGA	Thermo Gravimetric Analysis
TOF	Turnover Frequency
TON	Turnover Number
TPDC	terphenyl dicarboxylate
TPHP	Tert-butyl hydroperoxide oxidant
XRD	X-Ray Diffraction

1 Introduction and Motivation

Catalysis

The origin of catalysis cannot be properly set while the origin of life still remains a mystery.

However, limiting catalysis to the production of chemicals, it firstly appeared around 3000 years BC in the production of wine or beer from fermentated sugars. If more specificity is needed and catalysis restricted to catalytic production process, then the first commercial application was the production of sulphuric acid in the mid-18th century [1].

After that, many processes involving catalysts have been studied and introduced in industry, been visibly present in nearly all plants, not only in the production of bulk but also fine chemicals and constituting the basis of novel or improved processes [1].

The users of catalysts are especially concerned with the catalyst manufacture because by knowing how they are produced a clear insight in the catalyst structure and behaviour can be achieved. Thus, catalyst preparation constitutes a critical issue in the development of a process.

Depending on the presence of just single or different phases in the system, catalysis can be classified as homogeneous or heterogeneous, respectively. Although both of them are important, this project will focus on heterogeneous catalysis.

In that class of catalysis, when solid phases are present, reaction takes place on the surface of the catalyst. With their high surface areas, porous materials constitute the most common catalysts due to their maximization of production rates.

Metal-Organic Frameworks

Porous materials such as zeolites, activated carbon or alumina have been reported in a wide range of reactions, acting both as catalyst or catalyst support.

However in the last decades, several research groups have concentrated their efforts in the development of new solid porous materials and the enthusiasm over this topic was motivated by the discovery of Hybrid Porous Solids which are constituted by both inorganic and organic molecules [2]. A brief diagram representing the evolution from zeolites to new types of materials is shown in Figure 1 [3].

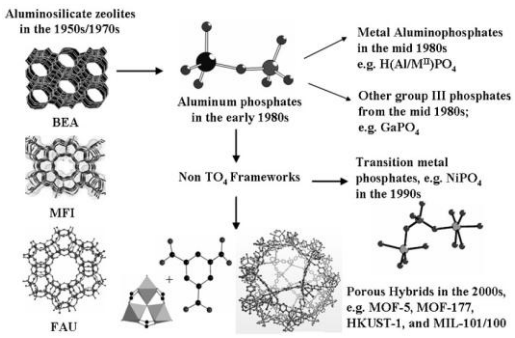

Figure 1- Evolution history of crystalline microporous materials.The 15th International Zeolite Conference (IZC) held in 2007 was entitled "From zeolites to Porous Materials: The 40th Anniversary of International Zeolite Conference". At the last IZC MOFs were also classified into a new class of zeolitic materials [3].

In the beginning Hybrid Porous Solids were simply considered coordination polymers but researchers from the area felt the need of using a term with a narrower sense [4].

A group of materials which result from solution chemistry linking by strong bonds polyatomic clusters (Secondary Building Units – SBUS) and organic molecules [5] and that could possess inorganic moieties with larger dimensionality, giving chains (1D), layers (2D) and inorganic frameworks (3D) led to a new term, Metal-Organic Frameworks (MOFs), more suitable to describe its nature [2]. This term did not include coordination polymers which have generally weaker bonds and lower stability, referred in terms of network charge formal bond valence and estimated link energy [6], [7].

These Metal-Organic Frameworks seem to be in what has been metaphorically called "runaway mode", due to the abundant number of discoveries in a brief period of time (Figure 2) [5].

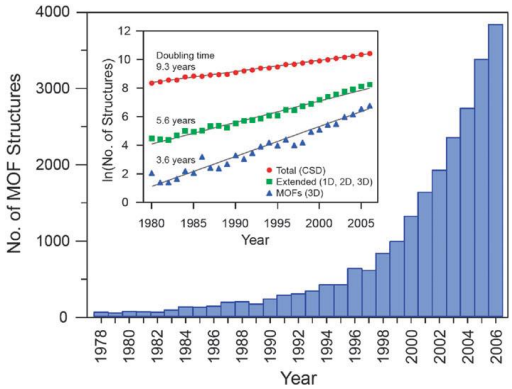

Figure 2 -Number of Metal-Organic Framework structures reported in the Cambridge Stuctural Database (CSD) from 1978 through 2006.The bar graph illustrates the recent dramatic increase in the number of reports, while the inset shows the natural log of the number of structures as a function of time, indicating the extraordinarily short doubling time for MOF structures, compared to the total number of structures archived in the database [5].

The interest over this topic was motivated by their important properties. These materials exhibit a high crystallinity, which enables the correct knowledge of the exact location and connection between the atoms. Thus correlations between the system properties and the chemical structure can be established [5].

Moreover MOFs detain high surface areas, low crystal densities, high storage capacity, magnetic ordering, selective carbon dioxide capture, guest dependent luminescence and also selective heterogeneous catalysis.

This justifies why the most common and well known applications of MOFs include gas storage, separation, drug delivery systems and catalysis [8].In this project we are focused in catalysis which application is particularly interesting since the pore size and functionality can be adjusted over a wide range for a variety of catalytic reactions [9].

An analogy between MOFs and aluminosilicate zeolites, one of the most important class of catalysts, was noted [10], [11]. Both share some of the most important catalytically relevant features such as internal surface areas, which facilitates catalytic reactivity, and uniform pore and cavity sizes, which in its turn enhances catalytic selectivity [10]. However, MOFs cannot compete with zeolites for catalysis under extreme conditions which indicates that their niche may be the high-value-added reaction of fine chemicals, delicate molecules and individual enantiomers under milder conditions [10]. This is possibly the only drawback of MOFs when compared to zeolites since most of their other

properties surpass the ones reported for the state of the art materials not only in terms of porosity - Figure 3 [7] [12].

Because most MOF structures are also neutral, they do not tend to collapse during the extraction of the template. Since the solvents, which act as templates, have weaker interactions with the framework, they easily evolve the structure at low temperatures, often keeping the framework intact and providing very quickly an important and readily available porosity [12].

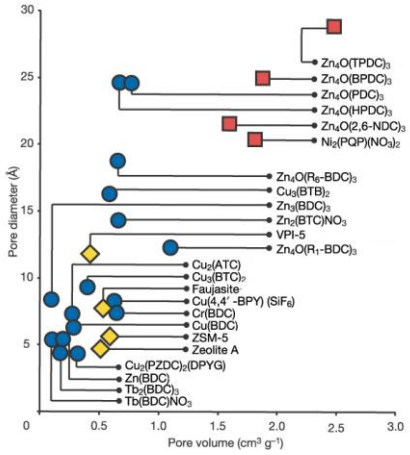

Figure 3 -Pore diameter as a function of pore volume. Blue circles, sorption and crystal MOF structures; red squares, crystal MOF structures; yellow diamonds, some typical zeolites [7].

Secondly, the existence of inorganic and organic parts allows hydrophilic and hydrophobic interactions within the same structure, which probably have some influence on the adsorption properties. MOFs also have a great variety of cations (di, tri or tetravalent) which can participate in the framework as well as a large choice of functionalized organic linkers [10], [12]. Therefore there are a huge number of possibilities for creating MOFs and thus for exploring its properties [12].

Although MOF properties and applications are really promising, the great majority of research concerning Metal-Organic Frameworks is focused on clarifying the rules of reticular synthesis and the development of a method for designing MOFs with the desired properties. Therefore, the work published concentrates on synthesis of novel structures and structure/property/function correlations [13].

In this project, it is intended to go in a slightly different direction in order to obtain an efficient and attractive way for application of MOFs in Industrial catalytic reactions.

Some previous studies have demonstrated that the use of MOF catalysts in slurry operation may cause attrition [14] apart from needing a subsequent separation process for recycling the catalyst which is always accomplished by some catalyst loss. This is not convenient when a catalyst is to be used several times, without losing its properties.

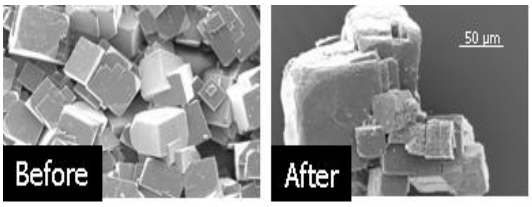

Figure 4 – SEM micrograph of IRMOF-3 samples before and after reaction [14].

The aim of this project was to test a possible route to get over this disadvantage. Thus, a possible method to coat Metal-Organic frameworks in some structured support, such as monoliths, was studied and then their performance in some reactions was also tested.

MIL-101 (Cr)

The Metal-Organic Framework used in this work was MIL – 101 (Material of the Lavoisier Institute 101). MIL-101(Cr) is a Chromium (III) carboxylate (terephtalate) Metal-Organic Framework, which formula is $Cr_3F(H_2O)_2O\left[(O_2C)-C_6H_4-(CO_2)\right]_3 \cdot nH_2O(n \approx 25)$ [15]. It was first synthesised and characterized in *2005* and was obtained by integrating the concepts of targeted chemistry and computational crystal structure design [15], [16].

This MOF combines a high surface area and pore volume and consists of μ_3-oxo bridged chromium(III) trimers cross-linked by terephtalate groups. The chromium ions of the MIL-101 structure have a pseudo/octahedral coordination whose vertices are occupied by the μ_3-O atom in the middle of chromium trimers and four oxygen atoms derived from the carboxylate groups of the terephtalate, the so called Supertetrahedra (ST) [9], [17], [15] [18]. The coordination sphere around each chromium is finally filled up by water molecules, a fluorine atom or a hydroxyl group [15], [17].

The molecules coordinated in the metallic cluster can be partially removed, generating unsaturated sites. These unsaturated sites are suitable to be used as catalytic sites. This open metal site can also be an anchoring place to guest molecules.

This MOF was chosen for the present study because it has features that make it particularly interesting for applications in heterogeneous catalysis. Its pores and pore windows are big enough to give access for even large reactant molecules diffusing into the pores and evacuation of guests does not affect the framework [15]. MIL-101 has a cubic cell with huge cell volume of 702 000 $Å^3$, a large free aperture of 12 Å (from pentagonal windows) and 16 Å x 14.5 Å (from hexagonal windows), two mesoporous cages of 29 and 34 Å [15], [17], [18]. These larger cages are also attractive because they allow the introduction of new species into them and could possibly enhance the reactions. Furthermore, MIL-101 has unsaturated sites that can be catalytic active themselves and coordinate others species.

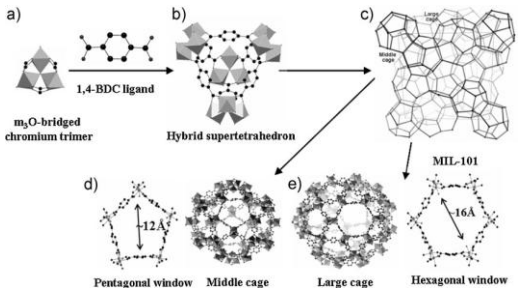

Figure 5 - Basic Building units and crystal structure of MIL-101 (Cr)[17], [15]..

Besides these properties, MIL-101 is also stable up to 375 ^{o}C, over months under air atmosphere and it is not altered when treated with various organic solvents at room temperature or under solvothermal conditions [17],[15].

First Steps

This work was intended to cover cordierite monoliths in MIL-101 (Cr) and test its catalytic performance.

A great part of the project was focused on the interfacing of the chosen MOF with support following different techniques.

First, a direct impregnation of a chromium source, chromium oxide, was tested, comparing a microwave with a hydrothermal synthesis by several characterization methods. Based on the results, the interaction with other kind of support, α-alumina disks, had to be tested and then the strategy skipped to application of some seeding techniques.

In order to perform these techniques, the most appropriate conditions for synthesizing nanoparticles to be used as seeds were selected and then both dip coating and spin coating were applied in α-alumina disks.

As the interaction between alumina support and MIL-101 (Cr) was effective, it was decided to see if we could benefit from a wash coating of cordierite with α-alumina in order to block the major pores of cordierite. Two different procedures were applied in order to wash-coat cordierite and after this sequence; a method for coating monoliths with MIL-101 (Cr) was successfully achieved.

A diagram illustrating the activities done for this purpose is shown in Figure 6.

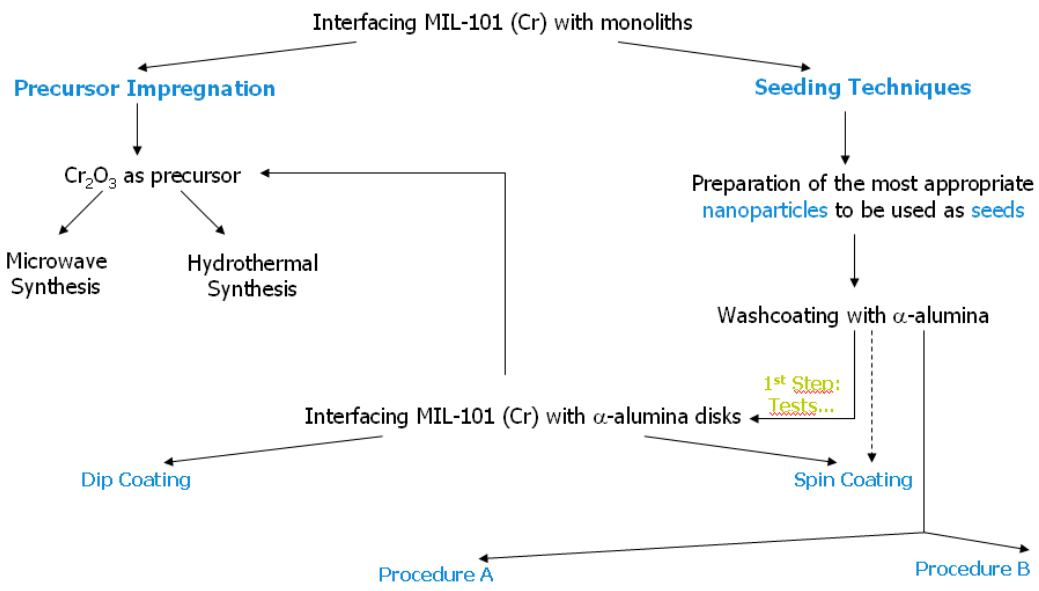

Figure 6 - Diagram illustrating the activities performed in order to interface MIL-101 (Cr) with monoliths.

Basic Catalysis with MOFs

Due to the focus of this work in heterogeneous catalysis, the steps that followed the interfacing of MIL-101 (Cr) with monoliths were surely to test the monolith behaviour when acting as catalysts.

Although research about MOFs performance in catalysis is relatively scarce, the interest over this application seems to be increasing and some post synthetic modifications have been successfully performed in order to develop new chemical methodologies for functionalizing their internal surfaces [5]. By this method some base catalysts that were only used as homogeneous catalysts before, can be introduced in the MOF structure and so been part of heterogeneous catalysis [14].

A large number of reactions are catalyzed by bases and carried out at industrial scale. Industrial base-catalyzed reactions are mostly catalyzed homogeneously by liquid bases due to economical reasons and the lack of other proven alternative. In fact, carrying out this reaction in a homogeneous medium causes some problems related to complex downstream processing and generation of vast amount of industrial waste especially in the synthesis of fine chemicals and pharmaceuticals. Replacing liquid bases used in homogeneous catalysis by solid bases is highly encouraged because it could solve at least one of these problems: high costs of product/catalyst separation, corrosiveness and costs associated with the disposal of spent or neutralized caustic [19].

In this project the reaction chosen for kinetic studies was Knoevenagel Condensation.

This reaction has been previously studied in this group using different MOF catalysts [14]. Very recently, MIL-101 (Cr) grafted with guanidine was shown to be a strong basic catalyst [18]. However, it would be ideal to interface this catalyst in order to avoid the considerable amount of powder and energy lost in the filtrations done to recover it after each run, as well as the attrition problems that damage catalyst particles. The approach of covering the MOF on a support and subjecting it to grafting techniques in order to confer the proper basic environment for the reaction is potentially a good solution for the problem.

Thus, in this project some catalytic tests with post synthetic modifications, using two different bases, guanidine and 1,5,7-Triazabicyclo[4.4.0]dec-5-ene, were tested.

Firstly some studies involving a slurry operation system were performed in order to be sure about the effectiveness of MOF functionalization. Then after selecting an appropriate reactor to perform the reaction using monoliths, some reactions were tried.

Although several problems were encountered in this last step, the discussion about the possible reasons for that occurrence are also within the scope of this project in order to help for further work.

So, the challenge of this project was to interface MIL-101 (Cr) with monoliths and start with the first reaction studies. A detailed description and discussion about the study developed is presented in the following chapters, starting with a small literature review followed by the studies about interfacing monoliths with MIL-101 (Cr), catalytic performance in a slurry reactor and first studies using a monolithic stirrer reactor.

Finally the main conclusions are summarized and suggestions for future work are given.

2 State of the Art

Coating supports with MOFs

As the main objective of the present project is to interface MOFs with monoliths, it is interesting to introduce what has been discovered in this area.

To our knowledge, no studies have been published so far concerning coating monolith surfaces with MOFs but there are a few studies about MOF films.

Zacher et al published a review about the recent developments in this field [13].

The MOFs already studied for this purpose were:

- $[Zn_4O(bdc)_3](MOF-5; bdc = 1,4-benzenedicarboxylate)$;
- $[Cu_3(btc)_2](HKUST-1; btc = 1,3,5-benzenetricarboxylate)$;
- $[Zn_2(bdc)_2(dabco)](dabco = 1,4-diazabicyclo[2.2.2\}oc\tan e)$;
- $[Mn(HCOO)]$;
- $[Cu_2(pzdc)_2(pyz)](CPL-1;\ pzdc = pyrazine-2,3-dicarboxylate;\ pyz = pyrazine)$

These MOFs were coated on supports and substrates such as silica, porous alumina, graphite, organic surfaces, self assembled monolayers (SAMs).

The film is usually grown by immersion of the selected substrates into specifically pre/treated mother liquors of the particular MOF material. The results were more or less densely packed films. Another way of making films is the layer by layer method in which an almost atomically flat and very homogeneous film is obtained. In this method there are individual growth steps separated by removing unreacted components via rinsing the substrate with the solvent[13], [20].

Two great challenges have to be faced when trying to create a MOF film. On the one hand, deposition or growth of MOF thin films, on substrates, should be ideally dense, homogeneous and oriented. On the other hand, MOF nanocrystals must be carefully prepared in terms of size, shape and surface funcionalization.

The deposition of MOF-5 coatings on alumina, silica and carbon substrates was performed by *Hermes et al* [21]. *Zacher et al* did a related study with HKUST-1 at 120 ^{o}C directly from the solvothermal mother solutions [22]. Using alumina supports the results obtained were better than silica which suggests that there is an obvious requirement of a basic electrostatically compatible surface for anchoring MOF-5 or HKUST-1. This requirement was not observed in case of $[Zn_2(bdc)_2(dabco)](dabco = 1,4-diazabicyclo[2.2.2\}oc\tan e)$.

Another study of *Yoo and Yeong* revealed a rapid deposition of MOF-5 on carbon coated anodic aluminium oxide (AAO) [23].

Gascon *et al* did a seeding approach for HKUST-1 and obtained dense coatings [20].

Other articles were more focused on oriented crystallization, such as the work of *Arnold et al* which is related to the crystallization of $[Mn(HCOO)]$ on porous alumina and graphite [24].

The first examples of pure phase MOF thin films showed a promising morphology. However a more detailed characterization of the adsorption properties of the films or coatings in comparison to the known bulk materials is needed [24], [13].

In *Gascon et al* work it was first tried to understand how they should control the size of the crystals and the nucleation velocity. To achieve this, some factors which might influence the synthesis, such as temperature and time, were maintained while varying the concentration of reactants. The results suggested that the synthesis should be performed with diluted solutions in order to have small crystals and controlled layer growth [20].

For the deposition of crystals on α-alumina supports, α-alumina disks were soaked in mother liquor followed by hydrothermal synthesis. This resulted in very poor densities, because nucleation and crystallization take place in the solution rather than on the support. To improve crystallization on the support, dipcoating with a dispersion of 5 microns $Cu_3(BTC)_2$ crystals in water was performed before hydrothermal synthesis and the results were much better [20].

Catalysis with MOFs

After coating monoliths with MOFs the following step was to prove its catalytic performance.

It has been 20 years since heterogeneous catalysis has been proposed for the first time as an application for crystalline MOFs [25] and 15 years since it was firstly demonstrated [26].

In 1994, the shape-specific catalytic activity for the cyanosilylation of aldehydes over $\left[Cd(NO_3)_2(4,4'-bpy)_2\right]_n$ was achieved although the structure did not survive after solvent removal [26].

Despite being strange that only now this field is truly explored, this can be explained by the need of understanding some principles about MOFs synthesis prior to test its potential applications [10], [12]. A list with the great majority of catalytic MOFs as well as the catalyzed reaction is given in Table 4 - Appendix 1.

Several types of catalytic systems or active sites have been used in MOFs applications.

Some groups have reported the synthesis of homochiral metal-organic frameworks useful for enantioselective reactions [12, 27], [28], [29], [30]. Particularly in [27] a pyridine functionalized derivative of tartaric acid and Zn (II) synthesised POST-1, a 2 D MOF, half of the six pyridine are coordinated by the zinc ions and the other protonated and directed toward the interior channel - Figure 7. These latter ones, when neutralized catalyze transesterification reaction in an enantioselective manner by deprotonation of the reactant due to the non-coordinated pyridil groups [10].

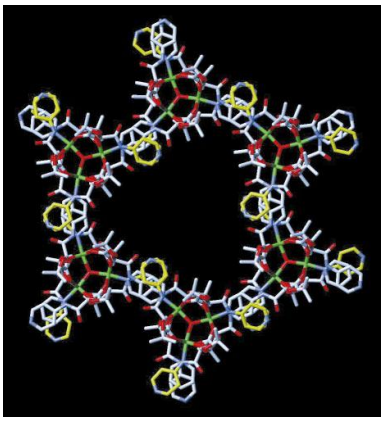

Figure 7- A hexagonal large-pore structure of POST-1 with trinuclear secondary building units.Three pyridyl groups pointing to the pore, Zn atoms in green, oxygen in red, nitrogen blue, C atoms in white and C atoms in pyridil groups In yellow [27].

Among others we can cite Lin and co-workers, as well as Hupp, Bu, Morris, Rosseinsky, Kim and Zheng research groups, being the latter who demonstrated that a synthesis of a homochiral compound could be made using totally achiral ones [31]. Although they are inferior to zeolites in terms of thermal or hydrolytic stability, this kind of catalyst is particularly interesting for the production of optically active organic compounds. However, the success achieved with the synthesis of homochiral frameworks is very limited specially because few are the cases reported where the MOF has maintained its structure after solvent removal [12], [31], [32] [33] . A review about this topic was published this year elsewhere[31].

The most common catalyst system is metal ions or ligands in Metal-Organic frameworks although most of the time they are only chosen as building blocks rather than as catalysts [12].

The first catalytic reaction reported [26], the cyanosilylation, used the metal Cd (II) as active site , with Lewis acid catalysis occurring via substrate displacement of axially coordinated water molecules. Also a pioneering work on phosphonates was done by Clearfield also showing a Lewis acid character [34], [35], [36] of Palladium, Pd (II) in alcohol oxidation, olefin hydrogenation, and Suzuki C-C coupling [37]. Moreover, MOF-5 proved to be selective as an alkylation catalyst with its Zn_4O nodes, for the Friedel-Crafts tert-butylation of both toluene and biphenyl [38]. Other examples include $Cu_3(btc)_2(H_2O)_3$ also known as HKUST-1, *Hong Kong University of Science and Technology*, in the cyanosilylation of benzaldehyde and acetone [39], and the anhydrous version in isomerization of α-pinene oxide, cyclization of citronellal, rearrangement of α-bromoacetals [40]. Reactions which require stronger Lewis acids such as Mukiyama aldol reaction have also been catalyzed by a MOF, $Mn_3[(Mn_4Cl)_3BTT_8(CH_3OH)_{10}]_2$ as well as an alkene oxidation, although there was some degradation after a few dozens of turnovers [41].

Although most of catalytic activity belongs to the inorganic component of the MOF, there is some work concerning the catalytic activity of the organic one. For instance a three dimensional coordination network using a tridentate amide ligand as the three connector part, {[Cd(4-btapa)$_2$(NO$_3$)$_2$]·6H$_2$O·2DMF}*n*, avoid hydrogen bond formation with amine groups and so the amine groups could act active sites. This framework, with pores of molecular dimensions catalyzed the Knoevenagel Condensation of benzaldehyde with maloninitrile [42].

In addition to this ones, also, Diels-alder Reaction [43], hydrogenations [44], esterifications [45], CO oxidation [46], photocatalysis [47] and basic catalysis [14], have been published.

Another method suggested for application MOFs in catalysis involves encapsulation of species. Both molecular catalysts and clusters have been encapsulated in MOFs.

Regarding the encapsulation of molecular catalysts, an unusually robust framework, $[In_{48}(H\,\mathrm{Im}\,DC)_{96}]$, rho-ZMOF has been proved to facilitate the oxidation of cyclohexane to cyclohexanol and cyclohexanone using tert-butyl hydroperoxide oxidant (TPHP)[48] Figure 8.

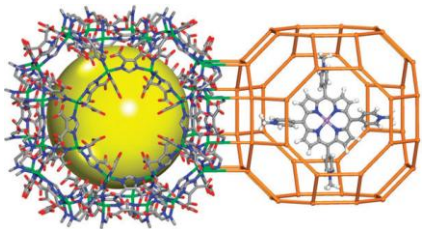

Figure 8 - The pore structure of rho-ZMOF (left) and the encapsulated $[H_2TMPyP]^{4+}$ porphyrin in rho-ZMOF α-cage (right). Solvent molecules and hydrogen atoms are omitted for clarity [10]

The cavities of the MOF are sufficiently large to encapsulate porphyrins, but the pores are too small to enable its exit, being encarcerated [10]. Loadings of >60% were achieved and base could be metallated subsequently with manganese, cobalt, zinc or copper ions.

The controlled growth of catalytic clusters or nanoparticles within MOF cavities is attractive but difficult to prove [10]. A proven example was the electrostatic encapsulation of keggin type polyoxometallates within MIL-101 [15]. Another example reported, is about encapsulation of the metal complex $[Mn(phen)_2(H_2O)_2]^{2+}$ into supramolecular frameworks through hydrogen bonding and $\pi-\pi$ interactions. This metal complex in supramolecular porous framework revealed size and shape selective catalytic activity in the oxidation of phenols with oxygen peroxide to form dihydroxibenzenes [29], [49]. Another oxidation process is facilitated with these active sites, the oxidation of α-pinene to the corresponding alcohol and ketone using hydrogen peroxide oxidant or oxygen depending on the keggin substituted ions, titanium or cobalt, employed in the cluster of the Metal-Organic Framework, such as MIL-101 [50].

Another type of catalyst systems in MOFs known so far is highly dispersed metal or metal oxide nanoparticles loaded into porous MOF host lattice. The work found in this area is even scarcer. It has been proved that Pd and Pt phosphonates were active catalysts for the photochemical production of hydrogen [51] and the production of hydrogen peroxide from streams of hydrogen and oxygen [52], [53]. On the other hand, it has been demonstrated that metal-organic chemical vapour deposition led to inorganic particles in MOF-5 which were moderately active for methanol synthesis and hydrogenation of cycloctene [49].

Post-Synthetic Modifications

For functionalization of MOFs, techniques involving Post Modifications are also becoming common. Post synthetic modifications are conceptually not new, not only they have been applied in carbon nanotubes, zeolites and mesoporous silica or organosilicas but also in MOFs [54], [25]. Nevertheless, it

took one decade to prove a covalent bond which was already cited due to its application as homochiral catalysts [27]. A covalent bond by post modification has also been achieved in IRMOF-3 by acetylation for targeting the amino groups of IRMOF-3 with acetic anhydride [55], latter the scope of its application has been enlarged for reaction with larger acid anhydrides [56] and using isocyanates as the modifying agent [57].

Other types of post synthetic methods include protonation and coordinative interactions. Non covalent interaction, with ion exchange and guest removal, and doping with metals are also cited as post synthetic methods but with less catalytic importance[54].

In what concerns the coordinative interactions as Post synthetic method used for functionalizing MOFs for catalysis, a homochiral porous MOF built from Cd(II) and BINOL (BINOL=1,1'-bi-2-naphthol) was treated with $Ti(O\mathit{i}Pr)_4$ and catalyzed the addition of $ZnEt_2$ to 1-naphthaldehyde, which affords (R)-1-(1-naphthyl)propanol. Later on it has been shown that the modified homochiral MOF also catalyzes addition of ZnEt2 to other aromatic aldehydes with conversion values similar to a comparable homogenous catalyst. It also has a remarkable size selectivity, and substrate conversion was found to decrease as the size of the aldehydes increased, indicating a true heterogeneous catalytic process [29].

MIL-101 (Cr) Catalytic Applications

MIL-101 (Cr) has found catalytic applications as Lewis acid, by coordinatively unsaturated sites (CUS) Cr(III) species, surface grafted amine species and encapsulation.

As these water molecules coordinated in MIL-101 (Cr) can be easily removed, Cr (III) sites that act as lewis active sites can be obtained. This approach has been applied in cyanosilylation reactions [10], [9].

Moreover its CUS Cr (III) species (Lewis acid sites), providing accessible sites for guest molecules showed oxidation ability of aryl sulfides to selectively produce the corresponding sulfoxides in the presence of hydrogen peroxide [3].

Successful immobilization of a Keggin heteropolytungstene was also achieved and the electrostatical attachement of a polyoxometalate (POM) such as Co and Ti monosubstituted Keggin-type heteropolytungstate was reported. These materials showed good activity and selectivity in the liquid phase oxidation or epoxidation of alkenes such as cyclohexene, α-pinene and caryophyllene with O_2 and H_2O_2.[50], [17].

MIL-101 (Cr) has also showed activity as basic catalyst when is treated with a number of organic multifunctional amines, after dehydration. Catalytic activity performance has been tested in Knoevenagel condensation reaction (base catalyzed model reaction). The bases grafted wee ED, ethylenediamine, DETA, diethylenetriamine and APS, 3-aminopropyltrialkoxysilane. ED-MIL-101 (Cr) presented conversions of 97.1% and selectivities ou 93.5%. The APS-MIL-101 (Cr) showed higher activity than when grafted in mesoporous silica [59].

MIL-101 (Cr) was also tested in acid catalysis after functionalization with SO_3H for the esterification of acetic acid with ethanol at 100 ºC. The functionalized MOF has 70.1% of conversion while with just the MOF 24.7% [3].

Besides this, Pd loaded APS MIL-101 and ED-MIL-101 exhibit high activities during the Heck reaction at 120 °, the most powerful method to couple alkenes with organic molecules. It also showed an activity similar to the Pd/C catalyst in the coupling reaction of acrylic acid with iodobenzene [60].

This project intends to be innovative because MIL-101 (Cr) was never coated on monoliths not even MOFs have been coated in that type of support.

Apart from this it was decided to perform test reactions using MIL-101 (Cr), in powder samples, grafted with two different bases and then some reactions with monoliths were tried.

3 Interfacing MIL-101 (Cr) with monoliths – Precursor Impregnation

3.1 Introduction

Monolithic catalyst supports are an attractive option for conventional carriers in heterogeneous catalysis.

Monoliths have several operational advantages such as energy input, efficiency, safety and catalyst separation. Their disadvantages are mainly the lower catalyst loadings (which can be compensated by the higher catalyst efficiency) and the catalysts replacement.

Concerning their intrinsic properties monoliths have a high mechanical strength, can stand high temperatures and temperature shocks as they have a low thermal expansion coefficient. On the other hand, the open structure makes the system less sensitive to fouling. However, they present a low BET (Brunauer-Emmett-Teller) specific surface area. That is the reason why it is usual to coat the monoliths with other materials such as Alumina, silica or carbon, which have high surface areas but low mechanical strength, establishing an optimal compromise using the best of both systems.

Cordierite, a ceramic material consisting of magnesia, silica and alumina in the ratio 2:5:2, was chosen due to the high thermal stability and low expansion coefficient comparing with metallic monoliths [61].

In order to start a first approach in coating monoliths with MIL-101 (Cr) some basic techniques were tested, as the interaction between Metal-Organic Frameworks and monoliths was never tried before.

The synthesis of MIL-101 (Cr), like most of the synthesis of metal-organic frameworks, is carried in solvothermal conditions using a solution containing both the organic and inorganic precursor. As a first trial in this project the inorganic precursor impregnation on the monolith was used, followed by synthesis. Both microwave and hydrothermal heating were tested, and characterization of the samples was performed. In order to be sure that the metal-organic framework obtained was, in fact, MIL-101 (Cr) further studies were done, involving another type of support: α-alumina disk.

The experimental procedure followed as well as the results achieved will be presented in the following topics.

3.2 Experimental Work

To interface MIL-101 (Cr) with monoliths, the first approach tried was the direct impregnation with Chromium oxide. The monolith chosen to do this test was Cordierite.

The cylindrical cordierite monolithic substrates had 5 cm of length and 1 cm of diameter, square channels and a cell density of 62 cells cm^{-2} (400 cpsi) and a wall thickness of 0.18 mm).

The monoliths were immersed in a Chromium Nitrate nonahydrate solution and under continuous stirring for 2 days. The amount of Chromium Nitrate used in the solution was that which could lead to 20% of the monolith final mass corresponding to Chromium Nitrate (or 10% in case of α-alumina disks). The water added to make the solution should be 20 mL per gram monolith.

After these two days the water is evaporated[1] from the solution and the monolith or the disk calcinated at 500 ºC for one hour, using a temperature ramp up to 500 C during 9 hours..

The monoliths were then impregnated with Chromium oxide; the following step was to perform a synthesis using it as inorganic precursor.

The standard conditions normally used to synthesize MIL-101 (Cr) are 1,63 grams of Chromium (III) Nitrate, $Cr(NO_3)_3 \cdot 9H_2O$ (97%); 0,7 grams of Terephthalic acid, $C_6H_4 - 1{,}4 - (CO_2H)_2$ (97%); 0,20 grams of Hydrofluoric Acid, HF (40%) and 20 grams of water (adapted from [18]).

The microwave synthesis took 2 hours at 180 ºC with an initial ramp of 32 degree per minute. Regarding the hydrothermal synthesis it was performed during 8 hours at 220ºC in a Static oven.

The synthesis of MIL-101 on the monolith surface or on the α-alumina disks was done in a similar way as that used with powder samples, maintaining the same stoichiometric ratios between each reactant, and admitting that the difference in the monolith weight before and after the impregnation was due to the Chromium Oxide.

Moreover, it is important to note that in this case Chromium Oxide, Cr_2O_3, was used instead of Chromium (III) Nitrate, $Cr(NO_3)_3 \cdot 9H_2O$, so that the quantity of inorganic precursor was adjusted in order to have the same amount of chromium.

After the synthesis in monoliths or α-alumina it is important to perform some washing procedures which were done in a similar way to that reported for the powder and which are more detailed in the following section.

3.3 Impregnation of Chromium Oxide as Precursor on Cordierite

This was the first technique tested in order to interface monoliths with MIL-101 (Cr).

The major goal was to grow crystals preferentially on the support, avoiding crystallization on the solution and this was thought to be achieved using Chromium Oxide instead of Chromium Nitrate nonahydrate due to questions related with solubility in water.

Following the procedure mentioned before, in the process of impregnation we were first generating Chromium Hydroxide and then Chromium Oxide.

$$Cr(NO_3)_3 \cdot 9H_2O \xrightarrow{evaporating\ water} Cr(HO)_3 \xrightarrow{Calcinating} Cr_2O_3$$

[1] Some experiments were also performed without evaporating the water but after calcination it was realised that the coating was preferably on the surface and not on the channels so, this procedure was not taken for the following steps. That occurrence was already studied in [62]

Both Chromium (III) Nitrate and Chromium hydroxide are soluble in water, especially at lower pH, while Chromium Oxide is more difficult to dissolve. Thus, when introducing Terephthalic acid, water and hydrofluoric acid, the crystals would grow next to the chromium source, which, because of its low solubility, would be on the monolith surface.

To analyze the efficiency of this method, several characterization tests were performed in order to guarantee that MIL-101 was actually being synthesized.

Besides that, characterization methods could also give an idea about how much MOF is coated on the monolith. This latter information has a crucial importance for performing the catalytic tests that this project is proposed to pursue. To evaluate the performance of any catalyst, information about its amount or its active sites amount must be known.

Characterization of the new materials was essential to understand interactions and alterations in MOF structures.

The methods used during these research were Physical Adsorption (Nitrogen Adsorption), X-Ray Diffraction (XRD), Thermo Gravimetric Analysis (TGA) and Scanning Electron Microscopy. More details about the methods applied can be found in Appendix 2 and a brief summary about the characterization performed in each sample is shown in Table 5 of the same appendix.

Microwave Synthesis

Starting with SEM analysis, the results obtained by this technique were pretty satisfactory Figure 9 and Figure 10.

a) 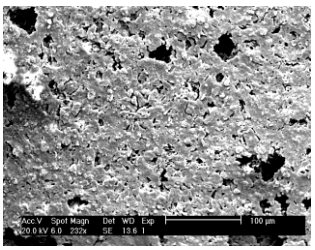

b) 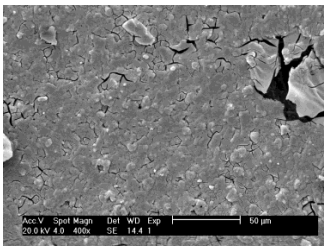

c) 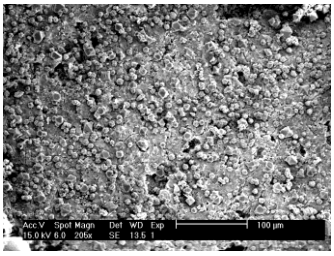

Figure 9 – SEM micrographs of a) monolith (Cordierite), b) monolith with chromium oxide, and c) Monolith with MIL-101 (Cr)).

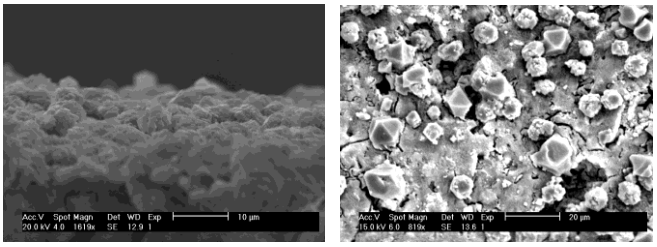

Figure 10- SEM micrographs of the layer obtained.

With these pictures it can be seen that some crystals grew on the surface although the coating was not very homogeneous and seemed to have different particle size.

After looking into the results of SEM characterization and suspecting that these differences in particle size could be due to the hot spots that usually occur under microwave heating, it was decided to also test the results of a coating followed by a hydrothermal synthesis.

With these samples, it was also necessary to continue with characterization.

To guarantee that we are in the presence of MIL-101, the XRD seemed to be the proper choice. In order to apply this technique and enable a XRD pattern beginning in 2θ equal to 5, there was a need to mill the samples and analyze them as powder. Nevertheless the results were not conclusive, probably because the amount of MIL-101 (Cr) was too small compared with the amount of cordierite, the inconclusive XRD pattern is presented in Appendix 3

In order to quantify the amount of MOF coated on the monolith and further perform the catalytic tests, nitrogen adsorption was performed with the monolith, the monolith with chromium oxide and the monolith with MIL-101 (Cr). In the isotherms obtained, as can be seen in Figure 11, the increase in the volume adsorbed was not sufficiently high to be accurately quantified. However, the sample coated with MOF adsorbed more N_2 than the rest, which is indicative of the MOFs presence.

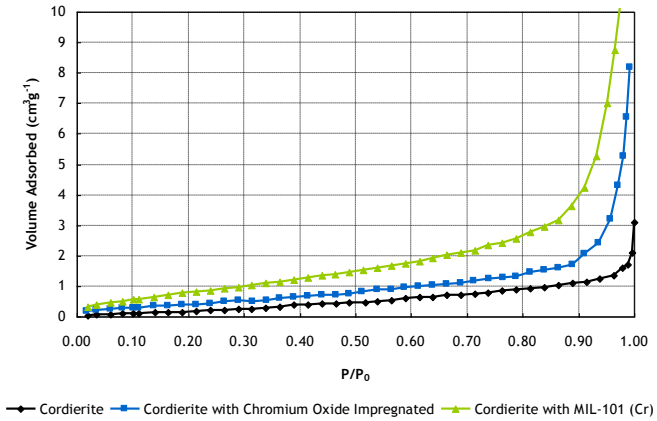

Figure 11 - Isotherms obtained for the monolith, monolith with Chromium Oxide impregnated, monolith with MIL-101 (Cr).

As nitrogen adsorption was not successful in detecting the MIL-101(Cr) amount in the monolith the next step followed was Thermo Gravimetric Analysis (TGA), which can also be useful in detecting the identity of the crystals, shown in SEM micrographs.

At the beginning it was decided to do the analysis in helium and using a heating rate of 10 degrees per minute up to 600 °. The TGA results suggested the presence of MOF, MIL-101 (Cr), as there was a decrease in the total mass which was not present in samples of the monolith and monolith with Chromium Oxide Impregnated. On the other hand the temperature at which the mass started decreasing is more or less the same that was observed with the MIL-101 (Cr) powder samples, according to the literature and some studies with particles shown in the next section.

However, the behaviour was far from perfect and there were still some doubts left. The temperature at which the mass starts decreasing was slightly lower than the observed for powder samples and also after around 500 ºC it was expected to see a clear plateau which is not present at all. Although the mass of monolith is also less than before, the decrease is not sufficiently high to justify the absence of a plateau Figure 12.

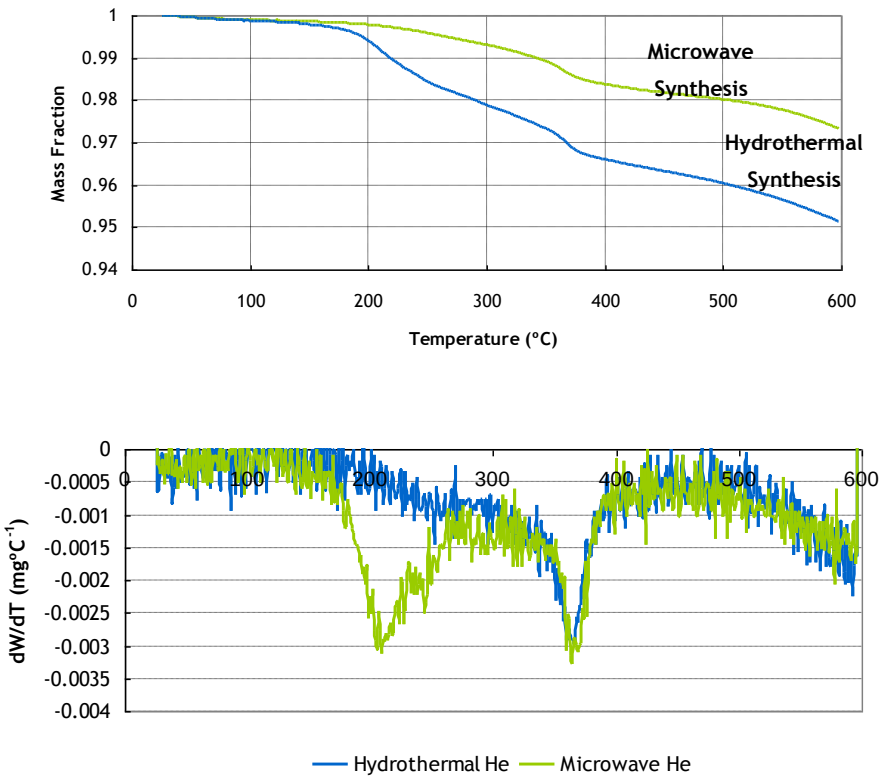

Figure 12 - TGA results for monolith with MIL-101 (Cr) both with microwave and hydrothermal synthesis and its derivative.

Besides this, another general observation that can be done is that the amount of a possible MIL-101 (Cr) obtained is not high enough to be subsequently used for catalytic applications.

Hydrothermal Synthesis

After analyzing SEM characterization, as it was said before, it was decided to do a hydrothermal synthesis in order to compare the crystals size and the coating obtained.

The SEM analysis was not as clear as it was desired. Although the surface did not have the same appearance as a monolith impregnated with Chromium Oxide, it was not possible to see any crystals.

Experimentally some difficulty was also detected in washing the MOF linker, and the colour of the monolith at the end was not homogeneous. Although the results were not the best, in the figure below, it can be seen the monolith appearance after MIL-101 synthesis by SEM characterization.

a) 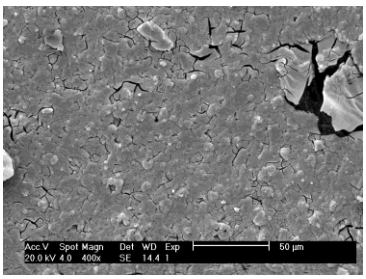

b) 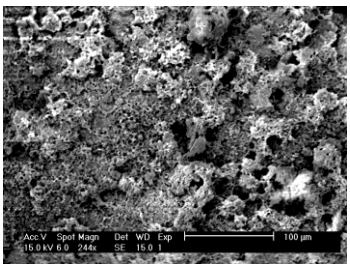

Figure 13 -SEM micrographs of the monolith impregnated with Chromium Oxide - a), monolith after hydrothermal synthesis of MIL-101(Cr)-b).

The XRD pattern obtained with this sample is also present in Appendix 3. Once again it was inconclusive although there was some trend in crystallinity, with a peak that was not present in the other samples without synthesis. Moreover, the Cordierite typical peaks at 2 theta equal to 10 it seems that there is some interference of two peaks but these observation pattern were not sufficiently clear to affirm that we are in the presence of MIL-101 (Cr).

The TGA results are presented in the Figure 12, to make a proper comparison among samples it was represented in the same graph as the microwave results.

Performing a hydrothermal synthesis, the same doubts about the temperature at which the mass started decreasing and the absence of a final plateau persist, although the amount of mass lost was greater. Possibly this can suggest that with a hydrothermal synthesis there are more crystals growing onto the monolith surface.

3.4 Impregnation of Chromium Oxide as Precursor on α-alumina disks

Although it was possible to see crystals after synthesis of MOFs, it was impossible to have a proof that using chromium oxide as inorganic precursor, instead of Chromium Nitrate, it was possible to synthesize MIL-101 (Cr).

In order to find an alternative route to ensure which crystals were being synthesized, two different tests were done: performing a synthesis in the standard conditions but using chromium oxide particles and selecting a different support, α-alumina disks and follow an identical experimental procedure.

α-alumina disk was the most attractive support to do these tests. Apart from its flat surface, which enables its characterization by XRD without the need of smashing the sample, it was also attractive to test the interaction with this substrate because it could be useful to do a wash-coat of the monolith with α-alumina.

The first test done, trying to synthesize MIL-101 (Cr) particles using Chromium Oxide in powder, did not lead to conclusive results, as can be seen in Appendix 4.

Regarding the tests using disks of α-alumina, after 2 hours of microwave synthesis it was not observed any layer on the surface although some crystals seemed to be growing – Figure 14 a). Because of this general observation, a secondary nucleation was done, during more ten hours of synthesis.

With 10 hours of synthesis, deposition of big crystals on the surface was clearly observed – Figure 14 b).

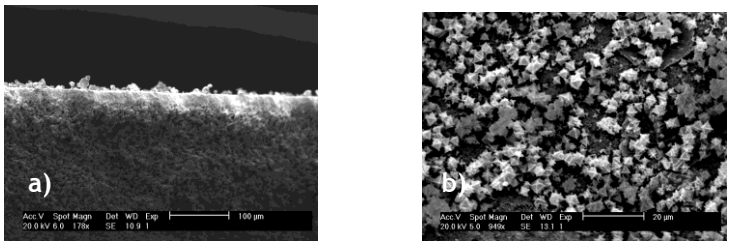

Figure 14 – SEM micrographs of a) α-alumina disk after2 hours of direct synthesis; b) α-alumina disk after a secondary growth during 10 hours.

These results were satisfactory. Nevertheless, an XRD analysis was essential in order to guarantee that it was MIL-101 (Cr) that was on the surface – Figure 15.

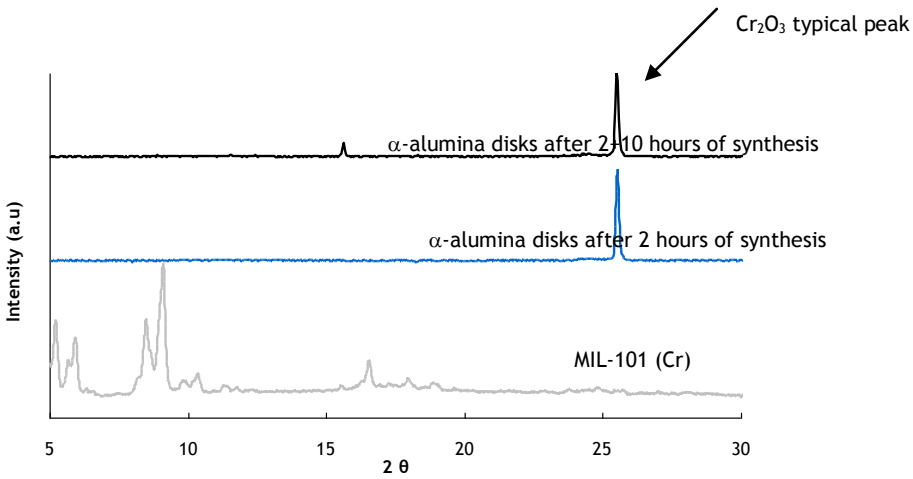

Figure 15 – XRD patterns of α-alumina disks after direct synthesis with impregnation of Chromium Oxide; α-alumina disk after a secondary nucleation during 10 hours.

As it can be seen, after two hours of synthesis the pattern was exactly the same as the Chromium Oxide Pattern. After the secondary nucleation a peak appear near the region where it was supposed to be for MIL-101 (Cr). However, as the major peak is absent we cannot conclude that this interfacing method is suitable.

4 Interfacing MIL-101 (Cr) with monoliths - Seeding Techniques

4.1 Introduction

For interfacing Metal-Organic framework with monoliths another technique was tested using a monolithic seeding with some crystals followed by a secondary growth.

The best match between substrate and the crystallizing solute exists when it is in fact a seed crystal of the solute. Nucleation of new crystals induced only because of the prior presence of crystals of the material being crystallized is termed secondary nucleation.

When some crystals are already adhered to the surface crystals tend to grow preferentially there rather then in solution, generating always new nuclei [63].

Although in some particular situations a seeding can be done directly on the support, in this case, a previous monolith wash-coating with α-alumina was needed to cover the cordierite big pores, as it will be discussed later.

So, a study about the interaction between a-alumina and MIL-101 (Cr) was needed as well as a decision about the most appropriate particles to be used as seeds.

Moreover, as it was desired to do an α-alumina wash coat, two different techniques were tested, differing essentially on the temperature of the α-alumina coating calcinations and the total time of secondary growth preparation.

4.2 Experimental work

The experimental work for this part is divided in three sections

- Preparation of the most appropriate nanoparticles
- Interfacing MIL-101 (Cr) with α-alumina disks by dip coating and spin coating
- Interfacing MIL-101 (Cr) with Cordierite wash-coated with α-alumina

Preparation of the most appropriate nanoparticles

The Metal-Organic Framework synthesis strongly depends on temperature for the coordination of metallic species, nuclearity and dimensionality of the inorganic framework. An increase in temperature favors the condensation of supplementary metallic polyhedra on the starting cluster, and then a change into chains, then layers of inorganic polyhedra occurs.

When synthesis is performed above 100 ^{o}C it is considered a hydrothermal synthesis. In this kind of synthesis, the dielectric properties of the solvent change, which result in a weakening of the interactions between the solvent molecules and therefore increasing its dissociation.

The parameters that have most influence on synthesis are: pH, concentration and temperature.

Solvothermal synthesis is the traditional way to obtain MOFs, however some new routes have appeared in the last years. One of them uses a mixture of non miscible solvents for the hydrothermal synthesis (heavy alcohols and water, for example) and then a solid forms at the interface of the biphasic mixture providing single crystals of the desired phase [12].

Besides that, another new way of synthesizing MOFs, particularly when there is copper involved is by an electrochemical route.

In this present project, for synthesizing nanoparticles, another route, different from the traditional solvothermal synthesis was also used - microwave synthesis. This method was already applied to dense solids and inorganic porous compounds. The major advantages of this method are lower crystallization times, phase selectivity, narrow particle size distributions, easy morphology control, and efficient evaluation of process parameters [12], [18]. The possibility of a synthesis in shorter times makes this way attractive for industrial scale production and a viable option.

Both MIL-100 and MIL-101 have been synthesized under microwave irradiation in less than one hour at 220 ºC. As this work is focused on synthesis of MIL-101 by microwave irradiation it was based on the method applied by *Jhung et al* with some slight deviations [18].

However, it should be noted that a new phase MIL-53 can be formed when increasing the synthesis time.

MIL-101 is synthesized from a mixture of 1,63 grams of Chromium (III) Nitrate, $Cr(NO_3)_3 \cdot 9H_2O$ (97%); 0,7 grams of Terephthalic acid, $C_6H_4-1,4-(CO_2H)_2$ (97%); 0,20 grams of Hydrofluoric Acid, HF (40%) and 20 grams of water.

The role of fluoride in this metal-organic framework has been under discussion. It possibly acts as a mineralizing agent to increase the crystallinity of the microporous materials and favors the formation of highly crystalline phases [64] Fluoride is involved in the terminal bond of the trimeric chromium species and partly substitutes the water molecules attached to Chromium. It is also suggested that the fluorine provides a strong interaction with chromium octahedral motif and the effective nuclei formation of MIL-101 (Cr). However, it should be noted that this issue is still under debate [3], [64].

The mixture is heated 2 hours at 180 ºC and once the synthesis is finished, the washing step start with the crystalline MIL-101 product in the solution. It is doubly filtered off using two glass filters with a pore size of 45 μm to remove the free Terephtalic Acid. Then a solvothermal treatment is sequentially performed using Ethanol 95% at 80 ºC for 24 hours. The resulting solid is soaked in 1 M of Amonium Fluoride (NH_4F) solution at 70 ºC for 24 hours and immediately filtered and washed with hot water. The solid is finally dried overnight at 150 ºC.

After synthesis the activation of MOF is important for obtaining materials with high surface areas and pore volumes[65]. The purification of MIL-101 (Cr) is still under development, being always synthesized with some organic and inorganic impurities in the pores as well as outside the pores. Terephtalic acid, having a low solubility in water and being the solvent of the synthesis, is a compound that highly contributes to these impurities.

The method for purification used during this project is based on [15] and comprises a three step process using double filtration, solvothermal treatment with ethanol and NH_4F and hot water. The use

of NH_4F is thought to be effective because the co-ordinated terephthalate anions probably exchange with fluoride anions and might be easily removed from the pores through the formation of ammonium terephthalate soluble in water[3]. Moreover, it is also believed that these treatments are also effective in the removal of inorganic species such as chromium hydroxide trapped in the pores, similar to what has been previously reported for MOF-5 [66].

To prepare the most attractive nanoparticles, a basic study about the influence of concentration has been done varying the standard condition from twice concentrated to 2.5 times diluted, by changing the quantity of water added to the autoclave.

Interfacing MIL-101 (Cr) with α-alumina disks by dip coating and spin coating

The secondary growth technique has been proved to be successful for the synthesis of MOF coatings on α-alumina substrates [20]. This method consists on coating the disks surface with some crystals of the desired MOF and then performing a secondary nucleation, with exactly the same synthesis procedure described before.

For the present work, a nanocrystals seeding is desired and two different techniques were performed: Spin coating and Dip coating.

Spin coating is a technique used to develop thin films on flat substrates. A certain amount of solution is put on the disk surface and then rotated at high speed in order to spread the fluid by centrifugal force – Figure 16. To apply this technique, a solution of the nanocrystals selected, those synthesized with 50 mg of water, was prepared using ethanol as a solvent.

Dispersion was prepared by sonicating a solution of 100 mg of crystals and 100 mL of ethanol during 12 hours. This sonication is needed in order to avoid as much as possible the agglomerates of particles, and ethanol was chosen as a solvent because of its volatile character which enables its evaporation during the rotation of the disk.

The equipment used was a SPS Spin 150 Spincoater at 1500 rpm. Ten drops of the solution were placed on the disk before rotating it, and this procedure was repeated five times for each disk.

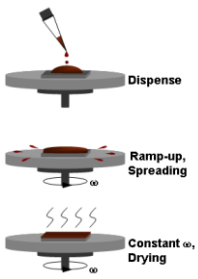

Figure 16 - Schematic representation of spin coating technique [67].

Dip coating technique is slightly different from the spin coating as it does not involve any centrifugal force. In this technique the substrate is immersed on the solution containing the seed material at a constant speed - Figure 17.

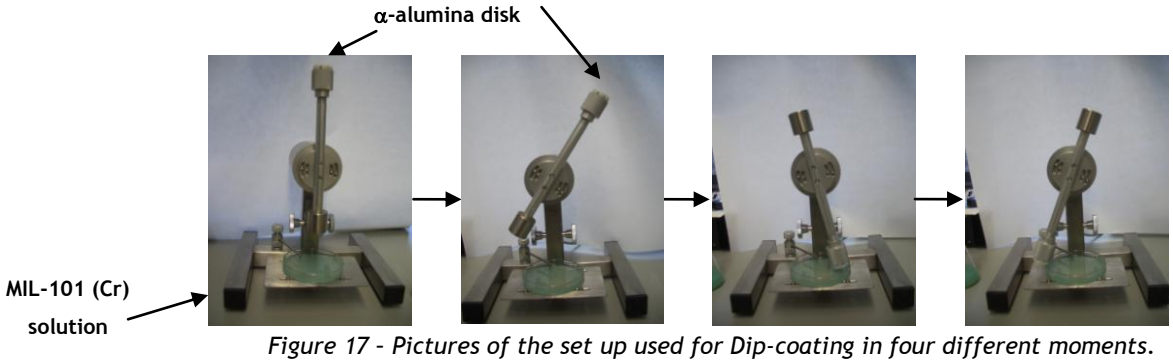

Figure 17 - Pictures of the set up used for Dip-coating in four different moments.

Then it remains fully immersed and motionless to allow the coating material to soak the disk and then it is withdrawn with constant speed too. This procedure was repeated 10 times. The seed solution was also a solution of MIL-101 (Cr) nanocrystals synthesized with 50 mg of water, after immersing in ethanol and sonication for 12 hours.

Polished asymmetric α-alumina disks (25 mm in diameter, 2 mm in thickness, top layer pore size 80 nm, and support layer pore size150 nm) supplied by Pervatech were used as supports. The α-alumina disks used in both spin and dip coating had the same characteristics as those used for direct impregnation with Chromium Oxide.

After seeding, a secondary nucleation is performed placing the support in a Teflon holder and immersed vertically inside a Teflon insert containing the synthesis solution. This position of the disk was adopted in order to avoid precipitation on the disk surface.

The synthesis conditions are the same as for particles synthesis, (2 hours at 180 ºC in microwave and 8 hours at 220 ºC in hydrothermal synthesis) but using 25 mL of water. For the hydrothermal synthesis the support and the synthesis solution are heated in a stainless autoclave. After the synthesis the cleaning procedure is done in the same way that is reported for the powder, without the consecutive filtration steps and being immersed in Ethanol at 80 ºC for 24 hours under reflux and in NH_4F at 70ºC for another 24 hours. After that it is activated overnight in a oven at 150ºC.

Interfacing MIL-101 (Cr) with Cordierite wash-coated with α-alumina

After observing a good interaction between α-alumina and MIL-101 (Cr) and in order to block the macropores of cordierite, as it will be explained latter on, it was decided to do a preliminary wash coating with α-alumina. The monoliths used during this stage were the same as reported in section 3.2.

Two different methods were followed and named Procedure A and B for convenience.

Procedure A was based on [68]. The criteria used to select the most convenient method were: having the highest amount of α-alumina deposited, and enabling a complete blocking of the cordierite macropores with only one coating step.

First a solution containing 50% of water and 50% of α-alumina (pores of 0.1 micrometer) was prepared under continuous stirring. Then, the cordierite monoliths were immersed on both NaOH (0,1 M) and the α-alumina solutions. After that the monoliths were flushed with a flow air (air knife) and dried under rotation at room temperature during 12 hours. The following step was calcination, which

was performed using an initial heating rate of 2 degrees per minute up to 1000 ºC, and then the calcination takes place during four hours.

After having the monoliths wash-coated with α-alumina a deposition of the active phase had to be done. In order to simulate a spin coating on the monoliths, which is not possible, due to its non flat geometry, first it was done a dip coating leaving the monoliths under stirring in a seeding solution (similar to the one used for the disks) for 1 hour. After that a vacuum treatment was performed, during another hour, in order to fix the crystals, as it happens in the disks. Then, the solvent, ethanol, is removed, in an oven at 100 ºC.

Thus, the monoliths were already ready for the secondary growth. The synthesis was performed in static and rotatory ovens and the conditions were exactly the same as the ones used for the secondary growth in disks with the only difference in the temperature used in rotatory oven. In this case, the temperature was 200 ºC instead of 220ºC due to equipment limitations. Once more the cleaning procedure was identical.

The procedure B differs essentially in the way of seeding. For this procedure, the strategy followed was preparing an initial suspension of α-alumina and seeds and then proceeding in exactly the same way as for procedure A but without the seeding step and with the heating up to 370 ºC

4.3 Preparation of the most appropriate nanoparticles

After performing the synthesis, washing the samples obtained (in order to remove the linker, terephtalic acid) and activating the catalyst the first distinctive difference detected among the samples was that the greater the amount of water added, the finer was the powder obtained. With these results we tended to conclude that the most diluted conditions were the most suitable for performing the coating or seeding in monoliths.

Furthermore, when performing the synthesis in conditions twice more concentrated than the standard, it seemed that the synthesis did not occur because the liquid kept its deep blue colour and we could not filter any powder.

It was also observed that we seem to have more MOF production with the diluted samples; however that must be confirmed because that can be due to density effects.

The SEM micrographs of MIL-101 produced with different quantities of water revealed an agglomeration of crystals, which was consistent with the results presented in some previous work [18] also done with microwave synthesis. It seemed also that we need a higher magnification in order to clearly see the crystals –Figure 18.

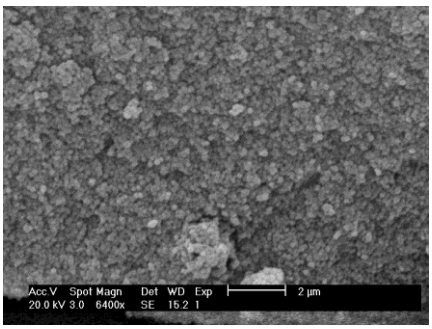

Figure 18 - SEM micrograph of MIL-101 (Cr) obtained with samples 2.5 more concentrated than the standard conditions.

Before proving the relation between the concentration of the reactants and the particle size, it was important to perform a characterization of the samples to see if it was consistent with the MIL-101 reported in the literature.

The isotherms obtained with physical adsorption are presented in Appendix 6, just to check that they were very similar for the different concentrations. As an example it can be seen in Figure 19 the isotherm obtained for the sample with the standard conditions diluted 2.5 times.

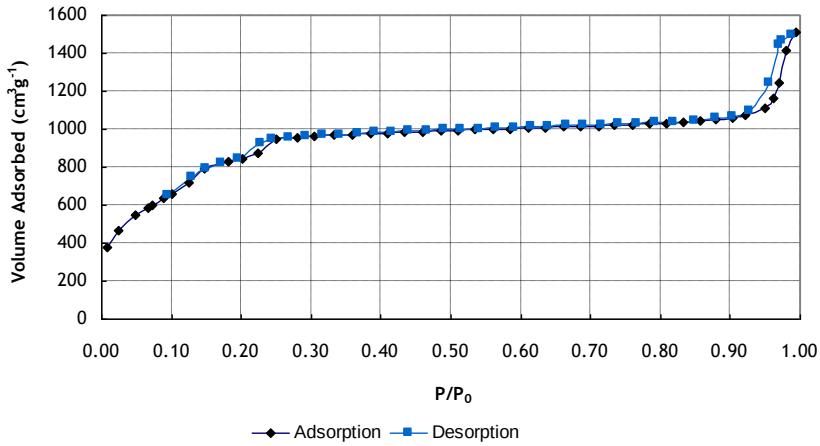

Figure 19- Nitrogen Adsorption Isotherm of the sample synthesized with the standard conditions 2.5 times diluted (blue line-desorption curve; black line-adsorption curve).

The isotherms show the typical shape of the MIL-101, [15] with the two typical steps at the beginning which have previously been attributed to the presence of two mesoporous cages [18]. The isotherms also show a hysteresis loop at high relative pressure that is attributed to the adsorption in the interparticles space, due to the small particle size.

With the values of uptake shown in the previous figure and in appendix the BET surface area was calculated using the figures of partial pressures between 0,05 and 0,25, see Appendix 6 for the method description. To estimate the microporous volume, the method followed was the t method –Appendix 8. The results are presented in Table 1.

Table 1 - BET surface area and Pore volumes calculated for each sample prepared.

	S_{BET} (m^2g^{-1})	$V_{micropores}$ (cm^3g^{-1})	$V_{mesopores}$ (cm^3g^{-1})
Standard Conditions	3428.2	1.50	0.18
1.5 times diluted	3352.1	1.43	0.29
2 times diluted	3548.5	1.57	0.25
2.5 times diluted	3334.5	1.44	0.28

Although the BET surface area and the microporous volume are pretty consistent with the literature [15], [18], [69], concentration influence was not clear enough to lead us into a conclusion. And also the differences observed can be due to an inefficient cleaning of the sample, as this issue is still under investigation [3].

Also as a way to characterize the sample and know the identity of the crystals, the XRD pattern was obtained – Figure 49 in Appendix 9 – and proved to be consistent with the literature. The same happened in the TGA characterization. The curves present two steps, the first one due to the water loss (around 100 ^{o}C) and the second one corresponding to the organic part of the metal organic framework. As all the samples belong to the same compound, the behaviour is almost the same in each one.

This study about the most appropriate nanoparticles was essentially based on the crystal size obtained. This analysis was necessary in order to achieve the optimal crystals of MIL-101 (Cr) to be used as seeds for a secondary nucleation.

It was admitted that the smaller particles were the most suitable for seeding techniques because it is easier to obtain a good dispersion.

The general observation was that the highest amount of water (and thus the lower concentration of reactants) led to the finest particles. However more evidences about this conclusion were necessary.

Crystal size measurement was performed using Laser Scattering and solutions corresponding to synthesis with standard conditions, 2 and 2.5 times diluted. The solutions were prepared using powder previously synthesized suspended in ethanol and then subjected to sonication during one day.

Although these seemed to be the ideal method to know the real crystal size, the drawbacks encountered made it impossible.

Firstly, the method could induce us to an error conclusion because of the porous character of the material. Secondly, even after sonication for more than 12 hours the agglomerates still subsist and so a reliable analysis was not achieved.

However, a peak corresponding to the lowest values of particle diameter (and not agglomerates) showed a tendency of decreasing from the standard sample to the most diluted. In the latter the value of the peak corresponded to 140 nm, with values ranging from 40 nm to 500 nm, which were pretty consistent with the results obtained with SEM – Figure 20.

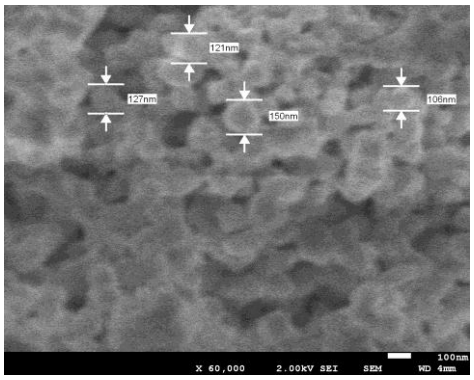

Figure 20 -SEM micrograph for powder samples synthesized 2.5 times diluted and a magnification of 60 000.

The decrease in particle size when the concentration is lower is related with the limited solubility of terephthalic acid in water. This synthesis reactant is probably present as suspended crystals during the MIL-101 (Cr) crystallization and the solvent mediated transformation of Terephthalic acid into MIL-101 (Cr) occurs. Because the organic linker is present as a crystalline material the concentration of terephthalic acid in the liquid is equal to its solubility. Thus, when the overall composition increases the quantity of organic reactant ready to be transformed in MIL-101 (Cr) does not increase. Therefore, solution conditions at different overall concentrations are quite similar. As the nucleation rates do not vary much for different experiments, the number of crystals is the same. At higher overall concentrations the same number of crystals has more material available for growth. Crystals from experiments at higher concentrations will therefore be larger.

As the SEM pictures for conditions 2.5 times diluted revealed particles in a range that was considered reasonable for performing the seeding techniques, these particles were selected to perform both dip and spin coating.

4.4 1st Step Interfacing MIL-101 (Cr) with α-alumina disks by dip coating and spin coating

Dip Coating

As it was already stated, dip coating coating technique was used to seed nanocrystals onto the α-alumina support surface. These crystals act as nucleation sites and enhanced the growth of more crystals.

After synthesis it is important to perform SEM analysis in order to see if a layer has formed on the surface and if it has the desired characteristics. These results are present in Appendix 10 (Figure 51) but were not sufficiently conclusive.

In order to have more objective results, a semi-quantitative analysis of the species present in the support surface was made in terms of atoms present – Figure 21.

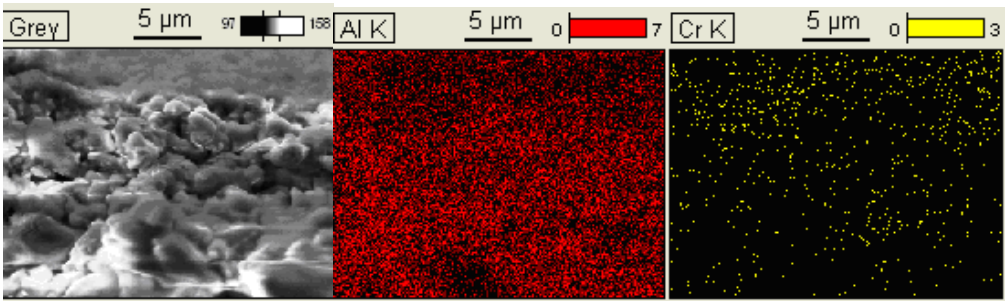

Figure 21 – SEM micrograph and atomic distribution in a cross section of a α-alumina disk after hydrothermal synthesis using dip coating seeding.

As it can be seen, there is a lot of alumina in the top layer which means that an uniform coating was not obtained and so this is not the most suitable method for interfacing MOFs in a support, at least with MIL-101 (Cr).

Before skipping to another method a XRD pattern was also analyzed, being the most reliable way to identify crystalline material – Figure 22.

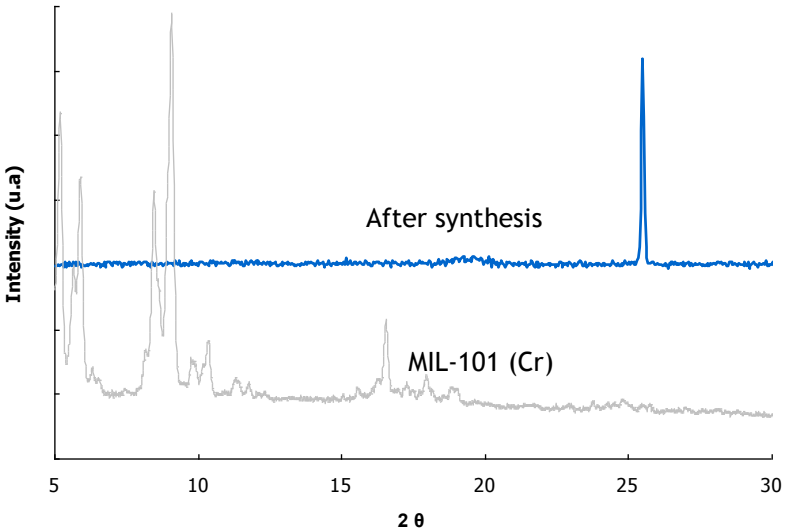

Figure 22 - XRD pattern of α-alumina disk surface after hydrothermal synthesis and with a previous seeding using dip coating technique. XRD pattern of MIL-101 (Cr) samples for comparison effects.

The XRD pattern did not reveal the presence of any MIL-101 (Cr) because the typical peaks of this material were absent.

Therefore, this result also supports the decision of not using this technique in order to interface MOFs in a support.

Spin Coating

Spin coating technique was also applied for seeding nanocrystals of MIL-101 (Cr) in the surface of α-alumina.

Both microwave and hydrothermal synthesis were tested.

The SEM micrographs can be seen in Figure 44.

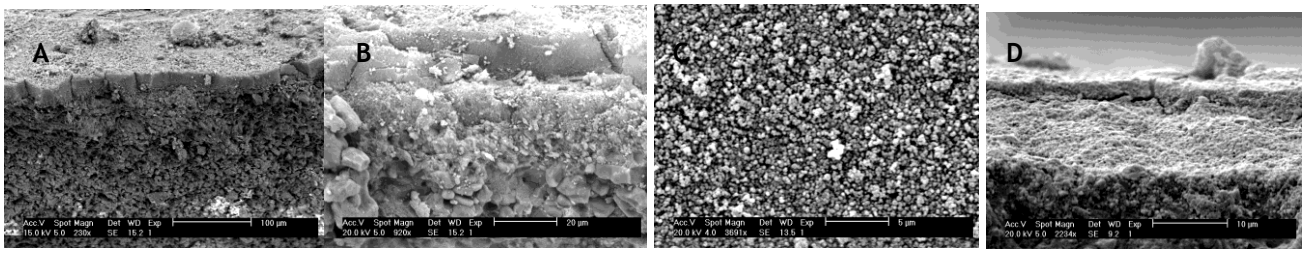

Figure 23-SEM micrographs of MIL-101 (Cr) hydrothermal synthesis in α-alumina disks (A and B) and microwave synthesis (C and D).

According to the SEM micrographs, the layer obtained with hydrothermal synthesis is much thicker than the layer obtained by microwave. This can be a consequence of the higher synthesis time that is used in hydrothermal synthesis.

However, cracks in the surface were observed with both methods.

In order to be sure about the origin of these cracks some analysis was also performed without washing the disk after synthesis. The results were nearly the same, which led to the conclusion that the temperature used for the washing as well as the activation at 150 ºC did not cause cracks but

possibly the growth of the crystals themselves, as the amount of MIL-101 (Cr) seems to be considerable.

For membrane applications, cracks in the surface of the coating should be avoided as well as too thick layers. As the interest of this project is mainly focused in catalytic applications these features are not so relevant. Although a thick layer could cause additional diffusion problems, it is important to ensure a considerable amount of catalyst on the monolith in order to accelerate the reaction. In a further study, it could be interesting to investigate if there are diffusion limitations and the optimal conditions to avoid them.

In order to be sure about the MIL-101 (Cr) present on the surface, XRD analysis was performed – Figure 24.

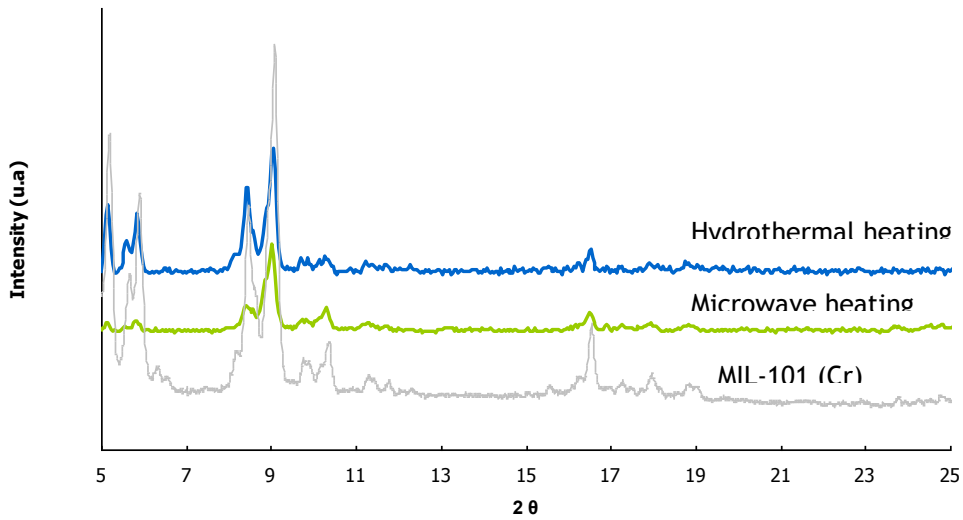

Figure 24 –XRD pattern of α-alumina samples with microwave and hydrothermal synthesis.

With both synthesis techniques it was possible to detect the MOF on the surface. The characteristic peaks are more defined using hydrothermal synthesis and so it was decided to pursue with this technique.

In order to see the distribution of the MOF in the surface, other SEM equipment was used.

With this analysis it was possible to ensure that the MIL-101 (Cr) was essentially on the surface of the support, as Chromium atom was detected on the top layer (yellow dots of Figure 46). Alumina, on the other hand, was preferentially on a deeper layer (red dots of Figure 46).

Some alumina was randomly detected on the surface, because of its non-constant appearance; this alumina on the top layer can be some small particles being taken to the surface when the piece of disk was cut for SEM analysis.

Spin coating seems to be a more suitable method to make a seeding for further secondary growth. Probably vacuum improves the retention of the crystals within the support.

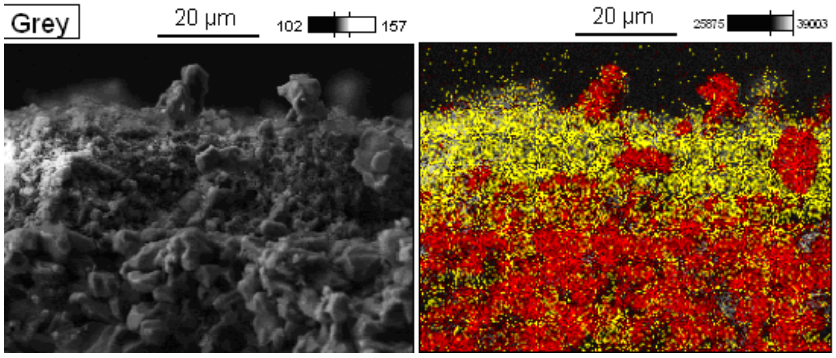

Figure 25 - SEM micrograph of α-alumina disk cross sectional view with the respective atomic distribution of Chromim (yellow dots) and Alumina (red dots)

4.5 2nd Step Interfacing MIL-101 (Cr) with Cordierite wash-coated with α-alumina

In this part of the project it was decided to do a preliminary α-alumina wash coat of the monoliths and not directly try to distribute the active phase on its surface[2].

Usually the route chosen to prepare a monolithic catalyst system strongly depends on the application and the catalyst. The advantage of using a coating technique is that the catalyst is used more efficiently, because the distance toward the active species will be smaller [61].

The reasons for choosing α-alumina, as it was already said, was two-fold, first its good interaction with MIL-101 (Cr) as shown in the previous experiments, and second in order to have a flat surface with a constant distribution of pores. For the wash coat a pore filling with high surface area wash coat material or a deposition as a layer in the pores of the ceramic support could have been used. The first one has the limitation of the amount of α-alumina that can be deposited, making sometimes the wash coat inaccessible. Moreover, the latter enables higher loadings, and diffusion into thicker walls does not influence the reaction because the diffusion distance is slower and can also be beneficial in terms of selectivity. However, care was taken in order to ensure that this "filter cake formation" is actually binded to the monolith, as in this case it is not confined to the pores of the monolith. So it was decided to try a strategy coating α-alumina as layer and not pore filling.

In what concerns the experimental procedure, some steps of the wash coating can also be discussed. The monoliths after being flushed in pressurized air were dried in horizontal position and rotated continuously around their axis. This avoids gravity to cause uneven washcoat distribution.

Besides that, pre-washing with NaOH and the concentration of 50% for slurry solution was chosen in order to just do the dip coating once and so decreasing the preparation time.

---

[2] The TGA results done in a sample without a wash coat with α-alumina can be found In Appendix 11 and in which is clear that the amount of MIL-101 (Cr) on the surface is so small to consider this an option for interfacing the MOF with monoliths.

After taking these considerations into account, the synthesis was performed in monoliths following both Procedure A and Procedure B, described in the experimental work, and the latter one, only tested in order to see if it was possible to reduce the synthesis time.

The secondary growth was firstly performed in a static oven. However, it was not possible to fix the monolith in a vertical position which resulted in a non uniform crystals distribution because of some precipitation effects Figure 26

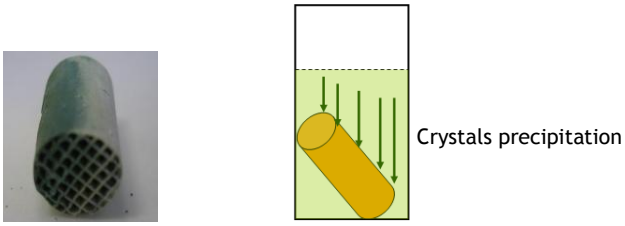

Figure 26 -Picture of the monolith synthesized using A procedure and static oven and a scheme illustrating the problem encountered.

Based on this, it was decided to perform the synthesis on a rotatory oven, although the monoliths were slightly damaged.

The appearance of the monoliths can be seen in Figure 27.

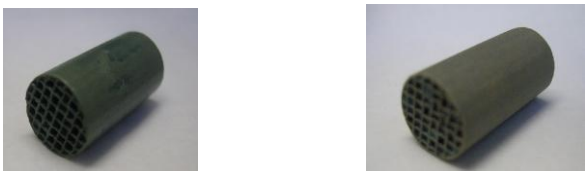

Figure 27 - Monolith after synthesis in rotatory oven and following procedure A and B for preparing the monoliths.

It seemed that Procedure A was the most convenient, however characterization of the samples was still needed.

SEM was performed in every sample as well as with a monolith just covered with alumina and alumina plus seeds after calcinations step - Figure 28 and Figure 29.

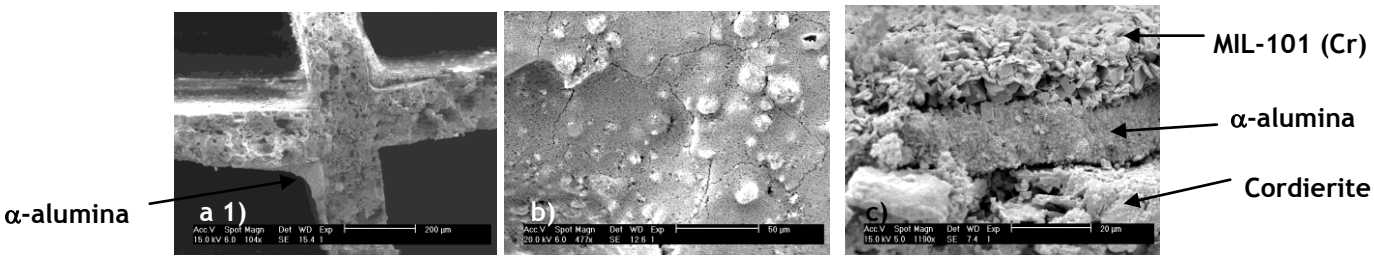

Figure 28 SEM micrographs of monoliths prepared with Procedure A) general overview of the α-alumina coating; B) surface of the monolith after being coated with α-alumina; c) cross sectional view of the monolith after secondary growth on a rotatory oven.

As it can be seen, α-alumina was coated on the monoliths. However, it should be noted that further study should be developed in order to have a more homogeneous coating.

Although SEM micrographs of the sample with secondary growth on a static oven were also taken, these results are only in Appendix 12 because they were inconclusive, not being possible to see any crystals.

The sample of the monolith synthesized using a rotatory oven was much more promising. It was, in fact, possible to see 3 clear layers and also some crystals seem to have an octahedral geometry, as we are expecting from MIL-101 (Cr) crystals.

Moreover, using a SEM with a higher magnification, it was also possible to detect more clearly the geometry of the crystals and also to see that they are all over the channels and not only on the edges - Figure 26

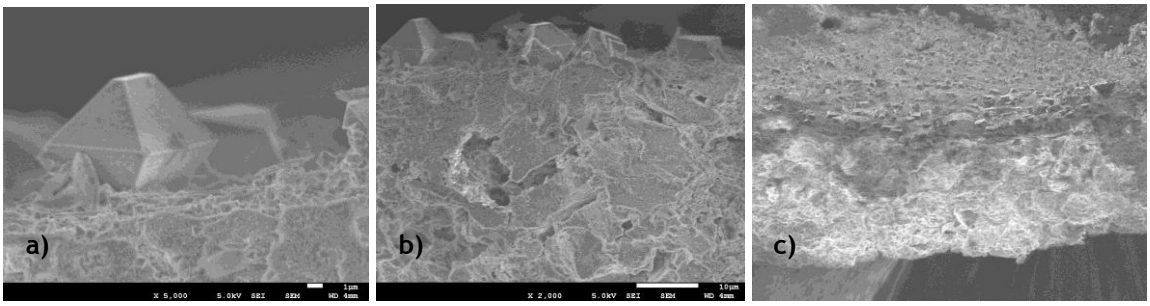

Figure 29 – SEM micrographs with a higher magnification with the octahedral geometry of the crystals perfectly clear- a) and b)- and the presence of MIL-101 (Cr) all over the channel. -c).

Skipping to the results of B procedure, surprisingly it was not possible to see any α-alumina coating, probably because a higher calcinations temperature was needed.

However, it seems that three different layers were obtained although much less clear than with B Procedure.

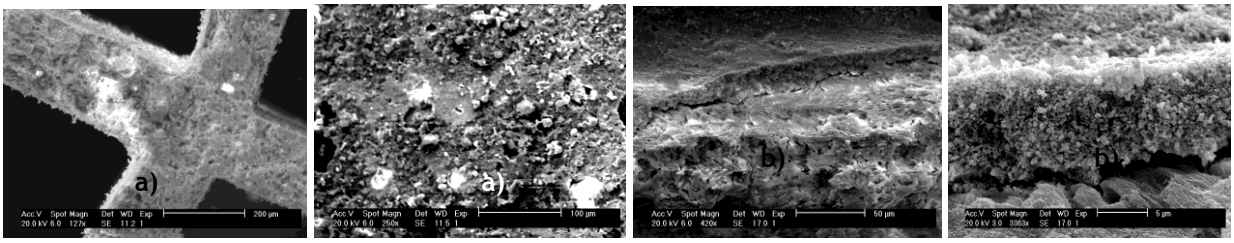

Figure 30 – SEM micrographs of monoliths prepared with procedure B a) monolith with just the coating; b) monolith after secondary growth in a rotatory oven.

XRD is known as being the best technique to confirm the identity of crystals. However, in this case, due to the cylindrical geometry of the monoliths and the typical MIL-101 (Cr) peak at 2 theta equal to 9, it was not the most advantageous. So, it was decided to use Raman spectroscopy.

The results obtained were pretty satisfactory, the presence of MIL-101 (Cr) being detected as the peaks were consistent with the ones assigned for the powder and also in a good agreement with the ones reported in literature for Terephthalic Acid [70]. Bands at 1612 and 1454 $cm^{-1}$are due to the C=O and C-O stretching modes of the carboxylates respectively. The bands at 1143, 866 and 633 cm^{-1}also correspond to terephthalic linkers, Figure 31.

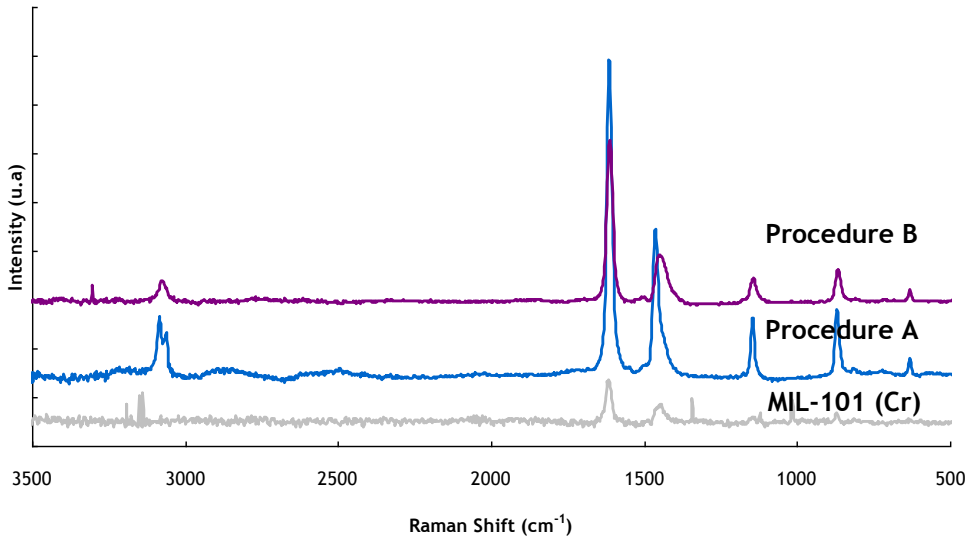

Figure 31 -Raman Spectra of the monolith's surface after secondary growth and with the coating prepared by both Procedure A and B and also MIL-101 powder.

Although the results were similar and both proving the presence of MIL-101 (Cr) it seems that with procedure A the crystals on the surface are more defined.

Last but not the least, it was important to check the thermal stability of MIL-101 (Cr) on the monolith surface. Thus, it was decided to do a Thermo Gravimetric Analysis (TGA). This information was also useful to have a rough estimation about the quantity of MOF that is actually covered on the monolith.

The first TGA tests, similarly to the ones reported in the chapter before, were done in He at a heating rate of 10 degrees per minute and up to 600 ºC. However the results were also strange with the absence of a plateau again.

Facing with this result, several assumptions were made that could have led to this occurrence.

First of all, it was wondered that the heating rate of 10 degrees per minute was too high and so the material reached temperature of decomposition too quickly and there was no time to be totally decomposed and keep decomposing at higher temperatures. Moreover, maybe it was better to increase the maximum temperature to 900 ºC. Some experiments were done having these considerations into account but no significant difference occurred.

Then, the use of Helium flow in the analysis and not air was questioned. As when TGA is performed in air, organics are reacting to form mainly CO_2 and Water, both gases leave the sample and this is probably the right way to calculate the amount of organics. However, when it is performed in Helium it is mainly creating carbon due to the thermal decomposition of the linker, so we get rid of the Hydrogen in the linker of MIL-101 (Cr) but most of the carbon stays with the material as coke, then when the temperature is higher coke starts gasifying, in a much slower process, contributing more strongly to a continuous decrease instead of a plateau.

So that, it was decided to perform the tests again but with an air flow, instead of a helium Flow. As it can also be seen in Figure 32 the TGA profile was much better and the decrease corresponding to the linker of MIL-101 (Cr) at around 375 ºC was steeper.

However, there is still a continuous mass decrease between the steps, which can be assigned to an inefficient cleaning for the first one, and the other could be assigned to some remaining crystals occluding from the monolith surface.

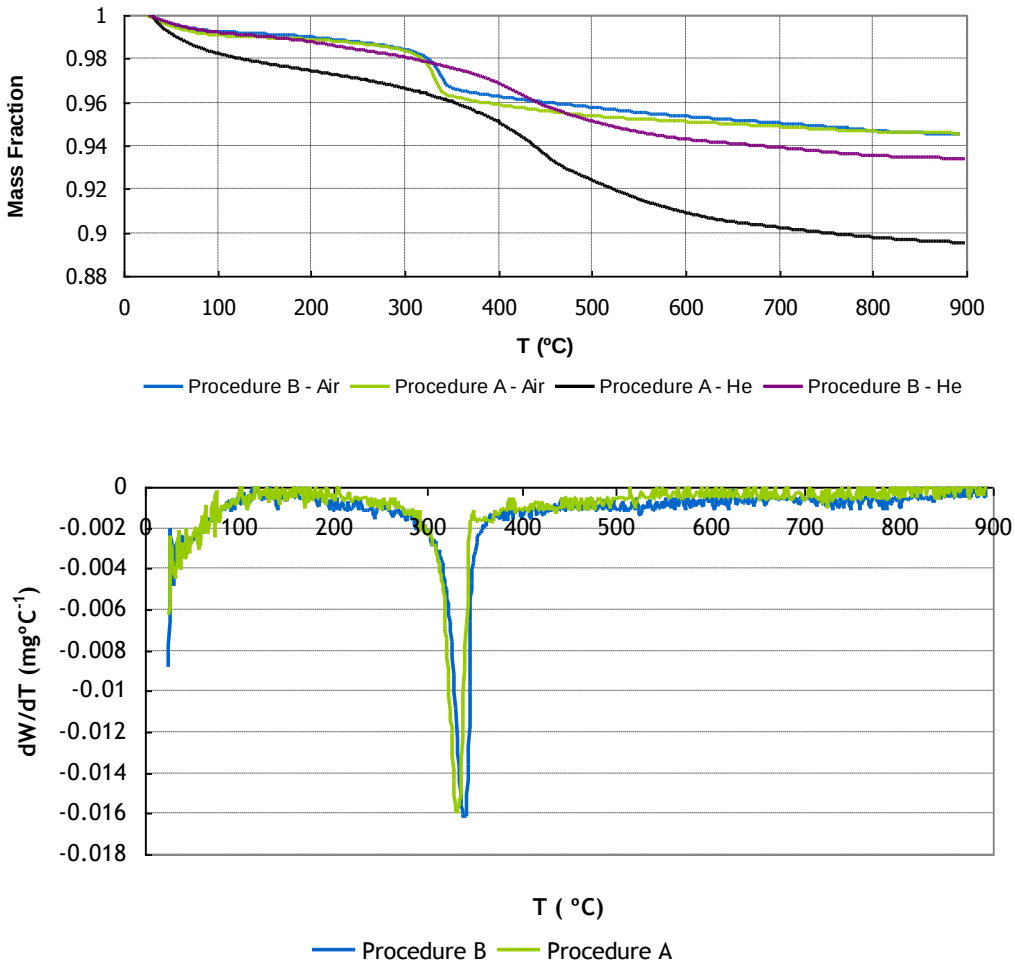

Figure 32 - TGA of MIL-101 (Cr) covered in the monoliths and respective derivative.

Apart from these conclusions, the results obtained with both procedures were particularly similar and it is almost impossible to distinguish between both monoliths - Figure 32 .

The mass percentage of the linker is around 5.5%, which can be translated in 8% of MIL-101 (Cr).

Although it was possible to grow MIL-101 (Cr) on the surface with both procedures, it was decided to pursue the catalytic studies doing procedure A because the layer seemed more homogeneous in SEM micrographs.

5 Catalytic Performance in Slurry Operation

5.1 Post-synthetic modification of MIL-101 (Cr)

A post-synthetic modification is characterized by a first assembly and then a modification of metal-organic frameworks with chemical reagents, maintaining the lattice structure. It is a chemical derivatization of MOFs after their formation, sometimes involving covalent bond formation.

A good way to access advanced MOF materials suitable for more sophisticated application is to integrate functionalities of greater complexity into these materials. The ability of modifying the physical environment of the pores and cavities within the MOFs would allow tuning the interactions with guest species and serve as a route to tailor the chemical stability and/or reactivity of the framework.

There are three well known strategies for MOF functionalization: use a functionalized organic ligand as the organic building block; functional properties associated with metal ions and functional "cartridge molecules" by non covalently bond within MOFs, which is sometimes called post grafting of CUS with chelating agents or electron rich molecules [71].

The disadvantages pointed for the first strategy cited are the interference with the formation of the desired framework, not compatible with MOF synthetic conditions and also it is time consuming and highly non trivial. That is why modifying MOFs after the synthesis seems a good alternative.

By doing this, it is possible to include a higher diversity of functional groups; purification and isolation of the modified products are easier; modification can be done with different reagents, generating a large number of topologically similar but functionally diverse MOFs [54].

Amines with a functional group of alkoxylane are often used as grafting reagents in base catalysis and immobilization and encapsulation of large molecules.

In this work it is intended to test the catalytic activity of MIL-101 (Cr) when covered in the monoliths. However, due to security reasons, it was not possible to test the direct activity of MIL-101 (Cr) but a post synthetic functionalization of the MOF seemed to be a good alternative to do so.

Before starting with the monolithic reactor, it was important to perform some studies in a slurry system, so that we can be sure about the activity of the catalyst grafted in the MIL-101 (Cr) and collect data for further comparison.

It was decided to do so connecting two different bases, guanidine nitrate and 1,5,7-Triazabicyclo[4.4.0]dec-5-ene acting to the OH group present on the super tetrahedra of MIL-101 (Cr) structure, Figure 33.

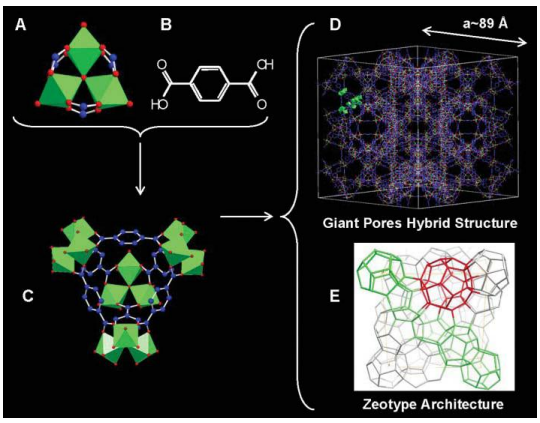

Figure 33 - Structure of MIL-101 (CR)A-trimeric building unit; B-Terephthalic acid; C-edges of the supertetrahedra; D Ball and stick representation E-3 D schematic representation .Chromium octahedral, oxygen and fluorine and carbon are in green, red and blue.

Characterization methods such as nitrogen adsorption and DRIFT were used to check if the base was being covalently bonded with OH or not.

5.2 Knoevenagel Condensation Reaction

The reaction chosen for testing the catalytic activity was Knoevenagel Condensation.

The Knoevenagel Condensation reaction is a modification of the Aldol Condensation which was first conducted by Emil Knoevenagel. It is based on the nucleophilic addition of an active methylene compound to a carbonyl group in presence of a base Figure 34. The reaction is usually catalysed by basic amines, although it can be also catalyzed by acids. The liquid-phase Knoevenagel condensation between a C=O functionality and an activated methylene group is an interesting classic route to C-C coupling for the preparation of important intermediates in the pharmaceutical industry and is often used as a test reaction for probing the activity of various solid base catalysts [72].

The reaction can proceed by two different mechanisms, depending on the nature of the catalytic material used as solid base.

If a strong base is used there is a direct deprotonation of the methylene group on the catalyst surface and reaction of the protonated intermediate with slightly acidic benzaldehyde takes place, leading to the product.

When weak bases, such as amino groups, are involved in the catalytic process, formation of an imine intermediate occurs with the benzaldehyde. As a consequence of the higher basicity of the formed benzaldimine compared with the free amine, the deprotonation of the methylene group takes place followed by reaction, regenerating the active site. The active methylene group can also react directly with the amino groups to form amides, inhibiting then the interaction amine-benzaldehyde and causing the deactivation of the catalyst [14], [73].

As reacting benzaldehyde with compounds containing active methylene groups with different p*K*a values, such as ethyl cyanoacetate (p*K*a ≤ 9) or ethyl acetoacetate (p*K*a ≤ 10.7), makes it possible to evaluate the basic strength of a catalyst.

This reaction has been previously studied in this group using different MOF catalysts [14].

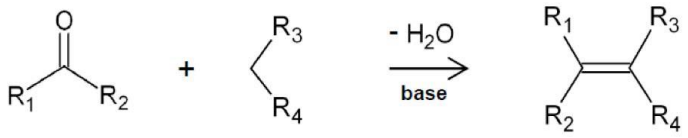

$$Benzaldehyde + EthylCyanoacetate \rightarrow Ethyl-trans-alpha-cyanocinnamate$$

Figure 34 -Reaction Scheme of Knoevenagel Condensation.

Very recently, MIL-101 (Cr) grafted with guanidine was shown to be a strong basic catalyst. However, it would be ideal to interface this catalyst in order to avoid the considerable amount of powder lost through reuse. The approach of covering the MOF in a support and subjecting it to grafting techniques in order to confer the proper basic environment for the reaction is potentially a good solution for the problem.

In this project, the performance of MIL-101 (Cr) grafted with guanidine and bicyclo guanidine in powder samples will be tested.

5.3 Experimental work

Grafting with guanidine nitrate and 1,5,7-Triazabicyclo[4.4.0]dec-5-ene

The mechanism of post-synthetic modification adopted – grafting of a base - consists of contacting a solution of the salt with a stable MOF, MIL-101 (Cr), synthesized in the last step, leaving the basic molecules interact with the OH groups connected directly with the metal cluster of MOF. This technique can be done with just pore volume impregnation or excess impregnation. The latter has been proved to be more effective, in previous studies in the group.

In this case, the amount of solution used is larger than in pore volume and an apolar medium is used. As the base, guanidine, is strongly polar, it is preferentially attracted to the OH groups of the MOF structure.

The amount of base added should be in agreement with the ratio mmolBase/gMOF equal to 1.5 (which corresponds to mmolBase/mmolOH equal to 1). Then it is mixed with toluene excess (30 mL) and heated under reflux at 100 ºC. After 12 hours, the solution is filtered and the catalyst recovered and stored at 160 ºC in an oven.

Knoevenagel Condensation Reaction

The typical experiment, 0.14 miliequivalents (referred to basic groups in the MOF) of the basic catalysts are added to a solution of ethyl cyanoacetate (0.792 g, 7 mmol) in 5 mL of Toluene while being stirred under inert atmosphere (N_2).

After establishing the temperature of 40 ºC, benzaldehyde (0.850 g, 8 mmol) is added to the solution. The reaction and formation of the product is periodically monitored by gas chromatography. The reaction conditions are typically kept for 2 to 4 hours.

After reaction, the catalyst is recovered from the reaction mixture by filtration.

5.4 Grafting with Guanidine Nitrate

DRIFT spectra of guanidine nitrate, MIL-101 (Cr) and MIL-101 (Cr) were particularly in good agreement with what was thought to be a covalent connection between the base and the MOF Figure 35.

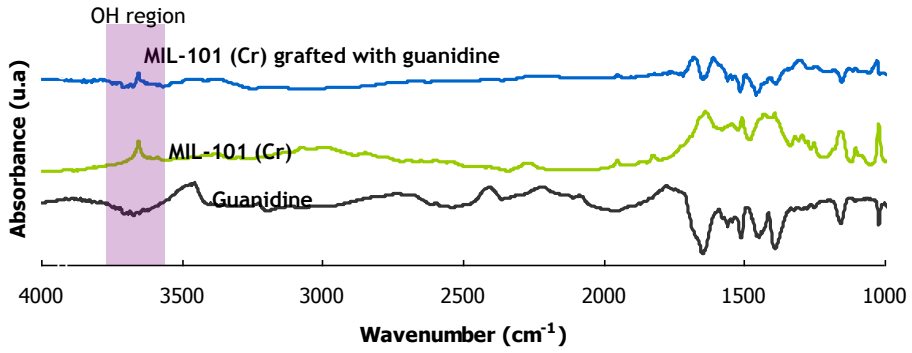

Figure 35 - DRIFT spectra of guanidine nitrate, MIL-101 (Cr) and MIL-101 (Cr) grafted with guanidine.

OH vibration stretching has its significant bands in the region between 3760 and 3550 cm^{-1}. As can be seen, the peak at a wavelength corresponding to OH, 3650 cm^{-1}, is not present in the guanide nitrate and becomes more diffuse when MIL-101 (Cr) is grafted inducing the presence of covalent bonds. Moreover there is a peak at a wavelength around 3400 cm^{-1} on the sample grafted belonging to the NH stretching which also supports the assumption that guanidine is connected to the MOF:

After characterizing by DRIFT, some test reactions were done. The reaction with the homogeneous catalyst was tested and then with the heterogeneous during three consecutive runs Figure 36.

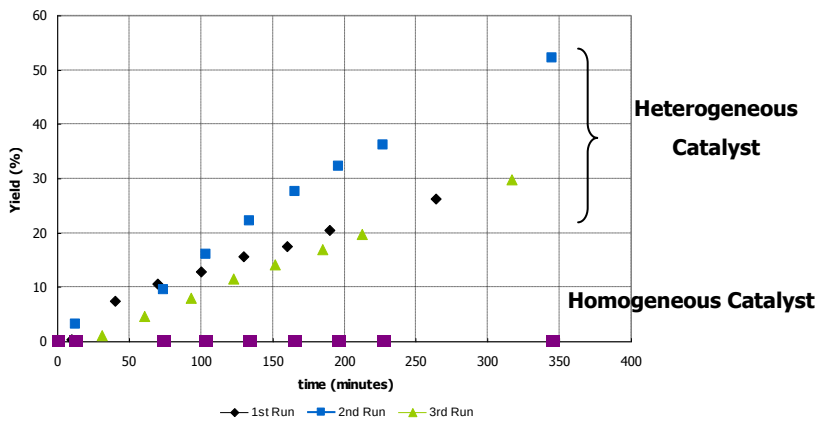

Figure 36 -Yield versus time for homogeneous reaction with guanidine nitrate and the heterogeneous catalyst, in three consecutive runs.

With these results it can be concluded that although the heterogeneous catalyst is active the homogeneous did not have any activity at all. This is because the cation of guanidine is stabilized by the nitrate and so it is not available for reaction.

Performing the grafting, the nitrate groups are removed and the guanidine connected to the OH of MIL-101 and so, the proton responsible for its basic catalyst character is available for catalyzing the reaction.

Besides that, an important conclusion that could be taken from this simple catalytic test is that the catalyst did not lose its activity from run to run, although we have observed a decrease in its mass due to the filtration step. This is also supported by the turnover number, TON, and the turnover frequency, TOF Table 3

Table 2 - TON and TOF values of the samples grafted with MIL-101 (Cr) guanidine after each run.

	Run	time (min)	TON	TOF (min^{-1})
Heterogeneous	1st	264	13.73	0.05
	2nd	227	18.09	0.08
	3rd	212	9.91	0.05

The turnover number (TON) and turnover frequency (TOF) can be defined as:

$$TurnoverNumber(TON) = \frac{[moles \cdot of \cdot ethyl \cdot cyanoacetate \cdot converted]}{[moles \cdot of \cdot active \cdot sites \cdot in \cdot the \cdot catalyst]}$$
$$TurnoverFrequency(TOF) = \frac{TurnoverNumber(TON)}{[unit \cdot time]} \quad (1)$$

5.5 Grafting with 1,5,7-Triazabicyclo[4.4.0]dec-5-ene

Another base that was also tested in slurry operation was 1,5,7-Triazabicyclo[4.4.0]dec-5-ene.

This base is supposed to be more active because the cation formed is more stable than the one reported to guanidine.

At the beginning the relation of one mole of base per mole of hydroxyl group was maintained.

The DRIFT results can be seen in Figure 37.

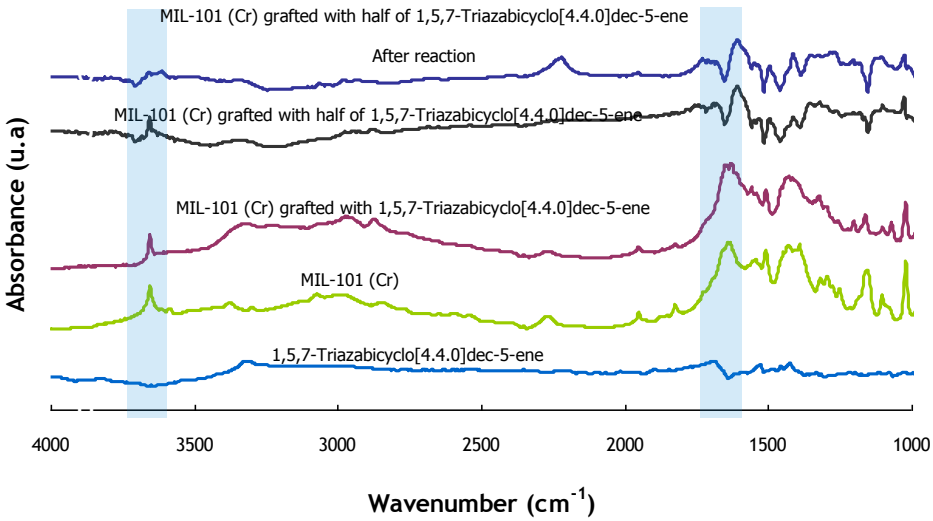

Figure 37 - DRIFT spectra of1,5,7-Triazabicyclo[4.4.0]dec-5-ene, MIL-101 (Cr)and MIL-101(Cr) grafted with both bicycle in the standard amount (1 mol of base per mol of OH group) and half of that quantity and after performing 3 runs of reaction.

In this case the presence of bicyclo in the MOF structure can be observed: there is a slight increase in the absorbance before a wavelength of 3500 cm^{-1} and also a CH stretching at around 1700

cm^{-1}. In what concerns the OH group, it is at around 3648 cm^{-1} and seems more diffuse. Moreover, there is a small shift in the stretching vibration of OH which indicates that bicyclo is being mildly coordinated with MOF. The NH stretching can also be seen at around 3330 cm^{-1}.

Similar to what was done before with guanidine nitrate, catalytic performance tests were also done with both homogeneous and heterogeneous catalysts.

Surprisingly, no conversion was observed when doing a grafting with the same molar quantity of base and OH groups in the MOF. The product peak was hardly visible, and there was not any change in the benzaldehyde quantity.

Supported by these results and also by the nitrogen adsorption isotherms, a pore blocking caused by 1,5,7-Triazabicyclo[4.4.0]dec-5-ene was suspected Figure 38.

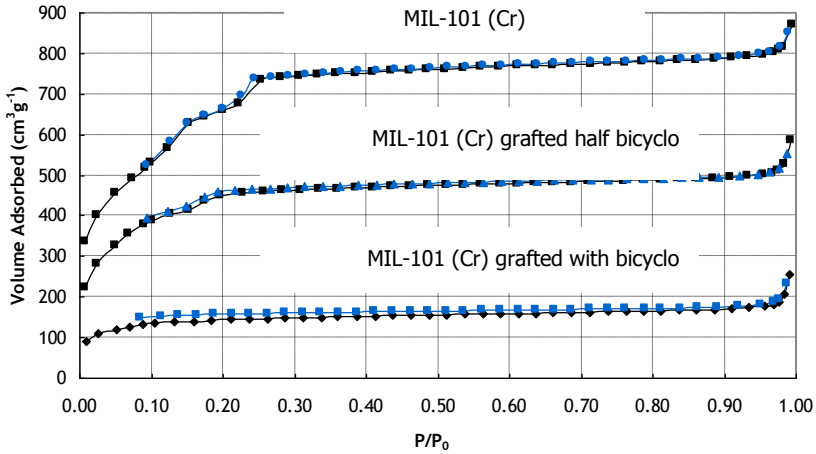

Figure 38 - N_2 adsorption isotherms of MIL-101(Cr), MIL-101(Cr) grafted with 1,5,7-Triazabicyclo[4.4.0]dec-5-ene and MIL-101(Cr) grafted with half of the amount of 1,5,7-Triazabicyclo[4.4.0]dec-5-ene..

As it can be seen, the volume adsorbed by MIL-101 (Cr) grafted with bicyclo is much lower than with MIL-101 (Cr). Moreover, the two steps behaviour belonging to the two mesoporous cages is absent, suggesting the blocking of the MIL-101 (Cr) pores.

In order to test this assumption, the grafting was repeated using half of the bicyclo guanidine amount, which means a relation of 0.5 moles of base per OH mole in MOF structure, and the results obtained were pretty consistent with what was expected.

The two steps belonging to the mesoporous cages were observed as well as a larger nitrogen volume was adsorbed Figure 38. However the step is less pronounced than in the bare sample, indicating that the mesoporous cavities are partially filled with the base. This is especially remarkable in the first step (it almost disappears), which indicates that the small cavities to a larger extent than the large one, as expected.

Besides that, the homogeneous catalyst proved to be active and with an activity similar to the one achieved with the heterogeneous catalyst. Moreover it remained active after 3 consecutive runs although there was some material loss.

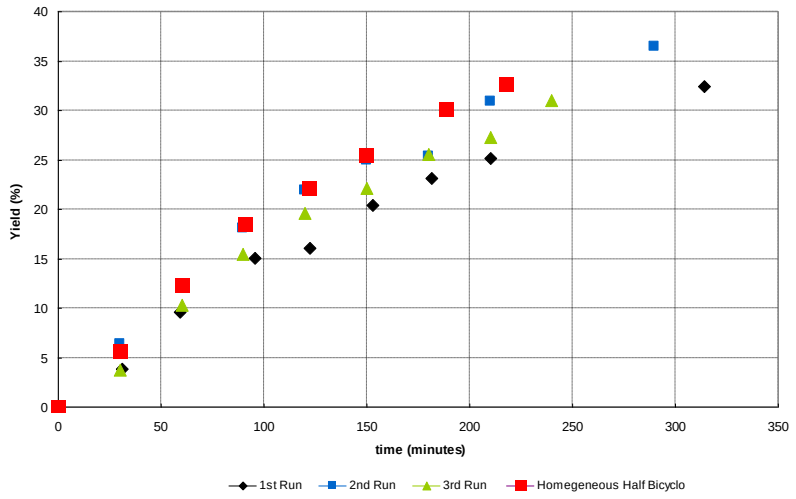

Figure 39 - Yield versus time for homogeneous reaction with 1,5,7-Triazabicyclo[4.4.0]dec-5-ene and the heterogeneous catalyst, in three consecutive runs.

Also interesting to note is that after 3 consecutive runs, the typical DRIFT peaks continue there, although more diffuse, Figure 37.

The turnover number and the turnover frequency were also calculated showing the activity of the catalyst in homogeneous and heterogeneous conditions after three runs Table 3.

Table 3 – TON and TOF values of the samples with MIL-101 (Cr) grafted with 1,5,7-Triazabicyclo[4.4.0]dec-5-ene, after each run, and also of the homogeneous catalyst.

	Run	time (min)	TON	TOF (min-1)
Heterogeneous	1st	210.43	26.98	0.13
	2nd	290	16.86	0.08
	3rd	240	36.33	0.15
Homogeneous	-	218	20.45	0.09

6 Monolithic Grafting and First Studies using a Monolithic Stirrer Reactor

The main goal of this project was to coat a monolithic surface with MIL-101 (Cr) and then to test its performance in some catalytic reactions.

However, grafting of the MOF and a study of its behaviour as particles was done, as reported in the previous chapter, for later comparison with a monolithic reaction.

Apart from the material loss observed in the slurry operation system, other disadvantages are often reported: separation, attrition, erosion of the equipment and hazards of handling. Moreover, the complex hydrodynamics of slurries makes scale-up difficult, which can lead to problems like incomplete suspension of particles and non-uniform distribution of the catalyst [74].

So, achieving a method to perform the reaction using monoliths instead of powder is a great challenge.

As the reaction chosen was Knoevenagel condensation, catalyzed by bases, the first step was to do a grafting in the MOF deposited on the monoliths and then performing the reaction.

Here the first drawback appeared; usually the quantity of MOF introduced for the grafting is high and it is difficult to achieve such quantity in the monoliths, as was previously said, it is around 8% of the monoliths mass, which, in average is not higher than 0.7 grams. Thus, it was not possible to introduce that quantity and it was decided to perform the guanidine grafting with an excess of the base.

Moreover, the grafting is usually done under reflux and in the first tests, a proper monolith stirring was not available and so it was done without stirring.

Being aware that the conditions for a proper post-synthetic functionalization were not met, a different strategy was tested which involved the encapsulation of a heteropoly acid by the method “bottle around the ship” – Appendix 13 - which did not involve any grafting.

A TGA characterization of both functionalized monoliths was done Figure 40. However, as the heteropoly acid encapsulation was not in the scope of this project it is only incorporated in Appendix 13 of this project.

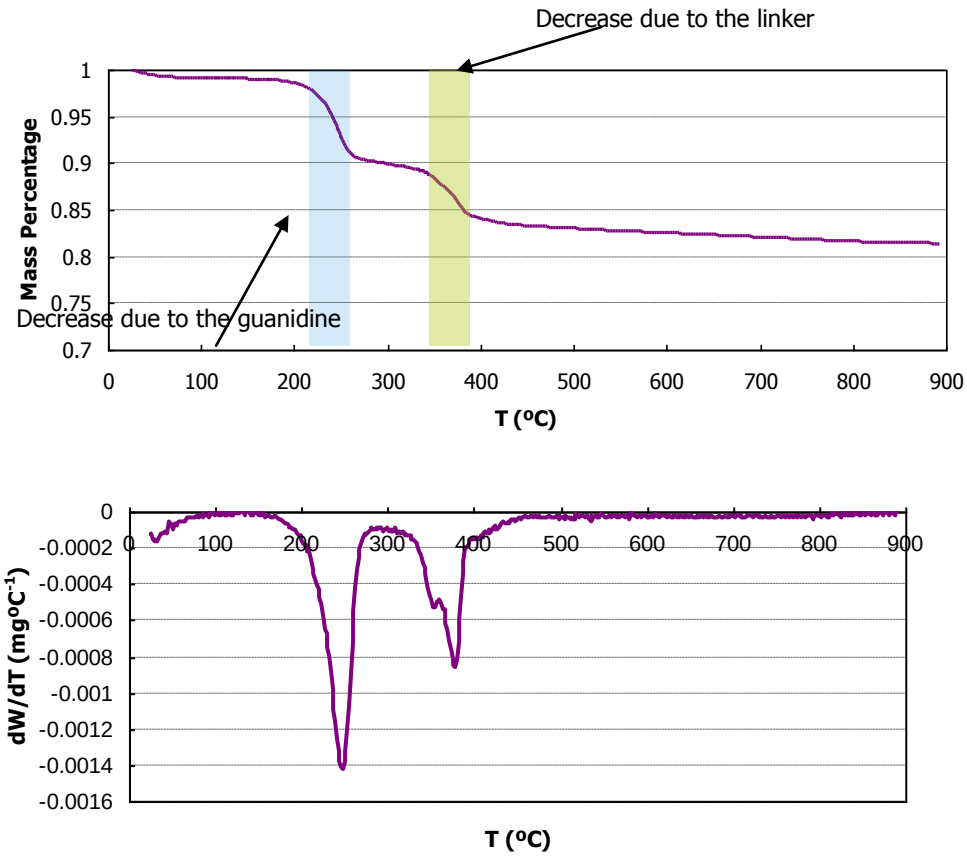

Figure 40 -TGA analysis of the monolith grafted with guanidine and the corresponding derivative.

The TGA was consistent with what was expected with two different steps: one belonging to the base decomposition and the other to the linker from the MOF decomposition.

Nevertheless, it should be noted that the decrease belonging to the linker should be steeper and more similar to the powder. The absence of a clear plateau was foreseen because in the case of the MOF connected to a surface, some crystals will continue occluding after the typical temperature of its decomposition as particles, 375ºC.However the absence of a clear step at the beginning could be assigned to the presence of some linker not been well removed during the washing procedure.

Besides the grafting and the characterization, it was also necessary to find proper reactor geometry in order to perform the reaction. The main difficulty was stirring the reactant mixture so that it could enter inside the channels.

The first reactor setup tried is shown in Appendix 14 - Figure 57.

A reaction with heteropoly acid was tried, however it was not successful. In fact, this setup was not the most convenient and the monolith channels were not being filled with the reactants mixture as the monoliths were not following the movement of the liquid.

Another strategy was tested, by putting the monoliths more spaced from each other Figure 41.

Figure 41 – Monolithic support for a monolithic stirrer reactor bare cordierite and cordierite impregnated with MIL-101 (Cr).

However, a reactor with this stirring geometry needs to have a bigger size than the one used in the slurry operation system. Thus, although the quantity of MIL-101 (Cr) coated in the monoliths is similar to the one used in the test reactions in powder and also the reaction is done with two instead of just one monolith, the scale up needed to be used in order to submerge the monoliths is six times higher then the quantity used in a slurry reactor.

Two reactions were firstly tried in this new setup: heteropoly acid encapsulated within the MIL-101 (Cr) structure and guanidine grafting of the MOF. It was not possible to detect any peak from the product even after 8 hours.

Two different explanations for this occurrence were considered: problems with encapsulation and probably a too high amount of base in the guanidine grafted reaction (blocking the pores) or the quantity of the MIL-101 (Cr) that is in fact on the monolith too small to detect the product.

In order to test the latter hypothesis, the procedure followed was performing a reaction with exactly the same conditions but instead of using monoliths coated with MIL-101 (Cr) putting "naked" ones and using in powder the same amount of MIL-(Cr) that is potentially on the monoliths.

The conversion registered was not high but it was possible to detect the product and calculate the conversion. Thus, assuming that quantity is actually on the monolith surface its amount should not constitute a drawback - Figure 42.

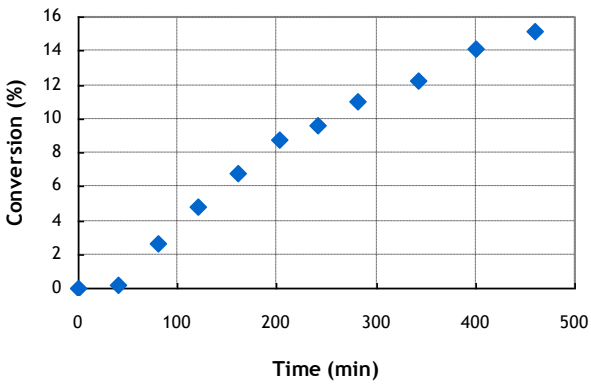

Figure 42 – Conversion versus time for the reaction carried on the monolithic slurry reactor using, in powder, the same quantity of MIL-101 (Cr) that is on the monolith surface.

Facing these results, this hypothesis of possible reason for non reaction occurrence was excluded.

In order to get over this drawback, the step that followed was performing the reaction with the 1,5,7-Triazabicyclo[4.4.0]dec-5-ene grafted in the monolith with a relation of 0.5 moles of base per moles of OH in MIL-101 (Cr).

In this reaction a peak of the product was visible but too low to calculate any conversion. However, it seemed to be increasing with the time. As in this case, the homogeneous catalyst was also active, it was necessary to check if this occurrence was only based on a deposition of bicyclo in the surface of the monoliths and not actually connected to the MOF. To prove so, the reaction was stopped, the monolith was removed and then after 50 minutes another samples was taken. As this sample has the same areas as the one taken almost one our before, it can be concluded that the basic character that was slowly catalyzing the process belonged to MIL-101 (Cr) grafted with bicyclo.

In order to increase the conversion, other strategy was performed, increasing the reaction temperature to 70 ºC. This favours the kinetics of reaction and is also favourable to the product desorption. Usually it is used a lower temperature, 40 ºC, because in some previous work at this group some catalytic activity comparison was done and only strong bases were active at that temperature.

Unfortunately, although the areas of the product were higher than the ones obtained at 40 ºC and also some increase in product peaks were continuously seen, it was not sufficiently relevant to be considered.

In order to find out the problem, the characterization results were looked more deeply. After observing SEM micrographs and also the TGA behaviour, some inefficient washing was inferred. The TGA assumption was already explained and in SEM micrographs some needles, the typical shape of terephtalic acid, were sometimes visible. Problems in the purification step of MIL-101 (Cr) synthesis have already been reported [3] and are still the focus of some groups research. Possibly they become more expressive when it is tried to wash MIL-101 (Cr) on the monoliths surface due to the absence of stirring in that step.

Therefore, the last trial was: perform the washing steps in the reactor setup being in continuous contact with the washing solution and then repeat the reaction with four monoliths.

The conversion obtained as a function of time is presented in Figure 43.

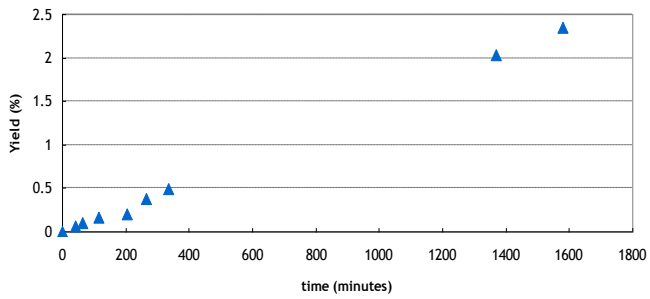

Figure 43 -Reaction Results of the last trial, performing the washing and the grafting in the monolithic stirrer reactor and using 4 monoliths.

After more than 24 hours, the conversion only reached 2.4% and so the problem perhaps is not the washing itself but the solutions used to do that. Although in powder the influence is not that much,

in monoliths it can be more difficult to remove. So, a study about other solvents to be used for cleaning would be interesting.

Some problems in weighting the quantity needed for the grafting were detected, because of its too low amount, and probably some crystals are not effectively dissolved in toluene.

Moreover it is not possible to guarantee that no product adsorption is occurring as well as an adsorption of the linker in the monolith surface could not be excluded.

It was not possible to test the performance of new reactions in new conditions due to time limitations.

7 Conclusions and Recommendations for Future Work

7.1 Conclusions

Studies about interfacing MOFs with structured supports are scarce; particularly, no work has been published so far on MOF coatings on monolithic supports. Thus, every work in this area always constitutes an important tool for further development.

Different techniques were tested in order to interface MIL-101 (Cr) with structured supports and some of them already excluded.

Using the direct impregnation of Chromium Oxide on a monolith or α-alumina surface followed by direct synthesis, it was not possible to prove the presence of MIL-101 (Cr) crystals. As in these case, a different Chromium source from the state of the art synthesis was being used, a confirmation that crystals belonged to MIL-101 (Cr) was essential.

Regarding the secondary growth approach, seeding turned out to be critical. Spin coating was considered the most suitable one, probably beneficiating from the vacuum that helps to attach crystals to the support. When using dip coating, it was not possible to detect MIL-101 (Cr) after the secondary growth with any characterization technique, probably due to a small quantity of MOF on the surface. Such small quantity is not attractive in terms of catalytic applications.

For coating the monoliths with MOF, a wash-coat with α-alumina, for blocking the major pores of cordierite, proved to be advantageous, and a particularly thick layer was obtained. Although a procedure to wash coat and seed the monoliths in less time was tested and showed the presence of MIL-101 (Cr) in the surface, the layer obtained was thinner and not adopted for the subsequent studies.

For testing the catalytic performance, some preliminary studies using MOF particles were done. A grafting was essential in order to give a basic character to MIL-101 (Cr), responsible for the catalytic activity in Knoevenagel condensation. Basicity was introduced in the MOF with the two different bases, guanidine and 1,5,7-Triazabicyclo[4.4.0]dec-5-ene, and it was possible to infer its covalent bonding to the OH group of MIL-101 (Cr), based on DRIFT tests. Moreover, while performing these studies, it was also noted that the pores of the structure could be blocked, if the grafting was done with a high quantity of base. Usually, the relation 1 mmolbase/mmol OH is maintained but we concluded that this relation was to high when grafting with 1,5,7-Triazabicyclo[4.4.0]dec-5-ene, a molecule with bigger size than guanidine.

In what concerns the reaction performed using the MOF supported on a monolith, TGA enables us to conclude that the base was in fact introduced in the MOFs. Nevertheless, several drawbacks were encountered in performing the reaction. First of all, the quantity of base used for the grafting was too small; secondly the washing procedure of the monoliths needs to be improved in order to get rid of the linker which can possibly be blocking the access of reactants to the active sites. Problems in product desorption can also be occurring.

Although the conversion obtained after more than one day was only 2.4 %, the catalyst covered in the MOF showed some activity and optimizing the conditions seems a great challenge for the future.

To summarize, the objectives proposed for this work were achieved. A successful method for interfacing MIL-101 (Cr) with monoliths was obtained and although some conditions still need to be optimized, basicity was introduced in the MOF covered on a monolith, and some conversion was detected in a reaction carried on a monolithic structured reactor.

7.2 Recommendations for Future Work

As this approach in Metal-Organic Framework research is very new, there is plenty of work that may be done.

First of all, reproducibility tests of the coating of MOF obtained on the support surface can be done and a deep study about the most relevant conditions that influence on it would be pretty useful.

Moreover, after the interfacing with a-alumina disks another possible research topic was found based on the study of MOFs potential as membranes.

Some improvements can also be made concerning the techniques already used in this project,. The conditions for secondary growth can be improved, especially because some monolith damage after being in the rotatory oven was noted and also, a proof that the synthesis solution is filling the monoliths channels needs to be found or at least the conditions optimized.

Using different solvents to clean MIL-101 (Cr) on the monolith surface would also be interesting, as there is a suspicion that this could be the reason why higher conversions are not being achieved in the monolithic stirrer reactor.

The grafting done in the MOF covered on the monoliths is a tricky question about this work and an alternative way in order to measure accurately the amount of base should be encountered.

Regarding the reaction performed in a monolithic stirrer reactor, a deep study about the optimal conditions is highly recommended in order to get data for further kinetic study and modelling.

Moreover, grafting other bases in MOFs and trying to find other reactions and MOFs to be covered on monoliths is always a good perspective of future work.

Therefore, there is still a long way to go and a lot of new challenges to face.

8 References

1. Prof. Dr. Jacob A. Moulijn, P.F.K., Dr. Guido Mul, *Heterogeneous Catalysis for Chemical Engineers*, ed. S.R.C. DelftChemTech. November 2005, Delft, The Netherlands: Technische Universiteit Delft.
2. Feng, P., X. Bu, and G.D. Stucky, *Hydrothermal syntheses and structural characterization of zeolite analogue compounds based on cobalt phosphate*. Nature, 1997. **388**(6644): p. 735-741.
3. Do-Young Hong, et al., *Porous Chromium Terephthalate MIL-101 with Coordinatively Unsaturated Sites: Surface Functionalization, Encapsulation, Sorption and Catalysis*. Advanced Functional Materials, 2009. **19**(10): p. 1537-1552.
4. O'Keeffe, M., *Design of MOFs and intellectual content in reticular chemistry: a personal view*. Chemical Society Reviews, 2009. **38**(5): p. 1215-1217.
5. Long, J.R. and O.M. Yaghi, *The pervasive chemistry of metal-organic frameworks*. Chemical Society Reviews, 2009. **38**(5): p. 1213-1214.
6. Kumar, D.K., et al., *From Diamondoid Network to (4,4) Net: Effect of Ligand Topology on the Supramolecular Structural Diversity*. Inorganic Chemistry, 2005. **44**(20): p. 6933-6935.
7. Yaghi, O.M., et al., *Reticular synthesis and the design of new materials*. Nature, 2003. **423**(6941): p. 705-714.
8. Rowsell, J.L.C. and O.M. Yaghi, *Metal-organic frameworks: a new class of porous materials*. Microporous and Mesoporous Materials, 2004. **73**(1-2): p. 3-14.
9. Henschel, A., et al., *Catalytic properties of MIL-101*. Chemical Communications, 2008(35): p. 4192-4194.
10. Lee, J., et al., *Metal-organic framework materials as catalysts*. Chemical Society Reviews, 2009. **38**(5): p. 1450-1459.
11. Davis, M.E., *New vistas in zeolite and molecular sieve catalysis*. Accounts of Chemical Research, 1993. **26**(3): p. 111-115.
12. Ferey, G., *Hybrid porous solids: past, present, future*. Chemical Society Reviews, 2008. **37**(1): p. 191-214.
13. Zacher, D., et al., *Thin films of metal-organic frameworks*. Chemical Society Reviews, 2009. **38**(5): p. 1418-1429.
14. Gascon, J., et al., *Amino-based metal-organic frameworks as stable, highly active basic catalysts*. Journal of Catalysis, 2009. **261**(1): p. 75-87.
15. Ferey, G., et al., *A Chromium Terephthalate-Based Solid with Unusually Large Pore Volumes and Surface Area*. Science, 2005. **309**(5743): p. 2040-2042.
16. Ryo Kitaura, K.S., George Akiyama, Susumu Kitagawa,, *Porous Coordination-Polymer Crystals with Gated Channels Specific for Supercritical Gases13*. Angewandte Chemie International Edition, 2003. **42**(4): p. 428-431.
17. Ferey, G., et al., *Crystallized Frameworks with Giant Pores: Are There Limits to the Possible?* Accounts of Chemical Research, 2005. **38**(4): p. 217-225.
18. S. H. Jhung, J.-H.L., J. W. Yoon, C. Serre, G. Férey, J.-S. Chang,, *Microwave Synthesis of Chromium Terephthalate MIL-101 and Its Benzene Sorption Ability*. Advanced Materials, 2007. **19**(1): p. 121-124.
19. Corma, A., et al., *Lewis and Brönsted basic active sites on solid catalysts and their role in the synthesis of monoglycerides*. Journal of Catalysis, 2005. **234**(2): p. 340-347.
20. Gascon, J., S. Aguado, and F. Kapteijn, *Manufacture of dense coatings of Cu3(BTC)2 (HKUST-1) on [alpha]-alumina*. Microporous and Mesoporous Materials, 2008. **113**(1-3): p. 132-138.
21. Hermes, S., et al., *Selective Nucleation and Growth of Metal−Organic Open Framework Thin Films on Patterned COOH/CF3-Terminated Self-Assembled Monolayers on Au(111)*. Journal of the American Chemical Society, 2005. **127**(40): p. 13744-13745.
22. Zacher, D., et al., *Deposition of microcrystalline [Cu3(btc)2] and [Zn2(bdc)2(dabco)] at alumina and silica surfaces modified with patterned self assembled organic monolayers: evidence of surface selective and oriented growth*. Journal of Materials Chemistry, 2007. **17**(27): p. 2785-2792.

23. Yoo, Y. and H.-K. Jeong, *Rapid fabrication of metal organic framework thin films using microwave-induced thermal deposition*. Chemical Communications, 2008(21): p. 2441-2443.

24. Mirko Arnold, P.K., Deborah J. Jones, Yannig Nedellec, Jörg Kärger, Jürgen Caro,, *Oriented Crystallisation on Supports and Anisotropic Mass Transport of the Metal-Organic Framework Manganese Formate*. European Journal of Inorganic Chemistry, 2007. **2007**(1): p. 60-64.

25. Hoskins, B.F. and R. Robson, *Design and construction of a new class of scaffolding-like materials comprising infinite polymeric frameworks of 3D-linked molecular rods. A reappraisal of the zinc cyanide and cadmium cyanide structures and the synthesis and structure of the diamond-related frameworks [N(CH3)4][CuIZnII(CN)4] and CuI[4,4',4",4'"-tetracyanotetraphenylmethane]BF4.xC6H5NO2*. Journal of the American Chemical Society, 1990. **112**(4): p. 1546.

26. Fujita, M., et al., *Preparation, Clathration Ability, and Catalysis of a Two-Dimensional Square Network Material Composed of Cadmium(II) and 4,4'-Bipyridine*. Journal of the American Chemical Society, 1994. **116**(3): p. 1151-1152.

27. Seo, J.S., et al., *A homochiral metal-organic porous material for enantioselective separation and catalysis*. Nature, 2000. **404**(6781): p. 982-986.

28. Kesanli, B. and W. Lin, *Chiral porous coordination networks: rational design and applications in enantioselective processes*. Coordination Chemistry Reviews, 2003. **246**(1-2): p. 305-326.

29. Wu, C.-D., et al., *A Homochiral Porous Metal−Organic Framework for Highly Enantioselective Heterogeneous Asymmetric Catalysis*. Journal of the American Chemical Society, 2005. **127**(25): p. 8940-8941.

30. Danil N. Dybtsev, A.L.N., Hyungphil Chun, Konstantin P. Bryliakov, Evgeniy P. Talsi, Vladimir P. Fedin, Kimoon Kim,, *A Homochiral Metal-Organic Material with Permanent Porosity, Enantioselective Sorption Properties, and Catalytic Activity13*. Angewandte Chemie International Edition, 2006. **45**(6): p. 916-920.

31. Ma, L., C. Abney, and W. Lin, *Enantioselective catalysis with homochiral metal-organic frameworks*. Chemical Society Reviews, 2009. **38**(5): p. 1248-1256.

32. Chuan-De Wu and Wenbin Lin, *Highly Porous, Homochiral Metal-Organic Frameworks: Solvent-Exchange-Induced Single-Crystal to Single-Crystal Transformations13*. Angewandte Chemie International Edition, 2005. **44**(13): p. 1958-1961.

33. Ma, L. and W. Lin, *Chirality-Controlled and Solvent-Templated Catenation Isomerism in Metalâˆ'Organic Frameworks*. Journal of the American Chemical Society, 2008. **130**(42): p. 13834.

34. Clearfield, A. and Z. Wang, *Organically pillared microporous zirconium phosphonates*. Journal of the Chemical Society, Dalton Transactions, 2002(15): p. 2937-2947.

35. Clearfield, A., Z.K. Wang, and P. Bellinghausen, *Highly Porous Zirconium Aryldiphosphonates and their Conversion to Strong Bronsted Acids. Solid State Chem.*, 2002. **167**: p. 376-385.

36. Clearfield, C.Y.Y.A., *The Preparation and ion-exchange properties of zirconium sulphophosphonates. React. Polym*, 1987. **5**: p. 13.

37. Llabrés i Xamena, F.X., et al., *MOFs as catalysts: Activity, reusability and shape-selectivity of a Pd-containing MOF*. Journal of Catalysis, 2007. **250**(2): p. 294-298.

38. Ravon, U., et al., *MOFs as acid catalysts with shape selectivity properties*. New Journal of Chemistry, 2008. **32**(6): p. 937-940.

39. Schlichte, K., T. Kratzke, and S. Kaskel, *Improved synthesis, thermal stability and catalytic properties of the metal-organic framework compound Cu3(BTC)2*. Microporous and Mesoporous Materials, 2004. **73**(1-2): p. 81-88.

40. Luc Alaerts, et al., *Probing the Lewis Acidity and Catalytic Activity of the Metal-Organic Framework [Cu_{<FONT SIZE='-1'>3</FONT>}(btc)_{<FONT SIZE='-1'>2</FONT>}] (BTC=Benzene-1,3,5-tricarboxylate)*. Chemistry - A European Journal, 2006. **12**(28): p. 7353-7363.

41. Ying Lu, et al., *A Cobalt(II)-containing Metal-Organic Framework Showing Catalytic Activity in Oxidation Reactions*. Zeitschrift für anorganische und allgemeine Chemie, 2008. **634**(12-13): p. 2411-2417.

42. Hasegawa, S., et al., *Three-Dimensional Porous Coordination Polymer Functionalized with Amide Groups Based on Tridentate Ligand: Selective Sorption and Catalysis*. Journal of the American Chemical Society, 2007. **129**(9): p. 2607-2614.

43. Sawaki, T. and Y. Aoyama, *Immobilization of a Soluble Metal Complex in an Organic Network. Remarkable Catalytic Performance of a Porous Dialkoxyzirconium Polyphenoxide as a Functional Organic Zeolite Analogue*. Journal of the American Chemical Society, 1999. **121**(20): p. 4793-4798.

44. Gomez-Lor, B., et al., *In2(OH)3(BDC)1.5 (BDC = 1,4-Benzendicarboxylate): An In(III) Supramolecular 3D Framework with Catalytic Activity*. Inorganic Chemistry, 2002. **41**(9): p. 2429-2432.

45. Paul M. Forster, N.S., Anthony K. Cheetham,, *A High-Throughput Investigation of the Role of pH, Temperature, Concentration, and Time on the Synthesis of Hybrid Inorganic-Organic Materials13*. Angewandte Chemie International Edition, 2005. **44**(46): p. 7608-7611.

46. Ru-Qiang Zou, H.S., Qiang Xu,, *Preparation, Adsorption Properties, and Catalytic Activity of 3D Porous Metal-Organic Frameworks Composed of Cubic Building Blocks and Alkali-Metal Ions13*. Angewandte Chemie International Edition, 2006. **45**(16): p. 2542-2546.

47. Jorge Gascon, María D.H.-A., Ana Rita Almeida, Gerard P. M. van Klink, Freek Kapteijn, Guido Mul,, *Isoreticular MOFs as Efficient Photocatalysts with Tunable Band Gap: An Operando FTIR Study of the Photoinduced Oxidation of Propylene*. ChemSusChem, 2008. **1**(12): p. 981-983.

48. Alkordi, M.H., et al., *Zeolite-like Metalâˆ'Organic Frameworks as Platforms for Applications: On Metalloporphyrin-Based Catalysts*. Journal of the American Chemical Society, 2008. **130**(38): p. 12639.

49. Stephan Hermes, M.-K.S., Rochus Schmid, Lamma Khodeir, Martin Muhler, Arno Tissler, Richard W. Fischer, Roland A. Fischer,, *Metal@MOF: Loading of Highly Porous Coordination Polymers Host Lattices by Metal Organic Chemical Vapor Deposition13*. Angewandte Chemie International Edition, 2005. **44**(38): p. 6237-6241.

50. Maksimchuk, N.V., et al., *Heterogeneous selective oxidation catalysts based on coordination polymer MIL-101 and transition metal-substituted polyoxometalates*. Journal of Catalysis, 2008. **257**(2): p. 315-323.

51. Byrd, H., et al., *Crystal Structure of a Porous Zirconium Phosphate/Phosphonate Compound and Photocatalytic Hydrogen Production from Related Materials*. Chemistry of Materials, 1996. **8**(9): p. 2239-2246.

52. Dokoutchaev, A., et al., *Platinum and palladium incorporation into phosphate/viologen-phosphonates of zirconium and hafnium: synthesis and characterization*. Journal of Molecular Structure, 1998. **470**(1-2): p. 191-205.

53. Reis, K.P., V.K. Joshi, and M.E. Thompson, *Molecular Engineering of Heterogeneous Catalysts: An Efficient Catalyst for the Production of Hydrogen Peroxide*. Journal of Catalysis, 1996. **161**(1): p. 62-67.

54. Wang, Z. and S.M. Cohen, *Postsynthetic modification of metal-organic frameworks*. Chemical Society Reviews, 2009. **38**(5): p. 1315-1329.

55. Wang, Z. and S.M. Cohen, *Postsynthetic Covalent Modification of a Neutral Metalâˆ'Organic Framework*. Journal of the American Chemical Society, 2007. **129**(41): p. 12368-12369.

56. Tanabe, K.K., Z. Wang, and S.M. Cohen, *Systematic Functionalization of a Metalâˆ'Organic Framework via a Postsynthetic Modification Approach*. Journal of the American Chemical Society, 2008. **130**(26): p. 8508-8517.

57. Dugan, E., et al., *Covalent modification of a metal-organic framework with isocyanates: probing substrate scope and reactivity*. Chemical Communications, 2008(29): p. 3366-3368.

58. Ingleson, M.J., et al., *Generation of a solid Bronsted acid site in a chiral framework*. Chemical Communications, 2008(11): p. 1287-1289.

59. Young Kyu Hwang, et al., *Amine Grafting on Coordinatively Unsaturated Metal Centers of MOFs: Consequences for Catalysis and Metal Encapsulation13*. Angewandte Chemie International Edition, 2008. **47**(22): p. 4144-4148.

60. Yin and J. Liebscher, *Carbonâˆ'Carbon Coupling Reactions Catalyzed by Heterogeneous Palladium Catalysts*. Chemical Reviews, 2006. **107**(1): p. 133-173.

61. Nijhuis, T.A., et al., *Preparation of monolithic catalysts*. Catalysis Reviews: Science and Engineering, 2001. **43**(4): p. 345 - 380.

62. Vergunst, T., F. Kapteijn, and J.A. Moulijn, *Monolithic catalysts -- non-uniform active phase distribution by impregnation*. Applied Catalysis A: General, 2001. **213**(2): p. 179-187.

63. Garside, R.J.D.J., ed. *From Molecules to Crystallizers*. Oxford Science Publications, ed. O.C. Primers. 2000, Oxford University Press: New York.

64. Loiseau, T. and G. Férey, *Crystalline oxyfluorinated open-framework compounds: Silicates, metal phosphates, metal fluorides and metal-organic frameworks (MOF)*. Journal of Fluorine Chemistry, 2007. **128**(4): p. 413-422.

65. Xiao, B., et al., *High-Capacity Hydrogen and Nitric Oxide Adsorption and Storage in a Metalâˆ'Organic Framework*. Journal of the American Chemical Society, 2007. **129**(5): p. 1203-1209.

66. Farha, O.K., et al., *Separating Solids: Purification of Metal-Organic Framework Materials*. Journal of the American Chemical Society, 2008. **130**(27): p. 8598-8599.

67. Engineering, I.C.S. *Solid State Group*. École Polytechnique Fédérale de Lausanne 28th of April]; Available from: ssg.epfl.ch/images/SpinCoating.png.

68. Pérez-Cadenas, A.F., F. Kapteijn, and J.A. Moulijn, *Tuning the morphology of monolith coatings*. Applied Catalysis A: General, 2007. **319**: p. 267-271.

69. Yingwei Li and Ralph T. Yang, *Hydrogen storage in metal-organic and covalent-organic frameworks by spillover*. AIChE Journal, 2008. **54**(1): p. 269-279.

70. Bordiga, S., et al., *Electronic and vibrational properties of a MOF-5 metal-organic framework: ZnO quantum dot behaviour*. Chemical Communications, 2004(20): p. 2300-2301.

71. Kapoor, M.P., Q. Yang, and S. Inagaki, *Self-Assembly of Biphenylene-Bridged Hybrid Mesoporous Solid with Molecular-Scale Periodicity in the Pore Walls*. Journal of the American Chemical Society, 2002. **124**(51): p. 15176-15177.

72. Corma, A., et al., *Zeolites as base catalysts: Condensation of aldehydes with derivatives of malonic esters*. Applied Catalysis, 1990. **59**(1): p. 237-248.

73. Wirz, R., D. Ferri, and A. Baiker, *ATR-IR Spectroscopy of Pendant NH2 Groups on Silica Involved in the Knoevenagel Condensation*. Langmuir, 2006. **22**(8): p. 3698-3706.

74. Rolf K. Edvinsson Albers, et al., *Novel monolithic stirred reactor*. AIChE Journal, 1998. **44**(11): p. 2459-2464.

75. Kozhevnikov, I.V., *Heteropoly Acids and Related Compounds as Catalysts for Fine Chemical Synthesis*. Catalysis Reviews: Science and Engineering, 1995. **37**(2): p. 311 - 352.

76. Misono, M. and N. Nojiri, *Recent progress in catalytic technology in japan*. Applied Catalysis, 1990. **64**: p. 1-30.

77. Yuichi Kamiya, T.O., Makoto Misono, Atsuyuki Miyaji, Katsuyuki Tsuji and Tetsuo Nakajo, *Catalytic Chemistry of Supported Heteropolyacids and Their Applications as Solid Acids to Industrial Processes* Catalysis Surveys from Asia, 2008. **12**(2): p. 101-113.

78. Rosi, N.L., et al., *Rod Packings and Metal - Organic Frameworks Constructed from Rod-Shaped Secondary Building Units*. Journal of the American Chemical Society, 2005. **127**(5): p. 1504-1518.

Appendix 1 MOFs with catalytic applications known so far

Table 4- Catalogue of known MOFs and summary of reactions catalyzed [10]

MOF material[a]	Substrate(s)	Reaction(s) catalyzed	Ref.
$[Cd(4\text{-btapa})_2(NO_3)_2]$	Benzaldehyde and malononitrile	Knoevenagel condensation	17
$[Cd(bpy)_2](NO_3)_2)]$	Benzaldehyde and cyanotrimethylsilane	Cyanosilylation of aldehyde	2
$[Cd_3Cl_6\mathbf{L1}_3]$	Aryl aldehyde and diethyl zinc	Alkylation of aldehyde	9
[Co(BPB)]	Cyclohexene	Oxidation of olefin	18
$[Cr_3F(H_2O)_2O(bdc)_3]$	Benzaldehyde and ethyl cyanoacetate; iodobenzene and acrylic acid	Knoevenagel condensation; Heck coupling	19
$[PW_{11}TiO_{40}]^{5-}@[Cr_3F(H_2O)_2O(bdc)_3]$, and $[PW_{11}CoO_{39}]^{5-}@[Cr_3F(H_2O)_2O(bdc)_3]$	α-Pinene, caryophyllene and cyclohexene	Oxidation of olefin	20
$[Cu(2\text{-pymo})_2]$ and $[Co(PhIM)_2]$	Tetralin	Aerobic oxidation of olefin	21
$[Cu(bpy)(H_2O)_2(BF_4)_2(bpy)]$	Various epoxides	Ring-opening of epoxide	22
$[Cu(\text{D-asp})bpe_{0.5}]$ and $[Cu(\text{L-asp})bpe_{0.5}]$	*cis*-2,3-Epoxybutane and methanol	Methanolysis of epoxide	23
$[Cu(\mathbf{L2})_2(H_2O)_2]$, $[Cu(\mathbf{L3})_2(H_2O)(Py)_2]$, $[Cu(\mathbf{L3})_3(H_2O)Cl]$ and $[Co(sal)(H_2O)(Py)_3]$	Linear and cyclic olefins	Epoxidation of olefin	24
$[Cu(SO_4)(pbbm)]$ and $[(Cu(Ac)_2(pbbm))\cdot CH_3OH]$	2,6-Dimethylphenol	Oxidative self-coupling	25
$[Cu_3(btc)_2]$	α-Pinene oxide; citronellal; ethylene acetal of 2-bromopropiophenone	Isomerization; cyclization; rearrangement	26
	Olive oil and mill waste waters	Oxidation of polyphenol	27
	Benzaldehyde (or acetone) and cyanotrimethylsilane	Cyanosilylation of aldehyde	28
[In(OH)(hippb)]	Benzaldehyde and α-methylbenzeneacetaldehyde	Acetalization of aldehyde	29
$[In_2(OH)_3(bdc)_{1.5}]$	Nitrobenzene and 2-methyl-1-nitronaphthalene; methylphenyl sulfide, (2-ethylbutyl)phenyl sulfide	Reduction of nitroaromatic; oxidation of sulfide	30
$Mn(porphyrin)@[In_{48}(HImDC)_{96}]$	Cyclohexane	Oxidation of alkane	7
$[Ln(OH)(1,5\text{-NDS})H_2O]$	Linalool	Epoxidation of olefin	31
$[(Mn(TpCPP)Mn_{1.5})(C_3H_7NO)\cdot 5C_3H_7NO]$	Cyclic alkenes; cyclic/linear alkanes	Epoxidation of olefin; oxidation of alkane	32
$[Mn_3((Mn_4Cl)_3BTT_8(CH_3OH)_{10})]_2$	Aldehydes and cyanotrimethylsilane; benzaldehyde and methyltrimethylsilyldimethylketene acetal	Cyanosilylation of aldehyde; Mukaiyama-aldol	12
$[(Na_{20}(Ni_8\mathbf{L4}_{12})(H_2O)_{28})(H_2O)_{13}(CH_3OH)_2]$	CO	Oxidation to CO_2	33
$[Pd(2\text{-pymo})_2]$	Cinnamyl alcohol; aryl halides and arylboronic acids; 1-octene, cyclododecene	Oxidation of alcohol; Suzuki–Miyaura coupling; hydrogenation of olefin	34
$Tb[V_6O_{13}\{(OCH_2)_3C(NH_2CH_2C_6H_4\text{-}4\text{-}CO_2)\}\{(OCH_2)_3C\text{-}(NHCH_2C_6H_4\text{-}4\text{-}CO_2)\}_2]^{4-}$	Propanethiol	Oxidation of sulfide	39
$[Zn_2(bpdc)_2\mathbf{L5}]$	2,2-Dimethyl-2*H*-chromene	Epoxidation of olefins	6
$[Zn_2(Py_2(PhF_5)_2PorZn)(TCPB)]$	Acetyl imidazole and pyridyl carbinols	Intermolecular transfer of acyl	35
$[Zn_3(\mu_3\text{-}O)(O_2CR)_6(H_2O)_3]^{n+}$	Esters and alcohols	Transesterification	36
$[Zn_4O(bdc)_3]$ and $[Zn_4O(ndc)_3]$	*tert*-Butyl chloride and toluene	Friedel–Crafts alkylation	37
$[(Zn_4O)(bdc\text{-}NH_2)_3]\cdot Vsal_{0.4}$	Cyclohexene	Oxidation of olefin	38

[a] Ac = acetyl; bdc = 1,4-benzenedicarboxylate; BPB = 1,4-bis(4′-pyrazolyl)benzene; bpdc = biphenyldicarboxylate; bpe = *trans*-1,2-bis(4-pyridyl)ethylene); Bpy = 4,4′-bipyridine; btc = benzene-1,3,5-tricarboxylate; btapa = 1,3,5-benzene tricarboxylic acid tris[*N*-(4-pyridyl)amide]; BTT = 1,3,5-benzenetris(tetrazol-5-yl); D-asp = D-aspartate; HImDC = 4,5-imidazole dicarboxylic acid; hippb = 4,4′-(hexafluoroisopropylidene)bis(benzoic acid); **L1** = (*R*)-6,6′-dichloro-2,2′-dihydroxy-1,1′-binaphthyl-4,4′-bipyridine; **L2** = (4-formylphenoxy)acetic acid; **L3** = 2-[2-[[(2-aminoethyl)imino]methyl]phenoxy]acetic acid; **L4** = 4,5-imidazoledicarboxylic acid; **L5** = (*R,R*)-(−)-1,2-cyclohexanediamino-*N,N*-bis(3-*tert*-butyl-5-(4-pyridyl)salicylidene)$Mn^{III}Cl$; nds = naphthalenedisulfonic acid; pbbm = 1,10-(1,5-pentanediyl)bis(1*H*-benzimidazole); PhIM = phenyl imidazolate; pymo = 2-hydroxypyrimidinolate; $Py_2(PhF_5)_2Por$ = 5,15-dipyridyl-10,20-bis(pentafluorophenyl)porphyrin; sal = salicylidene moiety; TCPB = 1,2,4,5-tetrakis(4-carboxyphenyl)benzene; TpCPP = tetra-(*p*-carboxyphenyl)porphyrin.

Appendix 2 Characterization Methods

During the research development, characterization of the new materials was essential to understand interactions and alterations in MOF structures.

The methods used during the research are listed and summarized in the next topics.

Physical Adsorption: N2 Adsorption

This technique is specially used to determine the specific surface area and pore volume.

The BET area of the sample can be calculated by measuring the amount of physisorpted nitrogen at 77 K.

Prior to the determination of the porous properties of catalysts by nitrogen physisorption the samples were pretreated at 200 ºC for 16 hours at a ramp rate of 10 ºC/min.

The isotherms were measured at 77 K using a Quantachrome Autosorb-6B unit.

The BET method was used to determine the surface are and Dubinin-Radushkevich to determine the pore volume.

X-Ray Diffraction (XRD)

This method consists on high-energy photons penetrating deeply into the solid sample. The position of the X-ray source is fixed and the angle between the incident and diffracted X-rays is 2θ degrees, the crystal and the X-ray detector are rotated coherently.

XRD results were obtained by using a Bruker-AXS D5005 diffractometer equipped with an incident beam monochromatic and a Braun Position Sensitive Detector (PSD) for a radiation $Cu_{k_{\alpha}1}(\lambda = 1.5405A)$. The measurements range was 5-90º in 2θ, with a step size of 0.039º in 2θ and a step time of 1 second.

Thermo Gravimetric Analysis (TGA)

Thermo Gravimetric Analysis is a technique performed to determine the stability and the thermal behaviour of the material. Also, the presence of adsorbed or weakly bonded substances may be observed.

A few amount of solid sample (approximately 14 mg) is introduced in the small container, and then is passed a flow of helium or air while some data is being recorded such as time, mass and temperature.

TGA equipment used was Mettler Toledo TGA/SDTA851e, under 60ml/min. In some of the experiments, it at 25ºC until 600 ºC with a heating rate of 10 ºC/min but then it was proved that a heating rate of 2 ºC/min and an increase up to 900 ºC were more convenient.

SEM (Scanning Electron Microscopy)

Electron microscopy techniques are widely applied for the characterization of solid catalysts, providing information about particle size, shape and chemical composition in certain areas of the sample.

Scanning electron microscopy enables a virtual look at the sample. This technique is based on the irradiation of the sample by primary electrons, those reflected by the sample are detected. SEM was performed on a Philips XL20 (15-30 kV) microscope, after coating with gold.

Diffuse Reflectance Infrared Fourier Transform (DRIFT)

Diffuse Reflectance Infrared Fourier Transform Spectroscopy enables a measurement of the intensity of the diffusely reflected light as a function of the wavelength when the catalyst is non transparent in the range of interest.

Infrared range of wavelengths is on the low energy side of electromagnetic spectrum and is typically identified by the region of 12500 to 20 cm^{-1}. Many of inorganic compounds adsorb irradiation in the region of 4000 to 400 cm-1, so the the adsorption of IR light is due from transitions between vibrational energy levels.

DRIFT spectroscopy was applied by using a Bruker model IFS66 spectrometer, equipped with a 633 nm laser and a DRIFT high-temperature cell with CaF_2 windows, in the 4000-400 cm^{-1} range. Samples were previously pretreated at 120ºC for 30 min, and then the spectra were collected at room temperature under air atmosphere by accumulation of 128 scans, applying a resolution of 4 cm^{-1} and using KBr as background.

Raman

Raman spectra were obtained at room temperature using a Renishaw Raman set up equipped with a 20 mW exciting Argon laser (λ=514 nm), coupled to a Leica microscope (x 20 magnification) with an incorporated CCD camera. All spectra were collected in the range of 4000 to 140 cm^{-1}, with a resolution of 2 cm^{-1}, at a detection time of at least 10 seconds.

Table 5 - Characterization Methods Performed in each sample,

			N2 Adsorption	SEM	XRD	TGA	Raman
Precursor Impregnation							
Monolith	Monolith		X	x	x	x	
	Monolith with Chromium Oxide		X	x	x	x	
	Monolith with MIL-101 (Cr)	Hydrothermal Synthesis		x	x	x	
		Microwave Synthesis	X	x	x	x	
α-alumina	Disk			x			
	disk with MIL-101 (Cr)	Microwave 2 hours Synthesis		x	x		
		Microwave 10 hours Synthesis		x	x		
Seeding Techniques and Secondary Growth							
Nanocrystals to be used as seeds	Microwave Synthesis with Chromium Nitrate	2 x more concentrated					
		Standard conditions	x	x	x	x	
		1.5 x more diluted	x	x	x	x	
		2 x more diluted	x	x	x	x	
		2.5 x more diluted	x	x	x	x	
α-alumina disks	Spin Coating	Microwave Synthesis		x	x		
		Hydrothermal Synthesis		x	x		
	Dip Coating	Hydrothermal Synthesis		x	x		
Monolith wash-coated with α-alumina	Monolith with Just α-alumina coating			x	x	x	
	Procedure A	Static Oven		x	x	x	
		Rotatory Oven		x	x	x	x
	Monolith with a-alumina and seed coating			x	x	x	
	Procedure B	Rotatory Oven		x	x	x	x

Appendix 3 XRD pattern of Cordierite impregnated with Chromium Oxide before and after synthesis

With this analysis it was expected to see a clear peak of MIL-101 (Cr) around 2θ equal to 9 but that did not happen. There is a peak in the sample with MOF that was not present in the others - Figure 44 - but it is not conclusive.

On the other hand, an assumption that there is no presence of MIL-101 (Cr) in the monolith shall also not be taken because what might be happening is that the amount of MOF is not sufficiently high to be detected among the large quantity of Cordierite present on the milled sample.

It was decided to perform again the measurements of the XRD pattern but this time without milling the sample but trying to analyze just a channel. As the MOF is coated on the surface, there is still a last hope that this could detect better any possible MIL-101 on the monolith although the technique is known to penetrate deeply in the solid.

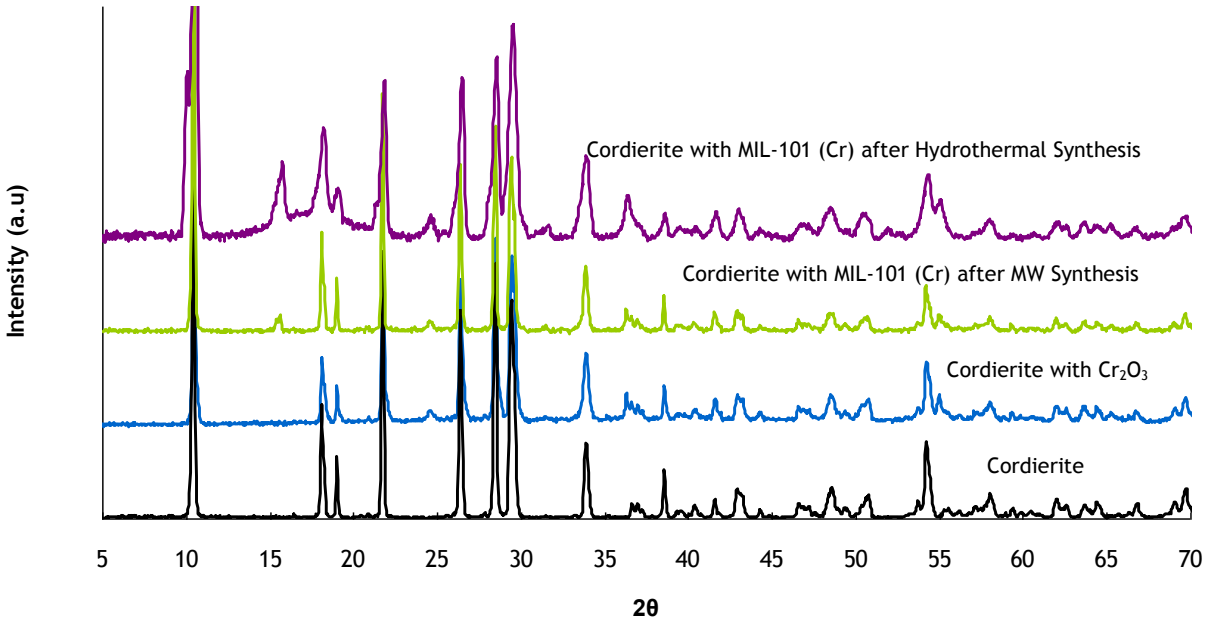

Figure 44 - XRD pattern of the codierite, cordierite impregnated with Cr_2O_3 and after direct synthesis MIL-101 (Cr).

The results achieved were very similar with the others so, XRD revealed to be an inconclusive technique to characterize these samples.

Appendix 4 Synthesis using Chromium Oxide Particles

The main objective of this project is to cover monoliths with MIL-101(Cr). The first technique that it was decided to perform in order to achieve this goal was Chromium Oxide Impregnation, followed by direct synthesis on the monolith.

Chromium Oxide is not the common precursor used to synthesize MIL-101 with Terephtalic Acid. So, to make this project consistent it is necessary to study what happens when trying to perform the synthesis with Chromium Oxide.

SEM characterization of two samples synthesized using the standard chromium conditions and a sample 1.5 times more diluted. The results were similar and a picture of the sample with the standard conditions can be seen in Figure 45.

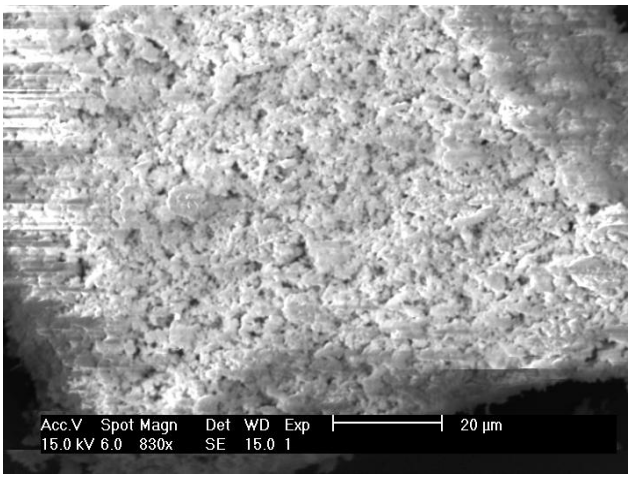

Figure 45- SEM Picture after the synthesis of MIL-101 (Cr) with Chromium Oxide.

Note that we do not have enough information to conclude that the synthesis of the MOF took place but some qualitative observations were a bit different from the samples previously prepared with Chromium Nitrate, the color of the powder was much darker and also there was some precipitation at the bottom of the container.

Apart from a SEM characterization, a XRD diffraction pattern was also studied.

In fact the XRD pattern for both samples did not indicate any presence of MIL-101 (Cr) as the pattern corresponds to the Chromium Oxide Pattern –Figure 46.

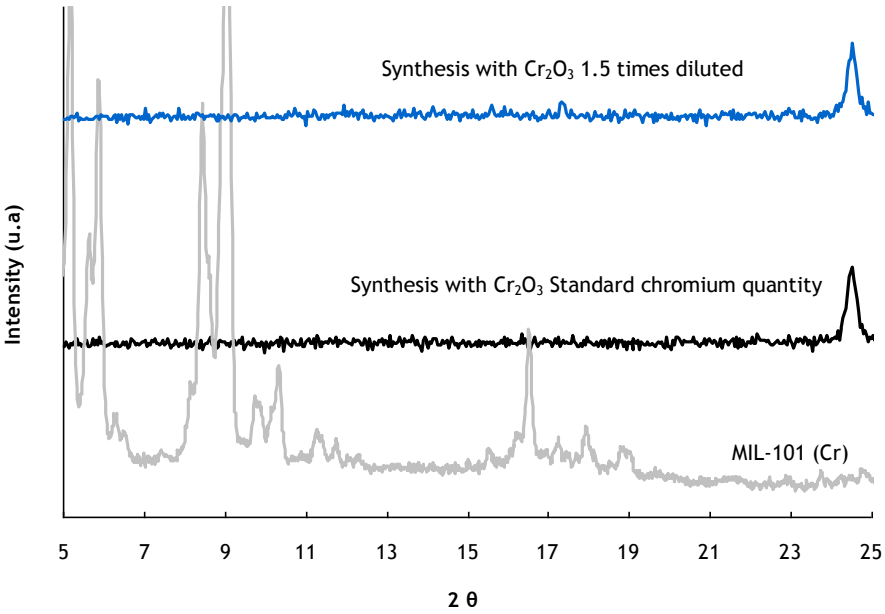

Figure 46 - XRD patterns of the powder obtained when performing a synthesis with Chromium Oxide.

Therefore, as it was not possible to prove the presence of MIL-101 (Cr) using this precursor. These results together with the ones obtained with the α-alumina disks led us to the conclusion that this was not the most convenient way to interface MIL-101 (Cr) with monoliths.

Appendix 5 Thermo Gravimetric Analysis of the Samples with Chromium Oxide Impregnated in Air using an air flow

TGA of Monoliths impregnated with Chromium Oxide Using Air Flow instead of Helium

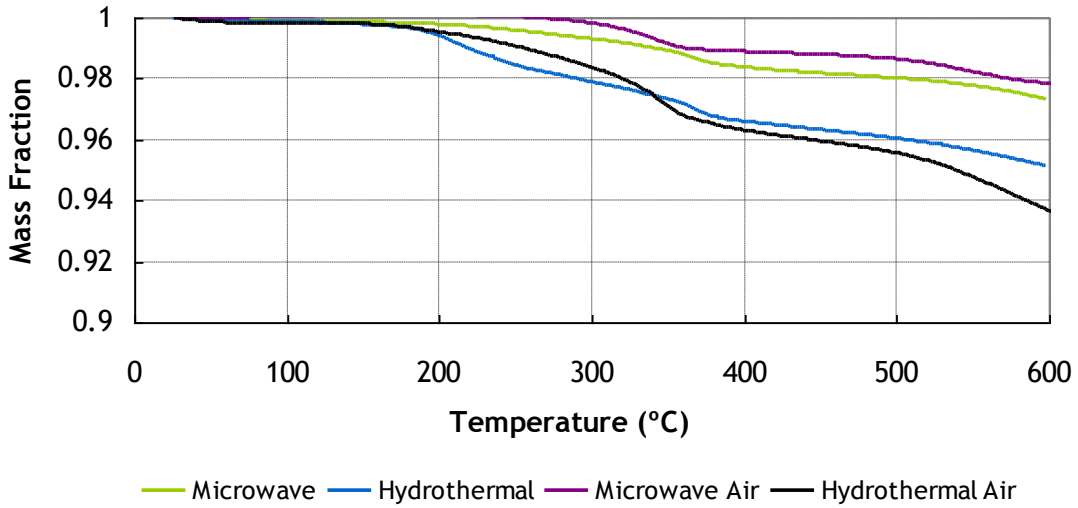

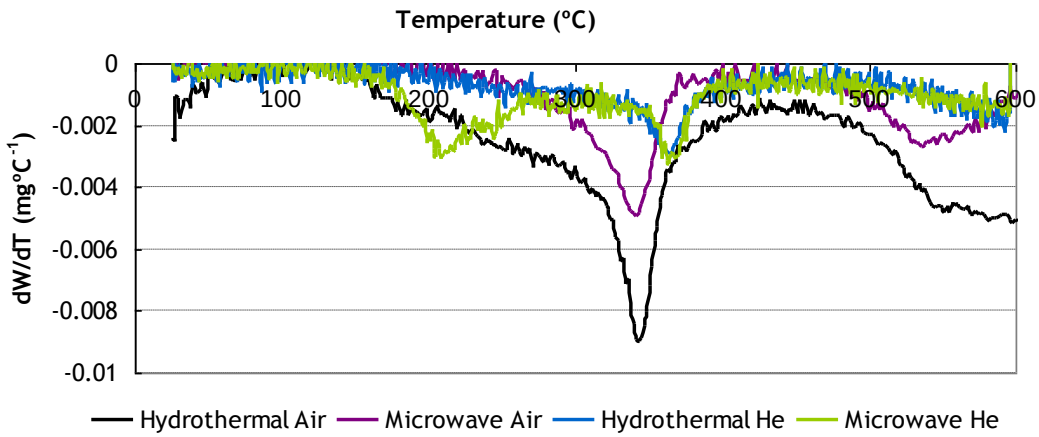

Figure 47 - TGA Results of the samples with direct synthesis both by Microwave and Hydrothermal Synthesis after Chromium Oxide Impregnation and with Helium an Air flow.

Similarly to what have happened with the monoliths coated using a secondary growth technique, the TGA in Air showed more defined plateaus than the TGA in Helium.

However, the decrease is not as steep as it was expected. Moreover, a decrease after 500 ºC was also register but not well understood.

The explanation for the occurrence of more defined plateaus has already been given. These curves were not shown in the main body of the report because the samples were analysed three months before the synthesis so, they possible have changed a bit their properties and the results are not so reliable.

Appendix 6 N_2 Adsorption Isotherms obtained for MIL-101 (Cr) particles with different synthesis reactants concentration

As it was said in the main body of the report, the N2 adsorption isotherms were determined for the samples from each concentration and were particularly similar.

a)

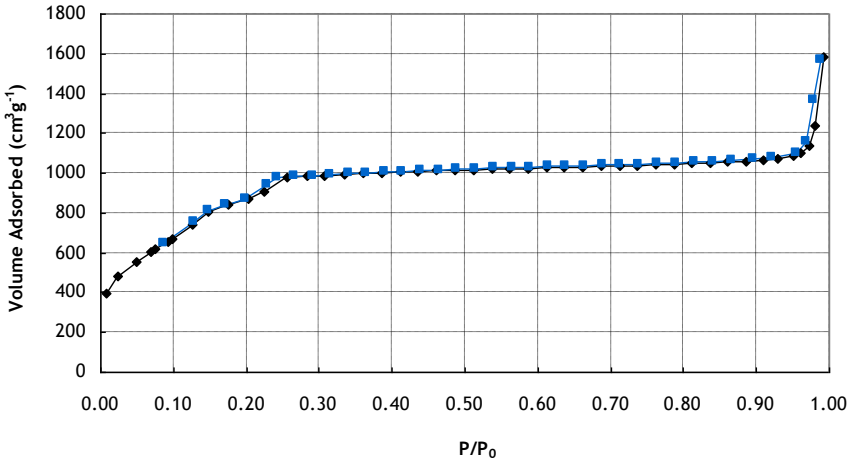

b)

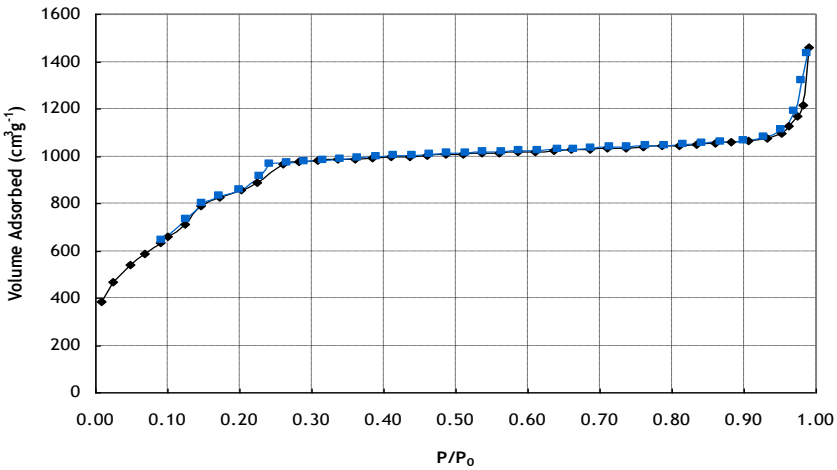

c)

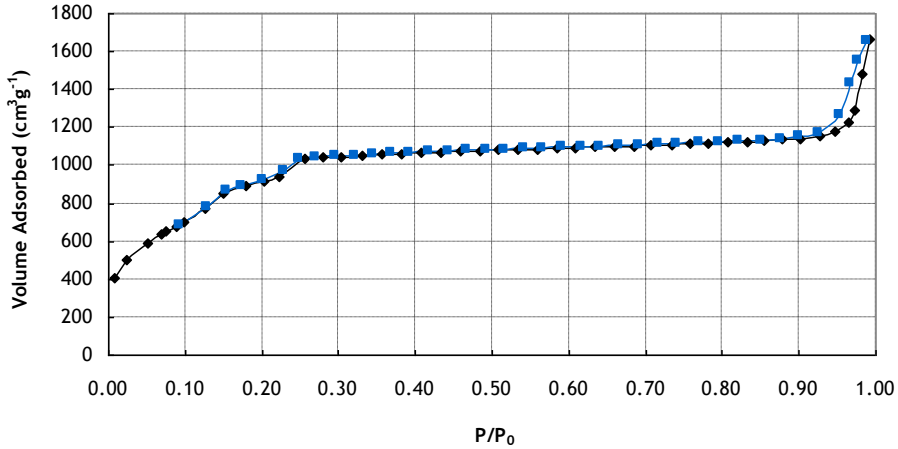

d)

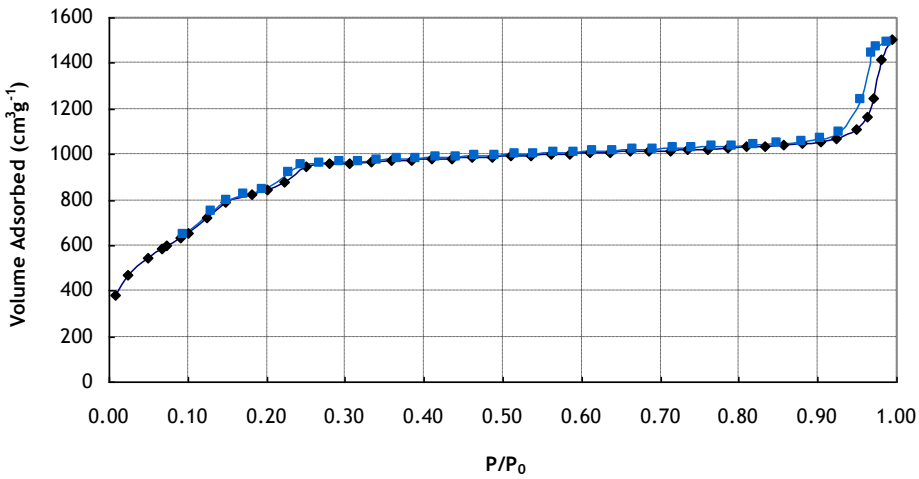

Figure 48 - N2 Adsorption Isotherms of MIL-101 (Cr) powder samples synthesized using a) standard conditions; b) 1.5 times more diluted synthesis conditions; c) 2 times more diluted synthesis conditions and d) 2.5 times more diluted synthesis conditions (blue is the dessorption curve and black the adsorption)..

Appendix 7 BET Method

The Brunauer, Emmett and Teller model describes in a quantitive way the physical adsorption of vapours and is essentially based on three hypotheses:

- In each layer the rate of adsorption is equal to the rate of desorption
- The heat of adsorption is constant and equal to the condensation heat after the second layer
- When the partial pressure reaches the atmospheric pressure the vapour condensates as a ordinary liquid and the number of layers adsorbed tends to infinite

With these assumptions they have obtained:

$$\frac{\frac{P}{P_0}}{n^a(1-\frac{P}{P_0})} = \frac{1}{n_m^a c} + \frac{c-1}{n_m^a c}\frac{P}{P_0} \qquad (1)$$

In which,

$n_m^a \rightarrow monolayer \cdot capacity$
$n^a \rightarrow quantity \cdot adsorbed$
$P \rightarrow system's \cdot pressure$
$P_0 \rightarrow saturation \cdot pressure$
$c \rightarrow parameter \cdot related \cdot to \cdot the \cdot heat \cdot of \cdot adsorption \cdot in \cdot the \cdot first \cdot layer \cdot and \cdot the \cdot heat \cdot of \cdot condensation$

This equation can be applied only to a restricted range of pressures, usually between 0.05 and 0.3.

Based on this equation it is possible to determine the BET surface area.

For the range indicated above when $\frac{\frac{P}{P_0}}{n^a(1-\frac{P}{P_0})}$ is represented as a function of $\frac{P}{P_0}$, a straight line can be obtained and with the slope $\alpha = \frac{(c-1)}{n_m^a c}$ and crosses the y axis at $i = 1/(n_m^a c)$. Which means $n_m^a = 1/(\alpha + i)$ - As this corresponds to the monolayer capacity, the BET area can be calculated as $S_{BET} = n_m^a N_A a_m$ (3)(*NA* Avogadro's number; *am* area occupied by one molecule).

For liquid nitrogen at 77K the *am* value is 0.162 nm^2.

Appendix 8 *t* method

Method consists in a comparison between the isotherm and a standard isotherm and drawing a graph with n^a as a function of t.

This method also allows a calculation of the material area as the slope of the curve already cited is proportional to the material's surface area.

$$\frac{n^a}{n_m^a} = \frac{t}{\sigma} \qquad (2)$$

$$t \rightarrow thickness \cdot of \cdot the \cdot layer$$
$$\sigma \rightarrow thisckness \cdot of \cdot a \cdot monolayer$$

And the area comes as

$$S = n_m^a N_A a_m = b_t \sigma N_A a_m \qquad (3)$$

in which b_t is the slope of the curve and σ is usually 0.354 nm.

When there is capilar condensation involved, for low values of t the curve presents a linear behaviour belonging to the physical adsorption, then, the quantities adsorbed surpass the one predicted due to the condensation.

In microporous materials, the adsorption occurs essentially at low pressures and is higher than the ones predicted by adsorption in multilayers. Only after the microporous saturation this phenomena occurs and a linear region of the curve is defined. From the slope, information about the area that belongs to the mesoporous and macroporous surface can be taken and from the point that it crosses the y axis the quantity adsorbed that saturates micropores. Considering it in a condensated state, similar to a liquid, an estimation about the micropores is:

$$V_{mic} = n_0^a V_M^L \qquad (4)$$

In which n_0^a is the point where the linear part of the curve crosses the y axis.

$$V_{micro} = micropore \cdot volume$$
$$V_M^L = molar \cdot liquid \cdot volume$$

Appendix 9 XRD Pattern and TGA of MIL-101 (Cr) particles synthesized using different reactants concentration

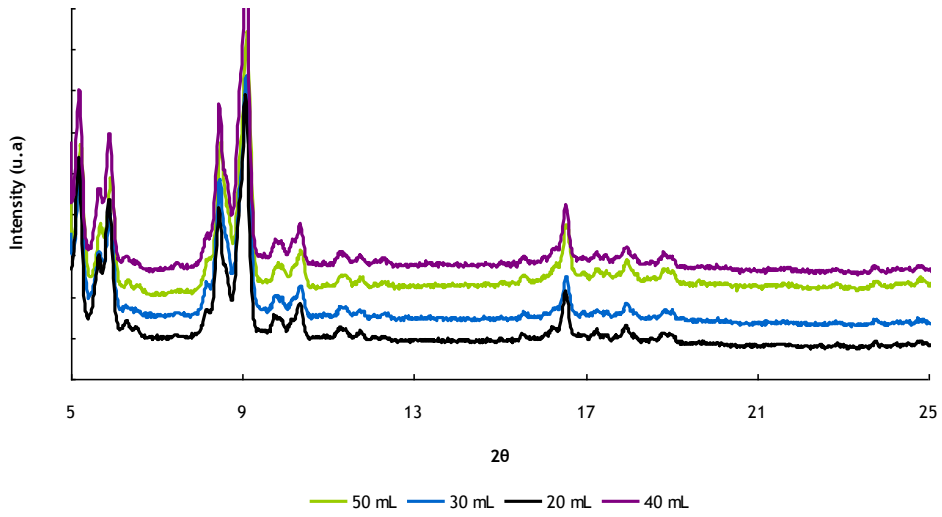

Figure 49 - XRD patterns of MIL-101 (Cr) samples from the most diluted (50 mL) to the standard (20mL).

The patterns obtained are also in conformity with literature, [15], with a major peak around 2 theta equal to 9.

The thermal stability has been also tested using TGA which give us information about the temperature at which the MOF, more particularly, the linker of the MOF, decomposes Figure 50.

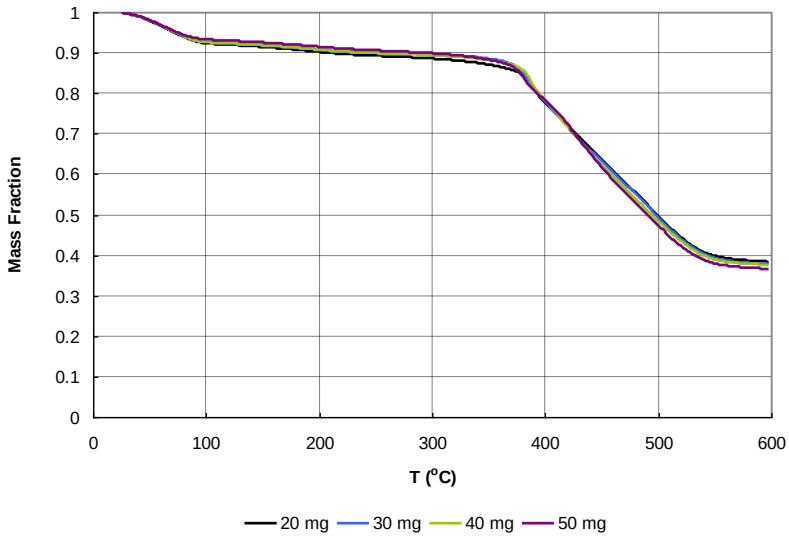

Figure 50 - TGA of MIL-101 (Cr) synthesized with different amount of water from the most diluted (50 mL) to the standard (20mL).

Appendix 10 SEM micrographs of α-alumina disk after a secondary growth in a sample seeded with dip coating

Dip coating cross-sectional view did not prove to be efficient in coating α-alumina disks.

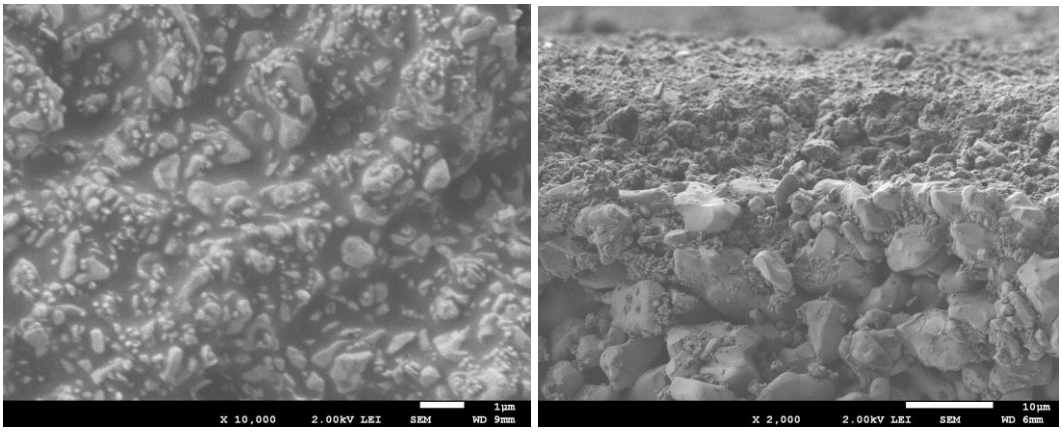

Figure 51 – SEM micrographs of: α-alumina disk top layer covered with MIL-101 (Cr) after dip coating technique – left image and cross sectional view of the same alumina disk.

As it can be seen, MIL-101 (Cr) crystals on the surface seem to be almost absent and also the cross sectional view is pretty similar to an α-alumina disk cross sectional view –Figure 52 .

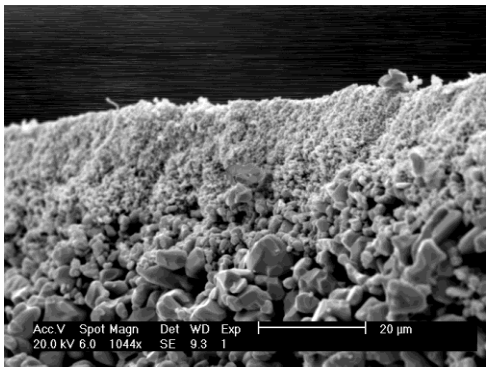

Figure 52 – SEM micrograph of an α-alumina cross-sectional view.

Appendix 11 Thermo Gravimetric Analysis of a Monolith after Secondary Growth and without a wash-coated with α-alumina

As the process to wash-coat a monolith with α-alumina takes a long time, it was decided to check if it was not possible to obtain a promising layer just by seeding cordierite with MIL-101 (Cr) and then performing a secondary growth.

A characterization using TGA was performed and as it can be seen in Figure 53, the decrease in mass at the temperature at which the MIL-101 (Cr) decomposed was not very pronounced and so, this was not definitely a good route to follow in order to interface MIL-101 (Cr) with monoliths.

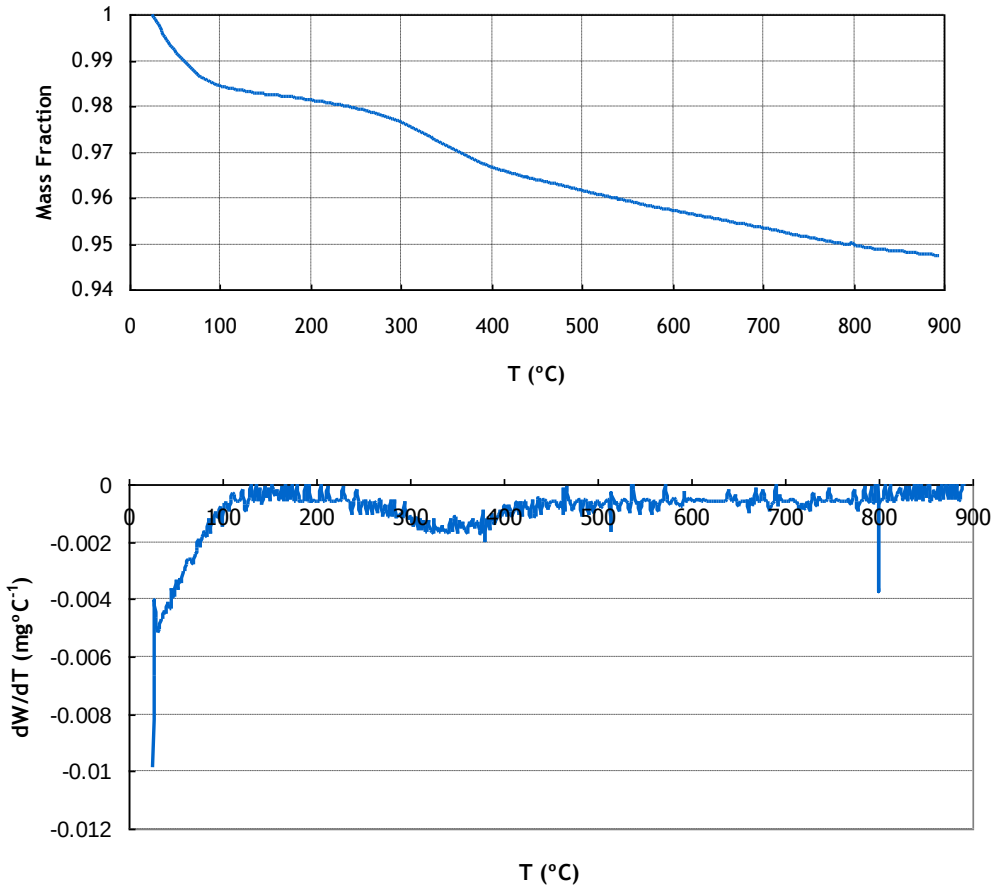

Figure 53 - TGA of MIL-101 (Cr) covered in the monoliths without doing a wash-coated with α-alumina and its derivative.

Appendix 12 SEM micrographs of Cordierite Wash-Coated with α-alumina and after Secondary Growth in Static Oven

After performing a secondary growth in a static oven, it was concluded that the coating was far from being homogeneous. Nevertheless SEM micrographs were also taken and revealed inconclusive. So, that, this it was decided to abandoned the static oven secondary groth for monoliths.

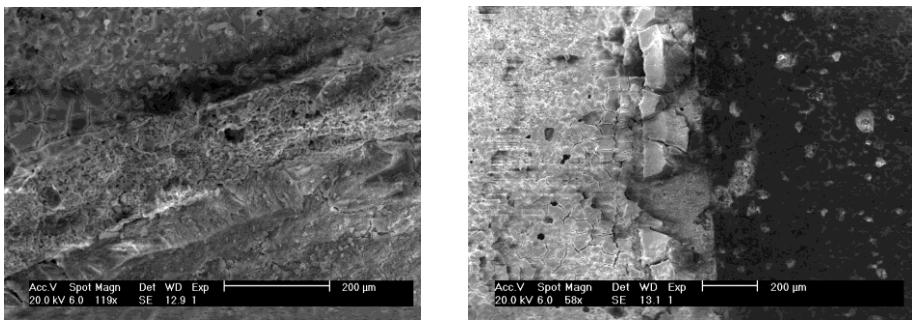

Figure 54 – SEM micrographs of the sample with a wash coat with α-alumina and with the Secondary Growth performed in a Static Oven.

Appendix 13 Thermo Gravimetric Analysis of the MIL-101 (Cr) covered in monoliths and with HPA encapsulation

Catalysis by heteropoly acids, HPAs, is an increasing field of study.

HPAs are polyoxometalates incorporating anions (heteropolyanions) having metal-oxygen octahedral as the basic structural units.

Among a wide variety of HPAs those belonging to the so called Keggin series are the most important for catalysis. They include heteropolyanions (HPANs),*XM12O40x-8* , where *M* is the central ion (Si^{4+}, P^{5+}, etc), *x* the oxidation state and M the metal ion (*Mo6+*, *W6+* and *V5+*). This HPANs have a well known Keggin structure with a central tetrahedron XO4 surrounded by 12 edge sharing metal-oxygen octahedral MO_6 [75].

Very high solubility in polar solvents and fairly high thermal stability in the solid state make them promising acid, redox and bifunctional catalysts in homogeneous as well as in heterogeneous systems.

In the last few decades, the broad utility of HPA acid and oxidation catalysis has been demonstrated in a wide range of synthetically useful selective transformations of organic substances.

Several industrial processes based on HPA catalysis, such as oxidation of methacrolein, hydration of olefins (propene and butene), olymerization of tetrahydrofuran, etc have been developed and commercialized [76].

In solution, the acid properties of HPAs are quite well documented in terms of dissociation constants and Hammet acidity functions.

HPAs have very high solubilities in polar solvents such as water, lower alcohols, ketones, etc and insoluble in non polar solvents.

However, acid forms of solid HPAs show very low activities for surface type reactions, due to their low surface areas (1-5 m^2g^{-1}). In these areas, the enlargement of surface area of solid HPAs, for example, by using supports, is indispensable to obtain active catalysts for practical applications [77].

The acidity and catalytic activity of supported HPA depends on the type of carrier, the HPA loadings, conditions of pre-treatment, etc.

Acid or neutral substances such as silica, active carbon, acidic ion exchange are suitable as supports. Basic solids like MgO tend to decompose HPA [75].

MOFs present clear advantages in the immobilization of HPA approaches. Several MOFs have mesoporous cages but communicate by smaller windows [78]. This structure presents excellent opportunities for the sequestration of Keggin like structures by growing MOFs around the HPA ("build bottle around ship").

Inferring that a possible reason for the non occurrence of reaction with guanidine grafting in the MOFs on the monoliths, a different route was studied, this did not need the use of grafting technique. So, it was decided to do an encapsultation of an Heteropoly acid in MIL-101 (Cr) structure.

The heteropoly acid used for this means was Phosphotungstic Acid, $H_3(PW_3O_{10})_4$, which has a Keggin like structure - Figure 55.

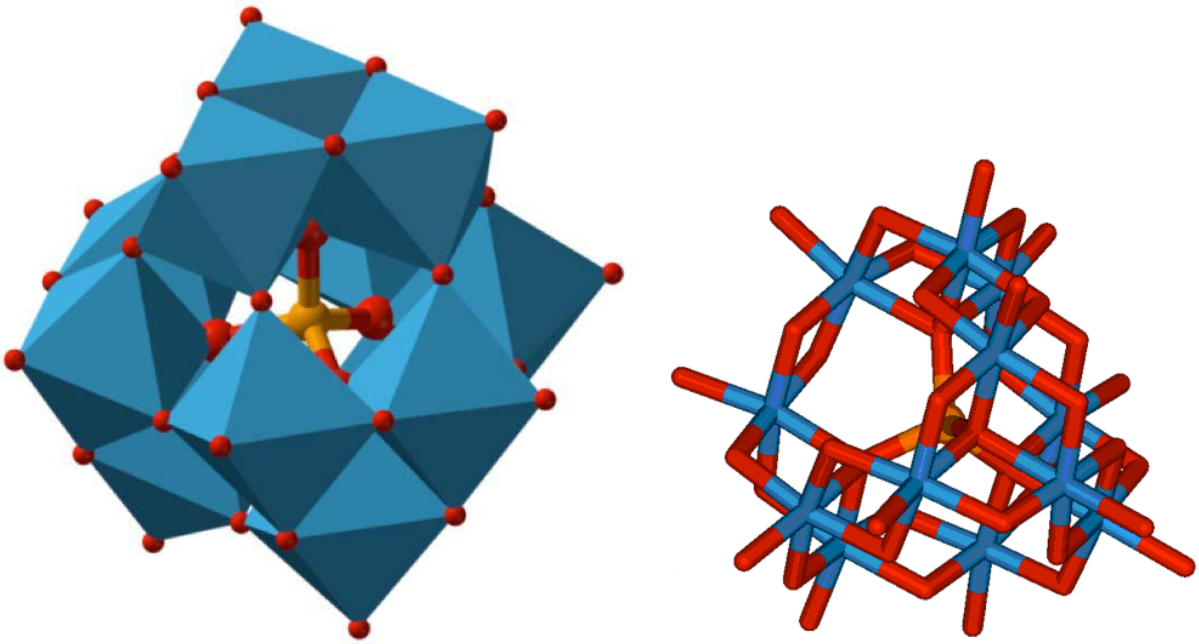

Figure 55 – Different representations of Phosphotungstic Acid molecule. Oxygen, Tungsten and Phosphorous are represented by red, blue and yellow, respectively.

To sequestrate this HPA inside the MOF structure, the synthesis was performed with the standard conditions but putting also 0.8 grams of Phosphotungstic Acid in the autoclave.

Then a TGA analysis was done and the decrease belonging to the heteropoly acid was present Figure 56.

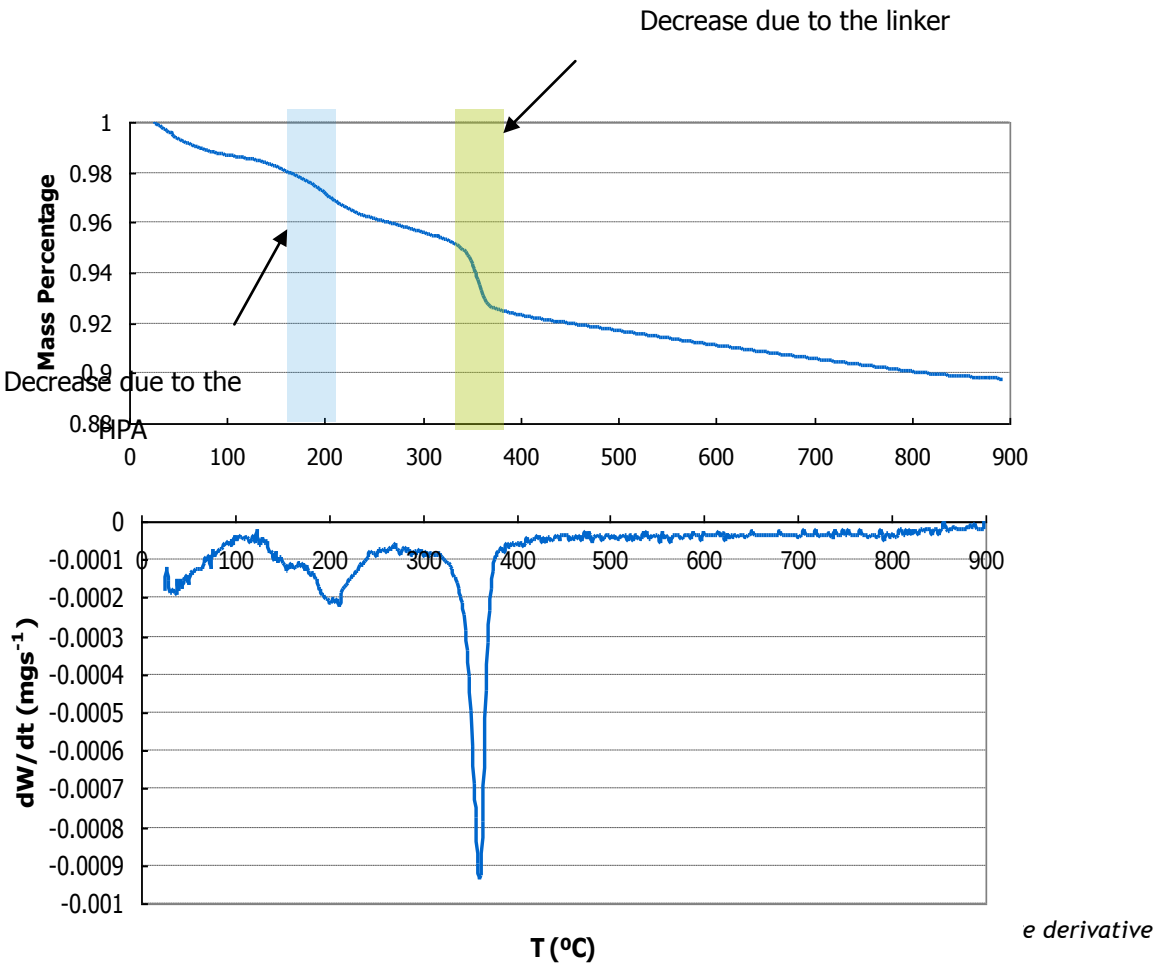

e derivative

However, no conversion was detected when performing the reaction. So, the problems is perhaps not on the grafting technique used.

Appendix 14 First Experimental Setup tested for the Monolithic Stirrer Reactor

The first reactor setup tested is shown in Figure 57. Using a setup like this a proper flow of the reactants mixture into the pores was not guaranteed.

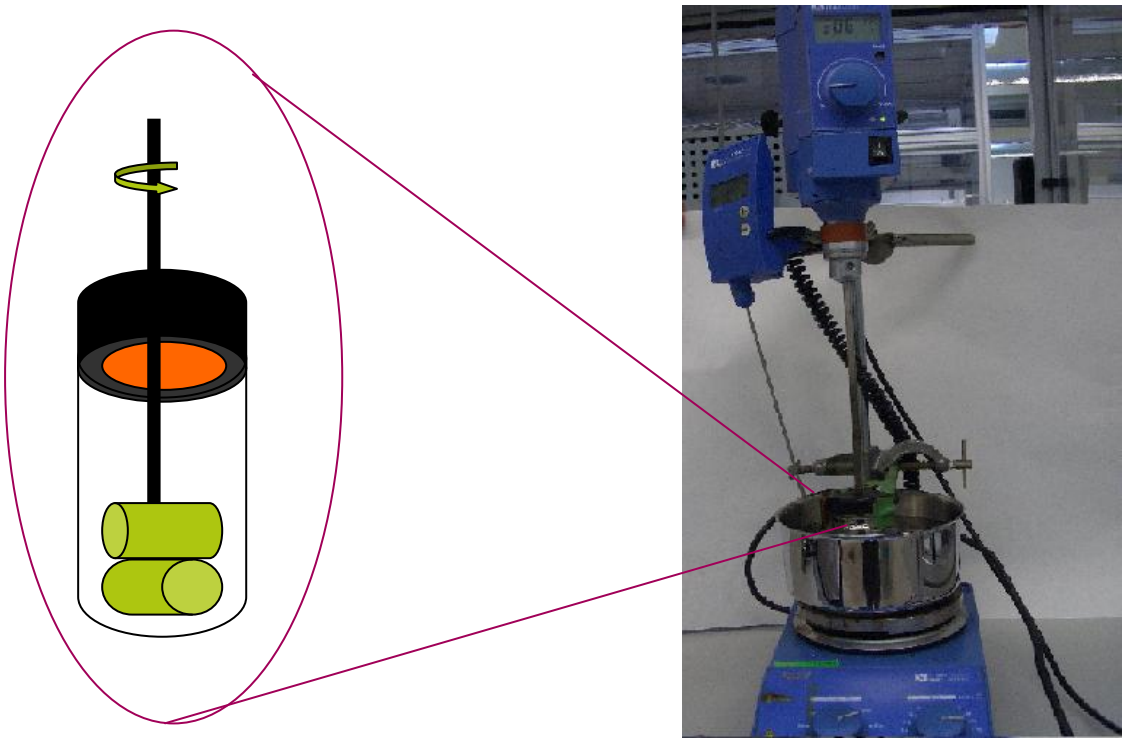

Figure 57 - First experimental setup tested.

Appendix 15 Poster Presented in MOFCAT Workshop 2009 - Metal Organic Frameworks on the Road to Applications in Oslo

Interfacing MIL-101 (Cr) with monolithic supports

M. Domingos, E.V. Ramos-Fernández, J. Juan-Alcañiz, J. Gascon, F. Kapteijn
Catalysis Engineering - Delft University of Technology
Julianalaan 136, 2628 BL Delft, The Netherlands

Introduction

Use MOF catalysts in slurry operation may cause attrition. Coating on a structured support eliminates this catalyst loss. Controlling their growth on surface becomes of a great challenge

1st Step Interfacing MIL-101 (Cr) with α-alumina disks

Dip coating | **Secondary growth** | **Spin coating**

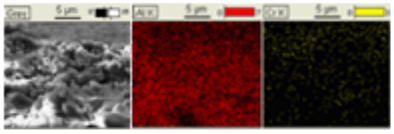

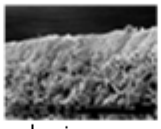

α-alumina support

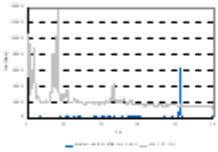

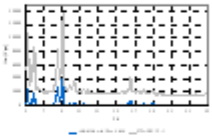

2nd step: Interfacing MIL-101 (Cr) with Cordierite wash-coated with α-alumina

Procedure A

- Washcoat with α-aluma
- Calcination @1000 °C
- Seeding with MIL-101 (Cr) nanocrystals
- Synthesis

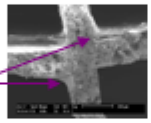

Alumina coating on the monolith

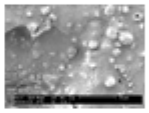

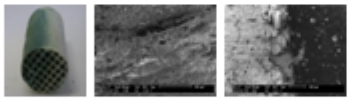

Procedure B

- Washcoat with a solution of α-alumina and seeds of MIL-101 (Cr) nanocrystals
- Calcination @ 400 °C
- Synthesis

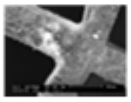

Coating

After Synthesis

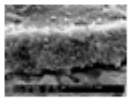

3 layers visible

- The Raman spectra of samples from both procedures show the presence of MIL-101
- TGA also shows a high weight loss, larger for sample A. The weight loss is ascribed to the MOF decomposition.

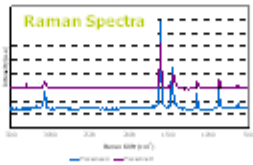

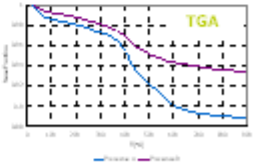

Conclusions

- Seeding appropriate technique to interface MIL-101 with different supports
- Cordierite monolith washcoated with alumina yields a 14wt% MIL-101 loading
- Promising for catalytic applications, e.g. in monolithic stirrer reactor.

TU Delft

Catalysis Engineering - DelftChemTech | Delft University of Technology